

INVESTIGATION OF THE ROLE OF A CANDIDATE EFFECTOR OF WHEAT
STRIPE RUST PATHOGEN IN PLANT IMMUNITY

A THESIS SUBMITTED TO
THE GRADUATE SCHOOL OF NATURAL AND APPLIED SCIENCES
OF
MIDDLE EAST TECHNICAL UNIVERSITY

BY

BAYANTES DAGVADORJ

IN PARTIAL FULFILLMENT OF THE REQUIREMENTS
FOR
THE DEGREE OF DOCTOR OF PHILOSOPHY
IN
BIOTECHNOLOGY

SEPTEMBER 2016

Approval of the thesis:

**INVESTIGATION OF THE ROLE OF A CANDIDATE EFFECTOR OF
WHEAT STRIPE RUST PATHOGEN IN PLANT IMMUNITY**

submitted by **BAYANTES DAGVADORJ** in partial fulfillment of the requirements for the degree of **Doctor of Philosophy in Biotechnology Department, Middle East Technical University** by,

Prof. Dr. Gülbilin Dural Ünver
Dean, Graduate School of Natural and Applied Sciences

Assoc. Prof. Dr. Çağdaş D. Son
Head of Department, **Biotechnology**

Prof. Dr. Mahinur S. Akkaya
Supervisor, **Chemistry Depart., METU**

Prof. Dr. Erdoğan Eşref Hakkı
Co-Supervisor, **Faculty of Agriculture, Selçuk University**

Examining Committee Members:

Assoc. Prof. Dr. Çağdaş D. Son
Biology Depart., METU

Prof. Dr. Mahinur S. Akkaya
Chemistry Depart., METU

Assist. Prof. Dr. Bala Gür Dedeoğlu
Biotechnology Depart., Ankara University

Assist. Prof. Dr. Urartu Şeker
UNAM, Bilkent University

Expert Dr. Anamika Pandey
Faculty of Agriculture, Selçuk University

Date: 06.09.2016

I hereby declare that all information in this document has been obtained and presented in accordance with academic rules and ethical conduct. I also declare that, as required by these rules and conduct, I have fully cited and referenced all materials and results that are not original to this work.

Name, Last Name: Bayantes DAGVADORJ

Signature : 

ABSTRACT

INVESTIGATION OF THE ROLE OF A CANDIDATE EFFECTOR OF WHEAT STRIPE RUST PATHOGEN IN PLANT IMMUNITY

DAGVADORJ, Bayantes

Ph.D., Department of Biotechnology

Supervisor: Prof. Dr. Mahinur S. AKKAYA

Co-Supervisor: Prof. Dr. Erdoğan Eşref Hakkı

September 2016, 157 pages

The advanced plant molecular biology and plant biotechnology tools were employed in this thesis, in order to understand the role of a candidate effector, PstSCR1, of *Puccinia striiformis* f. sp. *tritici* (*Pst*) causing yellow rust disease in wheat.

The homologues proteins of PstSCR1 were found to be only conserved in *Pst*, and in its closest relative, *Puccinia graminis* f. sp. *tritici* (*Pgt*). When PstSCR1 was expressed in *Nicotiana benthamiana* with its signal peptide (SP), it provoked the plant defense, whereas no such effect observed when it is expressed without SP, since SP facilitates crossing of proteins through cellular membranes, it is predicted that the effector is only functional (in triggering plant immune response) if secreted into plant apoplast. The subcellular localization of PstSCR1 was also investigated by microscopic analysis; the effector was indeed secreted to apoplast as the same as apoplastic marker C14 protein. It was also observed that the expression of the effector lowered the pathogenicity of *Phytophthora infestans* and *Peronospora*

tabacina on *N. benthamiana* leaves, respectively. Moreover, when PstSCR1 was overexpressed, it triggered cell death. Brassinosteroid insensitive 1-Associated Kinase 1 (*BAK1/SERK3*) silenced *N. benthamiana*, cell death was remarkably abated, indicating *BAK1* dependent function. Although SCR1-purified treatment on *N. benthamiana* showed a lack of cell death, it resulted in induction of defense genes *NbCYP71D20* and *NbACRE3L*, of which are induced in *BAK1* dependent immune response. Based on our results, *Pst*-secreted protein, SCR1 can activate PAMP-triggered immunity on non-adapted hosts and contribute to non-host resistance.

Keywords: Apoplast, small cysteine rich effector, wheat stripe (yellow) rust, PAMP, PTI.

ÖZ

ADAY SARIPAS PATOJEN EFEKTÖR PROTEİNİNİN BİTKİ İMMÜNİTESİNDEKİ ROLÜNÜN ARAŞTIRILMASI

DAGVADORJ, Bayantes

Doktora, Biyoteknoloji Bölümü

Tez Yöneticisi: Prof. Dr. Mahinur S. AKKAYA

Ortak Tez Yöneticisi: Prof. Dr. Erdoğan Eşref Hakkı

Eylül 2016, 157 sayfa

Bu tezde, gelişmiş bitki moleküller biyoloji ve bitki biyoteknoloji teknikleri kullanarak, kısa sistin bakımından zengin *Pst* aday efektörü; PstSCR1'in işlevi anlaşılmaya çalışılmıştır. PstSCR1 homolog proteinleri sadece *Pst* patojeninde ve bir de yakın akrabası olan *Puccinia graminis* f. sp. *tritici* (*Pgt*) patojende korunmuş olarak bulundu. PstSCR1 *Nicotiana benthamiana*'da signal peptit ile anlatımı yapıldığında bitki immün sistemini uyardığı halde signal peptitsiz anlatımı immün sistemini uyarmamıştır. Bu sonuç, efektötün signal peptit ile bitki hücresinin apoplastına salındığını ve apoplastda işlevsel olduğunu göstermiştir. Mikroskopik görüntüleme çalışmaları efektörün hücre içi lokalizasyonun apoplast olduğunu desteklemistir. Aynı zamanda immün sisteminin uyarılmasının *Phytophthora infestans* ve *Peronospora tabacina* *N. benthamiana* yapraklarında gelişmesini ve spor oluşturmasını yavaşlattığı saptanmıştır. Bununla birlikte, PstSCR1 çok fazla ekspres edildiğinde hücre ölümünü tetiklemektedir. Brassinosteroid duyarsız 1-

Associated Kinase 1 (*BAK1/SERK3*) susturulmuş *N. benthamiana*'da hücre ölümünün azalmış olması bu efektörün *BAK1/SERK3* reseptör tarafından tanıdığı ve bu nedenle immün sistemini uyarma mekanizmasının PTI olduğunu desteklemiştir. Bir başka destek ise, protein olarak izole edilmiş efektör *N. benthamiana* yapraklarına enjekte edildiğinde defans genleri olan *NbCYP71D20* ve *NbACRE31* indüklenmiştir. Bu sonuçlar konaklarda immün tepkisi oluşturabildiği ve bu efektör PTI yoluyla 'non-host' bağışlığı sağladığını bulunmuştur.

Anahtar Kelimeler: Apoplast, kısa sistin zengin efektör, buğday sarı pas, PAMP, PTI.

Dedicated to my family

ACKNOWLEDGEMENTS

First and foremost, I would like to express my sincere gratitude to my advisor Prof. Dr. Mahinur S. Akkaya for her time, contribution and supports that made my PhD study productive and stimulating. Her dedication and adventuresome to science always inspired me. For last seven year, what I learnt from her and in her laboratory is priceless. As being her PhD student, I am very fortunate and satisfied.

I would like to thank Dr. Tolga Osman Bozkurt for accepting me to study the part of this thesis in his laboratory. I also thank his postdoctoral fellow Dr. Pooja Pandey for her supervision. In Bozkurt lab, I had collected significant data including images of subcellular localization, and *P. infestans* and *P. tabacina* infection assays, which are included in this thesis.

I would like to acknowledge COST-STSM-FA1208 grant, TÜBİTAK (110T445, 113Z350 and BİDEB 2215), and METU-BAP financial supports.

I owe my gratitude to Prof. Dr. Erdoğan Eşref Hakkı for being my co-supervisor.

I would like to thank thesis committee members Assoc. Dr. Çağdaş D. Son and Assist. Dr. Urartu Şeker for their recommendation and criticism on the experiments.

I would like to acknowledge Dr. Kamoun and Dr. Nakagawa labs for providing the plasmid constructs.

I am grateful to Assist. Dr. Salih Özçubukçu for synthesizing FLAG peptide, which was used in immunoprecipitation experiments.

I am thankful to my fellow lab members Ahmet Çağlar Özketen for qPCR, and Ayşe Andaç for *Pst* infection. Also, I very appreciate their help on lab maintenance, brainstorming, discussions and collaboration on my research.

I thank to Akkaya lab members; Sayit Mahmut Erdoğan for his collaboration; Zemran Mustafa and Taylan Beyaztaş for their friendship.

I thank to Dr. Shan-Ho Chou lab for expressing PstSCR1 in *E. coli* for crystallization attempts.

I am grateful to Dr. Xianming Chen for supplying yellow rust *Pst-78* spores.

Last but not least, I specially thank to my mother Navchaa Lamjab, and my wife Mandakhtuya Gantulga for all their sacrifices that they have made on my behalf. I thank to my father-in-law Gantulga Sodnom, and my siblings Bayan-Undur Dagvadorj, Ariunmaa Dagvadorj and Saikhankhuu Dagvadorj for their endless support, encouragement and inspiration for me.

TABLE OF CONTENTS

ABSTRACT	v
ÖZ	vii
ACKNOWLEDGEMENTS	x
TABLE OF CONTENTS	xii
LIST OF TABLES	xvi
LIST OF FIGURES	xvii
LIST OF ABBREVIATIONS	xxi
CHAPTERS	
1. INTRODUCTION	1
1.2 Wheat yellow rust	1
1.3 Plant immunity	2
1.3.1 BAK1/SERK3 gene in PTI	7
1.4 Apoplast	8
1.4.1 Apoplastic effectors	8
1.5 <i>Pst</i> candidate effectors	11
1.5.1 <i>PstSCR1</i> candidate effector	12
1.6 <i>Agrobacterium tumefaciens</i> -mediated gene transfer	13
1.6.1 <i>Tobacco mosaic virus</i> derived pTRBO vector	14
1.7 Gateway cloning	16
1.7.1 Gateway destination vectors	18
1.8 Subcellular localization	20
1.9 Gene silencing	21
1.10 Immunoprecipitation	22
1.11 Objective of the research	23
2. EXPERIMENTAL PROCEDURES	25
2.1 Plants and pathogen materials	25
2.1.1 Plants used in the study	25
2.1.2 Pathogen	25

2.2 Isolation of total RNA	26
2.2.1 Preparation steps prior to isolation	26
2.2.2 Total RNA purification from plant tissue	27
2.2.3 RNA sample integrity check.....	27
2.3 First strand cDNA synthesis.....	28
2.3.1 Genomic DNA removal	28
2.3.2 cDNA synthesis	28
2.4 qPCR.....	29
2.5 Calculation of $\Delta\Delta Ct$ and fold change of treated sample	30
2.6 The PstSCR1 sequence analysis	31
2.7 PstSCR1 gene constructs.....	32
2.8 PCR amplifications.....	34
2.9 Cloning of a gene construct in pTRBO vector	36
2.9.1 pTRBO plasmid and insert DNA digestion	36
2.9.2 DNA purification	37
2.9.3 Ligation reaction.....	37
2.10 Gateway cloning	38
2.10.1 pENTR/D-TOPO cloning	38
2.10.2 LR clonase reaction	38
2.11 Bacterial transformation of plasmids.....	39
2.11.1 <i>E.coli</i> competent cell preparation	39
2.11.2 Transformation of <i>E. coli</i> Top10 competent cell	40
2.11.3 Preparation Agrobacterium GV3101 electro-competent cells.....	40
2.11.4 Agrobacterium GV3101 transformation	41
2.12 Agro-infiltration of plant leaves	41
2.13 Apoplastic fluid isolation	42
2.14 Apoplastic fluid infiltration	42
2.15 Virus induced gene silencing of BAK1	43
2.16 Infection assay	43
2.18 Protein extraction and immunoprecipitation	44
2.18.1 Total protein extraction.....	44

2.18.2 Tagged-protein immunoprecipitation	44
2.19 SDS-PAGE	45
2.19.1 Materials and preparation of the SDS-PAGE gel	45
2.19.2 SDS-PAGE	46
2.18 Western Blot	46
3. RESULTS and DISCUSSION	49
3.1 PstSCR1 homologs	49
3.2 Expression levels of PstSCR1 and its closest homolog during <i>Pst-78</i> infection	54
3.3 Subcellular localization of PstSCR1.....	59
3.4 PstSCR1 lowers pathogen infections.....	62
3.5 Overexpression of PstSCR1 in <i>N. benthamiana</i>	65
3.5.1 PstSCR1 cloning in TRBO vector	65
3.5.2 Overexpression of PstSCR1 cause cell death in <i>N. benthamiana</i>	71
3.6 Apoplastic extracts of PstSCR1 expressing leaves triggered cell death in a dose dependent manner.....	72
3.7 Stability of PstSCR1 in apoplast	73
3.9 PstSCR1 reducing the level of cell death in BAK1 silenced plants	76
3.10 Activation of <i>NbCYP71D20</i> and <i>NbACRE31</i> genes upon SCR1 treatment...85	85
3.11 Limitations of conducting expression of proteins in wheat.....	90
4. CONCLUSION	93
REFERENCES	97
APPENDICES	
A. pBSK-PstSCR1 (or pBSK-PSTHA2A5) PLASMID INFORMATION AND SEQUENCE	119
B. pBSK-PstSCR1 (pBSK-PSTHA2A5) PLASMID MAP	121
C. SEQUENCING RESULTS OF DNA BANDS IN FIGURE 3.5 A AND B IN SECTION 3.2	123
D. pTRBO CONSTRUCT SEQUENCES	131
E. SCR1-FLAG AND SP-SCR1-FLAG AMPLIFICATION	133
F. pTRBO CONSTRUCTS SEQUENCING CHROMATOGRAMS	135

G. pJL48-TRBO VECTOR SEQUENCE	139
H. pK7FWG2 GATEWAY DESTINATION VECTOR SEQUENCE	143
I. THE C _T VALUES OF qPCR IN <i>BAK1</i> SILENCING EXPERIMENT.....	147
J. THE AVERAGE OF C _T VALUES AND ΔΔC _T CALCULATION OF qPCR IN <i>BAK1</i> SILENCING EXPERIMENT.....	149
K. DAB STAINING OF <i>N. BENTHAMIANA</i> LEAF TREATED WITH PURIFIED SCR1	151
L. APOPLASTIC FLUID AND TOTAL PROTEIN WITH SCR1 INFILTRATION INTO <i>N. BENTHAMIANA</i>	153
M. AMINO ACID SEQUENCE OF PstSCR1	155

LIST OF TABLES

TABLES

Table 1.1	Fungal effector proteins.....	6-7
Table 1.2	Apoplastic effectors from various pathogens.....	10
Table 2.1	Genomic DNA elimination from RNA sample.....	28
Table 2.2	cDNA synthesis mix.....	29
Table 2.3	The primers used in qPCR amplifications.....	30
Table 2.4	The primers used in the cloning of gene constructs.....	33
Table 2.5	Components and their amounts used in PCR when using <i>Taq</i> DNA polymerase.....	34
Table 2.6	Annealing temperatures applied for <i>Taq</i> DNA polymerase amplifications.....	35
Table 2.7	Components and their amounts used in PCR when using <i>Q5</i> DNA polymerase.....	35
Table 2.8	Annealing temperatures applied for <i>Q5</i> DNA polymerase amplifications.....	36
Table 2.9	Contents and amounts for restriction enzyme digestions.....	37
Table 2.10	Components of ligation reactions.....	37
Table 2.11	LR clonase reaction components and their used amounts.....	39
Table 2.12	Selection of recombinant plasmids.....	40
Table 2.13	SDS gel casting contents.....	46
Table 3.1	The ΔCt , $\Delta\Delta Ct$, fold difference calculations in qPCR.....	81
Table 3.2	Relative quantification and its standard deviation of BAK1 silencing experiment.....	81
Table I	The Ct values of qPCR in BAK1 silencing experiment.....	147
Table J	Averages and standard deviations of Ct values.....	149

LIST OF FIGURES

FIGURES

Figure 1.1	The overview of effectors in plants defense.....	5
Figure 1.2	T-DNA binary vectors.....	14
Figure 1.3	pTRBO vector map.....	16
Figure 1.4	Gateway cloning.....	18
Figure 1.5	Destination vector pK7FWG2 map.....	19
Figure 1.6	<i>Tobacco Rattle Virus</i> (TRV) vectors schematic view.....	21
Figure 2.1	Inoculation of wheat with yellow rust <i>Pst</i> -78 spores.....	26
Figure 2.2	$\Delta\Delta Ct$ calculation.....	31
Figure 3.1	The multiple sequence alignment and the phylogeny tree of <i>PstSCR1</i> homolog proteins.....	51
Figure 3.2	The sequence comparisons of AJIL01000081.1 and GH737102	52
Figure 3.3	The quality of RNA from <i>Pst</i> -78 infected wheat samples	54
Figure 3.4	PCR primer design strategy to detect the presence of <i>PstSCR1</i> expression in <i>Pst</i> infected wheat samples.....	55
Figure 3.5	The <i>PstSCR1</i> and its closest homolog gene expression comparisons in different time points during <i>Pst</i> -78 infection...	58
Figure 3.6	The subcellular localization of <i>PstSCR1</i>	60
Figure 3.7	The co-localization of <i>PstSCR1</i> -RFP and <i>PstSCR1</i> -GFP.....	61
Figure 3.8	Pictures of representative <i>N. benthaminiana</i> leaf samples coexpressing pGWB554/C14 and pK7WGY2/REM1.3 and pGWB454/SP-SCR1-RFP and pK7WGY2/YFP-REM1.3.....	62
Figure 3.9	The assessment of the level of lesions by <i>P. infestans</i> in effector expressed samples.....	64
Figure 3.10	The evaluation of the level of <i>P. tabacina</i> spore formation in effector expressed samples.....	65
Figure 3.11	Schematic view of the positions of PCR primers on SCR1-	

FLAG and SP-SCR1-FLAG constructs.....	66
Figure 3.12 PstSCR1 with C-term FLAG amplification for cloning in pTRBO vector.....	67
Figure 3.13 Digestion followed by gel extraction of PstSCR1 PCR products and pTRBO vector agarose gel analysis.....	68
Figure 3.14 Colony PCR after cloning of PstSCR1 in pTRBO vector.....	69
Figure 3.15 Plasmid isolation and PCR of pTRBO/SCR1-FLAG and pTRBO/SP-SCR1-FLAG.....	70
Figure 3.16 The effector needs to be secreted to induce cell death in <i>N. benthamiana</i>	72
Figure 3.17 Apoplastic fluid with secreted effector triggers cell death in <i>N. benthamiana</i>	75
Figure 3.18 Appearance of <i>N. benthamiana</i> plants expressing pTRV2/GFP or pTRV2/BAK1 construct.....	77
Figure 3.19 The RNA quality of <i>BAK1/SERK3</i> and <i>GFP</i> silenced <i>N. benthamiana</i> plants.....	78
Figure 3.20 The qPCR profiles for <i>NbEF1α</i> and <i>NbBAK1/SERK3</i> gene expressions in BAK1 and GFP silenced plants.....	79
Figure 3.21 <i>BAK1/SERK3</i> was silenced by TRV2/ <i>NbSerk3</i> silencing construct.....	80
Figure 3.22 <i>BAK1</i> silencing.....	82
Figure 3.23 PstSCR1 triggered cell death reduced in the <i>BAK1</i> silenced in <i>N. benthamiana</i>	84
Figure 3.24 Western blot analysis of purified SCR1 from <i>planta</i>	86
Figure 3.25 The RNA isolated from <i>N. benthamiana</i> leaves injected with isolated PstSCR1 protein.....	87
Figure 3.26 The qPCR profiles for <i>NbCYP71D20</i> and <i>NbACRE31</i> gene expressions in SCR1 and GFP treated plants.....	88
Figure 3.27 The SCR1 treated plants were analyzed by qPCR for defense related genes of <i>N. benthamiana</i>	89
Figure B pBSK-PstSCR1 plasmid map.....	121
Figure C-1 The chromatogram of the sequenced DNA band of Figure 3.5A.	123

Figure C-2	The band of Figure 3.5A sequencing chromatogram.....	124
Figure C-3	The band (a) of Figure 3.5B sequencing chromatogram.....	125
Figure C-4	The band (b) of Figure 3.5B sequencing chromatogram.....	126
Figure C-5	The alignment of sequenced PCR product in Figure 3.5A by PstSCR1- SP-5-UTR-F primer was aligned with EST of PstSCR1.....	126
Figure C-6	The alignment of sequenced PCR product in Figure 3.5A by PstSCR1- Rev primer was aligned with EST of PstSCR1.....	127
Figure C-7	The alignment of sequenced PCR product (a) in Figure 3.5B by PstSCR1-TM-5-UTR-F primer was aligned with EST of PstSCR1.....	128
Figure C-8	The alignment of sequenced PCR product (a) in Figure 3.5B by PstSCR1-TM-5-UTR-F primer was aligned with whole genome shotgun sequence of PstSCR1 homolog.....	129
Figure C-9	The alignment of sequenced PCR product (b) in Figure 3.5B by PstSCR1-TM-5-UTR-F primer was aligned with whole genome shotgun sequence of PstSCR1 homolog.....	130
Figure C-10	Schematic view of the PCR product (b) in Figure 3.5B based on sequencing results.....	130
Figure D-1	PstSCR1 with SP fused with FLAG at C-terminus	131
Figure D-2	PstSCR1 without SP fused with FLAG at C-terminus	131
Figure D-3	PstSCR1 without SP.....	132
Figure D-4	GFP with SP fused with FLAG at C-terminus.....	132
Figure E-1	Sequence view of SCR1-FLAG construct.....	133
Figure E-2	Sequence view of SP-SCR1-FLAG construct.....	134
Figure F-1	pTRBO/SP-SCR1-FLAG sequence chromatogram.....	135
Figure F-2	pTRBO/SCR1-FLAG sequence chromatogram.....	136
Figure F-3	pTRBO/SP-GFP-FLAG sequence chromatogram.....	137
Figure F-4	pTRBO/SP-SCR1 sequence chromatogram.....	138

Figure J	The $\Delta\Delta Ct$ calculation.....	149
Figure K	DAB staining of <i>N. benthamiana</i> leaves (4-dpi) infiltrated with purified SCR1.....	151
Figure L	Representative <i>N. benthamiana</i> leaf infiltrated with samples possessing SCR1 protein.....	153

LIST OF ABBREVIATIONS

AE:	Apoplastic effector
AET:	Apoplastic effector target
<i>Avr</i> :	Avirulence
BAK1:	Brassinosteroid insensitive 1-Associated Kinase 1
CaMV:	Cauliflower mosaic virus
cDNA:	Complementary DNA
CE:	Cytoplasmic effector
CET:	Cytoplasmic effector target
CP:	Coat protein
DAB:	3,3'- Diaminobenzidine
DNA:	Deoxyribonucleic acid
dNTP:	Deoxy-nucleotidetriphosphate
dpi:	Days post-inoculation
EDTA:	Ethylenediaminetetraacetic acid
ETI:	Effector-triggered immunity
ETS:	Effector-triggered susceptibility
GFP:	Green fluorescent protein
GOI:	Gene of interest
HR:	Hypersensitive response
hpi:	Hours post inoculation
IP:	Immunoprecipitation
Kan:	Kanamycin
kb:	Kilobase
LB:	Lysogeny broth
LRR:	Leucine rich repeat
M:	Molar
MCS:	Multiple cloning site
mg:	Miligram

mRNA:	Messenger RNA
mL:	Mililiter
MP:	Movement protein
N:	Nopaline synthase terminator
NB:	Nucleotide binding
ng:	Nanogram
NT:	No Template
ORF:	Open reading frame
p:	plasmid
PAMP:	Pathogen-associated molecular pattern
PCD:	Programmed cell death
PCR:	Polymerase chain reaction
<i>Pgt</i> :	<i>Puccinia graminis</i> f. sp. <i>tritici</i>
pmol:	Picomole
POI:	Protein of interest
PRR:	Pattern recognition receptor
<i>Pst</i>	<i>Puccinia striiformis</i> f. sp. <i>tritici</i>
PTI:	PAMP-triggered immunity
PVPP:	Polyvinyl Polypyrrolidone
qPCR:	quantitative PCR
<i>R</i> :	Resistance
Rb:	Ribozyme
RdRp:	RNA-dependent RNA polymerase
RFP:	Red fluorescent protein
Rif:	Rifampicin
RNA:	Ribonucleic acid
ROS:	Reactive oxygen species
SAR:	Systemic acquired resistance
SCR:	Small cysteine-rich
SERK3:	Somatic embryogenesis receptor kinase 3
SP:	Signal peptide

T-DNA: Transfer DNA
Taq: *Thermus aquaticus*
Ti: Tumor-inducing
TMV: Tobacco mosaic virus
TPI: Tagged-protein immunoprecipitation
TRBO: TMV RNA-based overexpression
TRV: Tobacco rattle virus
TTSS: Type-III secretion system
u: Unit
Vir: Virulence
YFP: Yellow fluorescent protein

CHAPTER I

INTRODUCTION

1.2 Wheat yellow rust

The first description of wheat yellow (stripe) rust was documented in 1777 (Eriksson and Henning, 1896). Yellow rust, having spread worldwide, is considered as one of the three most threatening and detrimental diseases of cultivated wheat. The rust is recognized by yellow to orange dusty appearance, which is due mass urediniospores on infected wheat leaves. The infection frequently occurs on the lower leaves and the lesions likely to be distributed on whole area of leaves (Chen, 2005; Markell *et al.*, 2000).

The yellow rust on wheat plant is formed by fungal pathogen, *Puccinia striiformis* f. sp. *tritici* (*Pst*). Single *Pst* urediniospore has ability to infect the plant and generate mass number of urediniospores. *Puccinia striiformis* infection is largely influenced by climate factors in comparison to other diseases (Chen, 2005). Temperature is an important aspect for spore germination and infection, spore formation and durability, and host resistance. *Puccinia striiformis* is favored by cool environment (optimum 9-13 °C), which allows it to initiate the disease in the beginning of crop season. As a consequence, the pathogen can result more serious yield loss than its close relatives, preferring warmer climate for optimal growth (Brown and Sharp, 1969; Chen, 2005).

Another imperative factor for the pathogen life cycle is the humidity. Urediniospores need steady moisture on the surface of the plants for germination and infection. Therefore, light rainy days and night dew formations generate the

optimum condition for infection. However, elevated humidity is the reason to make spores more vulnerable than dry climate (Chen, 2005; Rapilly, 1979; Zadoks 1961).

Wind is a main factor for spore dispersal. Urediniospores were observed to spread over broad range in a short time. For instance, stripe rust urediniospores were traveled over 800 km within viable state by wind in Europe. Moreover, in USA, it was recorded that stripe rust spores was gradually driven by wind within distance of 2400 km in six months (Zadoks, 1961). Conversely, it is believed that the spread of viable urediniospore is limited to short distance due to high sensitivity to ultraviolet light (Maddison and Manners, 1972). In addition, wind can result drying of spores, which promotes stability but diminishes the germination and infection on the plant (Chen, 2005). Nevertheless, it spreads with wind flow and generates diseases worldwide.

1.3 Plant immunity

Plants are constantly under attack from various microorganisms such as fungi, bacteria, and viruses. To withstand this incursion, plants developed basal defense system called innate immunity. Unlike vertebrate, being absence of circulatory system and mobile defender cells (B cell immunoglobins and T cell receptors), plant cell has its self-recognition system of invaders and activates its basal defense (Jones and Dangl, 2006; Spoel and Dong, 2012).

In plant, there are two layers of defense strategies occurring against pathogens, namely pathogen-associated molecular pattern (PAMP)-triggered immunity (PTI) and effector-triggered immunity (ETI) (Figure 1.1). Molecules with roles in pathogen-associated molecular patterns (PAMPs) or microorganism-associated molecular patterns (MAMPs) such as lipopolysaccharides, lipoteichoic acid and flagellin from microbes are recognized by pattern recognition receptors (PRRs), which are found on the plant cell plasma membrane. PRRs are grouped in trans-membrane receptor kinases and trans-membrane receptor-like proteins. When these

proteins recognize the PAMPs, the composite defense system so called PTI is activated to fight back the pathogen invasion (Figure 1.1). PTI of plant provides quite powerful responses including shutting of stomatal pores, limiting the nutrients to apoplast from cytosol, secretion of antimicrobial substances, accumulation of reactive oxygen species (ROS) and programmed cell death (PCD), against most microorganisms or non-adapted pathogens (Bigeard *et al.*, 2015; Dodds and Rathjen, 2010; Zipfel and Felix, 2005).

However, plant pathogens, so-called adapted pathogens, conquer the host innate immunity or PTI by deploying clusters of molecules known as effectors into the apoplast, and the cytoplasm of the plant. The effectors modify the host defense mechanism to support pathogen propagation and invasion (Bozkurt *et al.*, 2012; Dodds and Rathjen, 2010; Kamoun 2006). Various types of effectors reported from diverse plant pathogens (Dou and Zhou, 2012; Kamoun, 2006; Zhang and Xu, 2014). Many effectors have direct roles in operating on PTI response. For instance, AvrPto and AvrPtoB, type-III effectors of *P. syringae*, interact and intervene the receptor kinases and, therefore, inhibit PTI in the plant (Shan *et al.*, 2008; Xiang *et al.*, 2008; Zeng *et al.*, 2012). In another example, Avr3a, an effector from *P. infestans*, suppresses infestin 1 (INF1) triggered-PTI. INF1 stimulates ubiquitin E3-ligase CMPG1 that results the programmed cell death in various plants. But, Avr3a binds and inhibits CMPG and thereby disturbing INF1-triggered-PTI (Bos *et al.*, 2010).

Effectors manipulate plant processes and prevent PTI, which support pathogenesis. This changed cellular state gives rise to the effector-triggered susceptibility (ETS). However, sometimes effector can be detected by another layer of detection apparatus and activates immune responses so-called ETI, in plants. ETI triggers stronger immunity in comparison to PTI, resulting in hypersensitive response (HR) or programmed cell death at pathogen infection site. The classical example of ETI recognition system is well explained by immune receptors such as nucleotide-binding leucine-rich repeat (NB-LRR) proteins in the cell (Figure 1.1). These immune receptors are the plant resistance (*R*) gene products that either directly or

indirectly recognize the specific effector molecules (Dodds and Rathjen, 2010; Jones and Dangl, 2006; Win *et al.*, 2012). NB domain of NB-LRR has several distinct motifs that have characteristics of one type of ATPases named ‘signal transduction ATPases’ with numerous domains (Albrecht *et al.*, 2006; Leipe *et al.*, 2004). It is believed that NB domain binds and hydrolyses the ATP, and resultant conformational changes modulate in signal transduction. On the other hand, LRR domain is thought to have roles in protein-protein interaction and ligand binding. Moreover, the LRR regions may determine the specificity of NB-LRR due to *R* proteins being divergent in these domains. It is implied that LRR domain functions to detect the pathogen proteins (Jones and Jones, 1997; Martin *et al.*, 1999; McHale *et al.*, 2006).

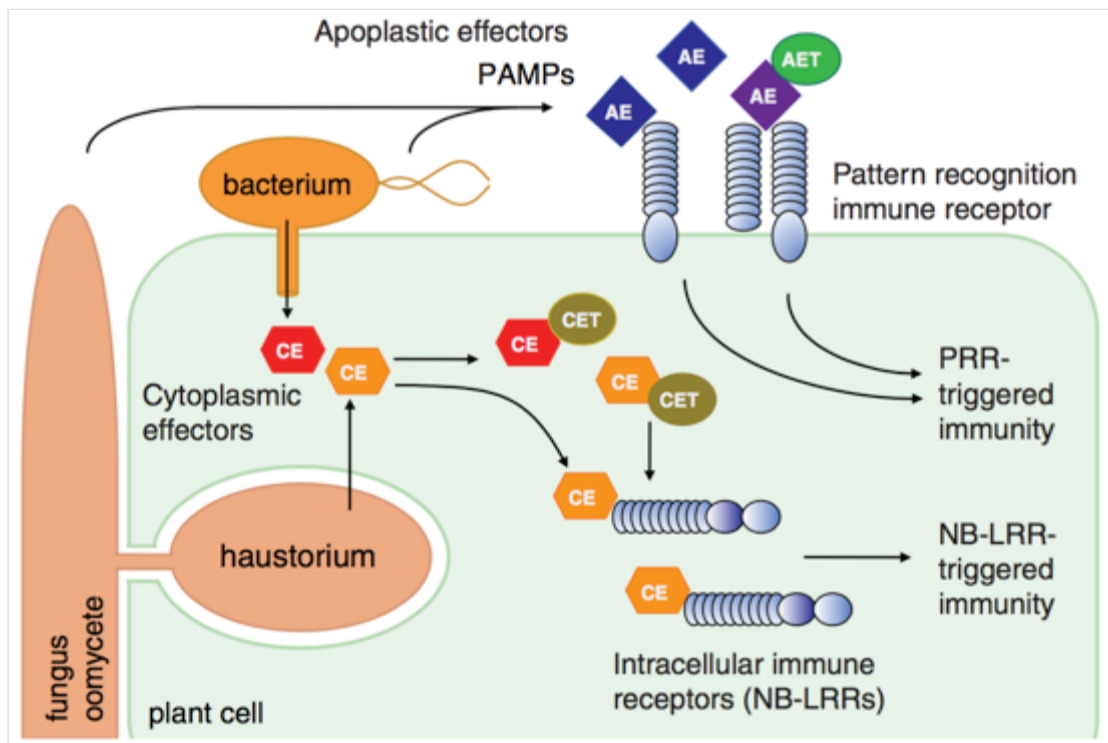


Figure 1.1 The overview of effectors in plant defense. Plasma membrane receptors known as pattern recognition receptors (PRRs) detect and associate with apoplastic effectors (AE) or the pattern associated molecular patterns (PAMPs). Thus, PAMP- or PRR-triggered immunity (PTI) is initiated. Fungus and oomycete pathogens form a construct named haustorium to benefit by depriving nutrients from the plant. Cytoplasmic effectors (CE) from fungus and oomycete might be delivered into the plant cell by haustorium. Conversely, the bacterial effectors are deployed *via* needle like structure known as Type-III secretion system. When they localized into the plant cell, effectors disturb and cease PTI. On the other hand, the plants expressing resistance (*R*) genes produce intracellular NB-LRR receptors, which detect the effectors and trigger effector-triggered immunity (ETI) or NB-LRR-triggered immunity. Apoplastic effector target and cytoplasmic effector target are designated as AET and CET, respectively (Taken directly from Win *et al.*, 2012).

Table 1.1 Fungal effector proteins

Effector	Function/homology	Localization	References
<i>Cladosporium fulvum</i> (tomato)			
Avr2	Protease inhibitor	Apoplast	Dixon <i>et al.</i> (1996)
Avr4	Chitin-binding	Apoplast	Joosten <i>et al.</i> (1994)
Avr4E	Unknown	Apoplast	Westerink <i>et al.</i> (2004)
Avr9	Carboxypeptidase inhibitor	Apoplast	Van Den Ackerveken <i>et al.</i> (1993)
Ecp1	Tumor-necrosis factor receptor	Apoplast	Van Den Ackerveken <i>et al.</i> (1993)
Ecp2	Unknown	Apoplast	Van Den Ackerveken <i>et al.</i> (1993)
Ecp4	Unknown	Apoplast	Lauge <i>et al.</i> (2000)
Ecp5	Unknown	Apoplast	Lauge <i>et al.</i> (2000)
Ecp6	LysM-domains; chitin-binding	Apoplast	Bolton <i>et al.</i> (2008)
Ecp7	Unknown	Apoplast	Bolton <i>et al.</i> (2008)
<i>Leptosphaeria maculans</i> (oilseed rape)			
AvrLm1	Unknown	Probably in cytoplasm	Gout <i>et al.</i> (2006)
AvrLm6	Unknown	Probably in apoplast	Fudal <i>et al.</i> (2005)
AvrLm4-7	Unknown	Probably in apoplast	Parlange <i>et al.</i> (2009)
<i>Fusarium oxysporum</i> f. sp. <i>lycopersici</i> (tomato)			
Avr3 (Six1)	Unknown	Xylem	Rep <i>et al.</i> (2005)
Six2	Unknown	Xylem	Houberman <i>et al.</i> (2007)
Six3	Unknown	Xylem	Houberman <i>et al.</i> (2007)
Avr1 (Six4)	Unknown	Xylem	Houberman <i>et al.</i> (2007)
<i>Magnaporthe oryzae</i> (rice)			
Avr-Pita	Homology to Metallproteases	Cytoplasm	Orbach <i>et al.</i> (2000)
Avr-Pita2	Homology to Metallproteases	Probably in apoplast	Khang <i>et al.</i> (2008)
Avr-Pita3	Homology to Metallproteases	Probably in cytoplasm	Khang <i>et al.</i> (2008)
Pwl1	Glycine-rich hydrophilic protein	Probably in apoplast	Kang <i>et al.</i> (1995)
Pwl2	Glycine-rich hydrophilic protein	Probably in apoplast	Sweigard <i>et al.</i> (1995)
Pwl3	Glycine-rich hydrophilic protein	Probably in apoplast	Kang <i>et al.</i> (1995)

Table 1.1 (Continued)

Effector	Function/homology	Localization	References
Pwl4	Glycine-rich hydrophilic proteins	Probably in apoplast	Kang <i>et al.</i> (1995)
Ace1	Hybrid polyketide synthase/nonribosomal	Not secreted	Böhnert <i>et al.</i> (2004)
Avr1-CO39	Unknown	Unknown	Farman <i>et al.</i> (2002)
<i>Rhynchosporium secalis</i> (barley)			
Nip1	Non-specific toxin/induces necrosis and plasma-membrane H ⁺ ATPase	Probable in apoplast	Rohe <i>et al.</i> (1995)
Nip2	Non-specific toxin/induces necrosis	Probable in apoplast	Rohe <i>et al.</i> (1995)
Nip3	Non-specific toxin/induces necrosis	Probable in apoplast	Rohe <i>et al.</i> (1995)
<i>Melampsora lini</i> (flax)			
AvrI, 567 (A, B and AvrM	Unknown	Cytoplasm	Dodds <i>et al.</i> (2004)
AvrP123	Kazal Ser protease inhibitor	Cytoplasm	Catanzariti <i>et al.</i> (2006)
Avr P4	Cystine knotted peptide	Cytoplasm	Catanzariti <i>et al.</i> (2006)
<i>Blumeria graminis f. sp. hordei</i> (barley)			
Avra10	>30 paralogues in Bgh and other f. sp.	Probably in cytoplasm	Ridout <i>et al.</i> (2006)
AvrK1	>30 paralogues in Bgh and other f. sp.	Probably in cytoplasm	Ridout <i>et al.</i> (2006)

Source: Modified from Stergiopoulos and de Wit, 2009.

1.3.1 BAK1/SERK3 gene in PTI

In *Arabidopsis thaliana*, leucine-rich BRI1-associated receptor kinase 1 (BAK1) was initially found to be interacting with plant hormone brassinosteroid receptor (BRI1) and, therefore, participating in the development of the plant (Li *et al.*, 2002; Nam and Li, 2002). BAK1 is also named as SERK3 since it is one of the family members of somatic embryogenesis receptor kinases (SERK) in *Arabidopsis* (Hecht *et al.*, 2001).

Later, *BAK1/SERK3* was discovered to partake in PTI triggering as positive regulator in innate immune system (Chinchilla *et al.*, 2007; Heese *et al.*, 2007; Shan *et al.*, 2008; Zipfel, 2008). The PAMP molecules are first recognized by PRRs, which leads to heterodimerization with *BAK1/SERK3*, phosphorylation of the complex and resulting PTI pathway activation (Dodds and Rathjen, 2010). In *N. benthamiana*, it was reported that *BAK1/SERK3* is involved in basal immune system so it is a method to investigate PTI pathway in this model plant (Chaparro-Garcia *et al.*, 2011). The *BAK1/SERK3* gene contributes to the plant cell death caused by PAMP molecules such as INF1 and XEG1 (Heese *et al.*, 2007; Ma *et al.*, 2015).

1.4 Apoplast

The external space between outer plasma membranes is known as apoplast in plants. This region is a domestic for various biological processes such as signaling, transport and storage of nutrients, and defense related activities against microbes (Sattelmacher, 2001). Apoplast is the key player of passage and balance of essential molecules including proteins, metabolites and ions in plant. Moreover, it is known that the first cell compartment to respond to the environmental stress, and it is believed to having critical role in plant physiological changes (Hoson, 1998; Sattelmacher, 2001). This region is abundant with hydrolytic enzymes such as glucanases, chitinases and proteases for plant cell defense. Moreover, plant surface receptors like PRRs, which function to detect PAMP molecules, are found on the outer plasma membrane and activate the resistance mechanism of the plant (Tör, 2008).

1.4.1 Apoplastic effectors

In plant, effectors secreted into the space outside of the plant plasma membrane (apoplast) are called apoplastic effectors. The apoplastic region is considered to be important for pathogen attack for several reasons. Apoplast is the first battleground

for invasion of the host cell. To achieve successful infection, the pathogen is projected to deliver effectors into apoplast to avoid the defense proteins, to manipulate the membrane receptors and other extracellular defense molecules of the host plant (de Jonge *et al.*, 2011; Oliva *et al.*, 2010; Rooney *et al.*, 2005; Shabab *et al.*, 2008; Tian *et al.*, 2007;). So far, apoplastic effectors identified are enzymes, enzyme inhibitors, cysteine-rich proteins and toxins (Kamoun, 2006; Ma *et al.*, 2015) (Table 1.1 and 1.2).

Table 1.2 Apoplastic effectors from various pathogens

Apoplastic effectors	Species	Reference
<i>Enzyme inhibitors</i>		
• Glucanase inhibitors GIP1 and GIP2	<i>P. sojae</i>	Rose <i>et al.</i> (2002)
• Serine protease inhibitors EPI1 and	<i>P. infestans</i>	Orsomando <i>et al.</i> (2001), Osman <i>et al.</i> (2001)
• Cysteine protease inhibitors EPIC1 and	<i>P. infestans</i>	M. Tian and S. Kamoun (2005)
<i>Small cysteine-rich</i>		
• INF elicitin	<i>P. infestans</i>	Ricci <i>et al.</i> (1989), Kamoun <i>et al.</i> (1997a)
• INF2A and INF2B elicitins	<i>P. infestans</i>	Kamoun <i>et al.</i> (1997b)
• PcF	<i>P. cactorum</i>	Orsomando <i>et al.</i> 2003
• PcF-like SCR74 and SCR91	<i>P. infestans</i>	Bos <i>et al.</i> (2003), Liu <i>et al.</i> (2005)
• SCR96	<i>P. cactorum</i>	Chen <i>et al.</i> (2015)
• Ppat12, 14, 23, and 24	<i>H. parasitica</i>	Bittner-Eddy <i>et al.</i> (2003)
<i>Nep1-like (NLP) family</i>		
• PaNie	<i>Pythium</i>	Veit <i>et al.</i> (2001)
• NPP1	<i>anhanidermatum</i> <i>P. parasitica</i>	Fellbrich <i>et al.</i> (2002)
• PsojNIP	<i>P. sojae</i>	Qutob <i>et al.</i> (2002)
• GP42 (PEP13) <i>Translutaminase</i>	<i>P. sojae</i>	Nurnberger <i>et al.</i> (1994), Sacks <i>et al.</i> (1995)
• CBEL	<i>P. parasitica</i>	Sejalon-Delmas <i>et al.</i> (1997), Villalba Mateos <i>et al.</i> (1997)
• XEG1 glucoside	<i>P. sojae</i>	Ma <i>et al.</i> (2015)

Source: Modified from Kamoun, 2006.

Some apoplastic effectors can be detected by plant and activate the immune responses (Hematy *et al.*, 2009). The classical examples is INF proteins from *Phytophthora*, which are small cysteine-rich apoplastic effectors such as INF1 inducing cell death, through recognition by cell surface receptors (Kamoun, 2006). Another cysteine-rich effector SCR96 from *Phytophthora cactum*, which was found

to be imperative for pathogen infection and oxidative stress tolerance, provoke cell death in its host plant (Chen *et al.*, 2015). Moreover, XEG1 apoplastic effector with xyloglucanase activity from *Phytophthora sojae* promotes the virulence but also acts as PAMP, independently by its enzyme activity, causing the cell death in plant species including *Solanum lycopersicum*, *Capsicum annuum* and *Glycine max* (Ma *et al.*, 2015). These types of immune response activators are called elicitors. Chaparro-Garcia *et al.* (2011) reported that BAK1/SERK3 receptor-like kinase contributes to the elicitor derived cell death. Silencing of the kinase gene promotes the susceptibility of the plant to the pathogen. Moreover, host-translocated effectors can block the elicitor derived cell death, showing pathogen being adapted to nullify the cell death trigger mechanisms (Bos *et al.*, 2006; Chen *et al.*, 2014; Gilroy *et al.*, 2011; Ma *et al.*, 2015).

1.5 *Pst* candidate effectors

Thanks to advancements in incorporation of genome sequencing, transcriptome, and bioinformatics and gene annotation tools, researchers have been computationally predicting numerous candidate effectors of *Puccinia striiformis* f. sp *tritici* (Cantu *et al.*, 2013; Yin *et al.*, 2009; Zheng *et al.*, 2013). One of the popular examples of *Pst* effectors prediction was illustrated in Cantu *et al.* (2013). In short, they sequenced genomes of *Pst*-21 (US), *Pst*-43 (US), *Pst*-130 (US), *Pst*-87/7 (UK) and *Pst*-08/21 isolates by selecting from different geographic regions. The sequenced genomes were filtered sequentially by proteomic analysis, secretome analysis, clustering of secreted proteins, and followed by the selection of tribes with *Pst* member(s) to determine the candidate effectors of *Pst*. Then the filtered sequences were annotated by comparing with known effector features such as cysteine content, effectors motifs, genome architecture, and similarity to known haustorial proteins and fungal AVR. Afterwards, the sequences were ranked according to the content of effector features. The final identified twenty-two candidates were further analysed by qPCR. Among them, five were marked as highest possible *Pst* effectors (Cantu et

al., 2013). Later in 2016, Petre *et al.* characterized these five candidate effectors (Cantu et al., 2013) among other candidate effectors of *Pst* by expressing them in model plant *N. benthamiana* via Agrobacterium-gene transfer method.

Although there are significant efforts on the identification of pathogen effectors (Djamei *et al.*, 2011; Dou and Zhou, 2012; Fernandez *et al.*, 2012), our knowledge of the molecular machinery underlying pathogen development in the host cell is still largely unknown (Doehlemann and Hemetsberger, 2013; van Esse *et al.*, 2006).

1.5.1 PstSCR1 candidate effector

In 2009, Yin *et al.* generated haustorial cDNA library from *Pst*-78 strain. Selecting by the uniqueness of sequence and the presence of secretion signal, they predicted 15 candidate effector EST sequences of *Pst*-78. Moreover, six of them showed induction during the pathogen infection period (Yin et al., 2009). In this study, we focused on one of these predicted effectors. By our preliminary analysis, two of these six, one of which is the candidate Pstha2a5 (GH737102) (we refer to it as PstSCR1 in the entirely of this thesis), were appeared as a whole cDNA preserving predicted signal peptide (SP) from NCBI database. In addition, the sequence of the predicted protein possess N-terminal FKC amino acid sequences which fits to (Y/F/W)x(C) the conserved motif reported in rust and other wheat pathogen effector candidates (Cantu *et al.*, 2011; Duplessis *et al.*, 2011; Godfrey *et al.*, 2010; Hacquard *et al.*, 2012; Morais do Amaral *et al.*, 2012). Moreover, the level of gene expression by qPCR revealed that the candidate effector expression was almost 120 times more in infected wheat than in urediniospores (Yin *et al.*, 2009). To up to date knowledge, there are no homologies found in the databases of plant genome. From sequence analysis, it was prominent that the N-terminal FxC motif is next to SP and the six-cysteine residues, two of which are adjacent. The small cysteine-rich candidate effector of *Pst* (PstSCR1), with SP, conserved motif, high cysteine content, and small size is convincing for being a candidate effector. According to

gene expression analysis, the PstSCR1 might have role in late stage of infection such as beginning of spore formation during the pathogenesis.

1.6 *Agrobacterium tumefaciens*-mediated gene transfer

In plants, *Agrobacterium tumefaciens* has been the most widespread used tool for gene transfer into plants and thanks to it for being low-cost, straightforward and stable transformation agent (Opabode, 2006; Wydro *et al.*, 2006). *A. tumefaciens* and related species are the gram-negative and soil-borne pathogen of plants. *Agrobacterium* causes tumor in dicotyledonous plants by transferring its infective genes into host chromosome. An infectious *Agrobacterium* strain possesses a tumor inducing (Ti) plasmid, which is the only cause for DNA transfer and tumor development. The plasmid is made up two important portions, which are called virulence (*Vir*) region and transfer-DNA (T-DNA) region. The bacterium can secrete T-DNA and insert it into host chromosome by the involvement of cluster of *Vir* gene products (Pitzschke and Hirt, 2010).

However, the Ti plasmid is oversized and forming tumor in plants and hence it is unsuitable to apply this system in research. Therefore, researchers developed T-DNA binary vector system by improving the original plasmid for commercial applications. The T-DNA and *Vir* region were split into separate replicons (plasmids) (Figure 1.2). The former one is inserted into much smaller plasmid, which makes it more relaxed to introduce into target gene and operate the plasmid *in vitro*. Moreover, by introducing the *E. coli* origin of replication, the plasmid with T-DNA has ability to duplicate in both *E. coli* and *A. tumefaciens*. In addition to this, the tumor inducing parts such as oncogenes and opine synthase genes were discarded from the *Vir* region because they have no significant function in gene transfer but form tumor and tissue damages in host plants. Owing to these valuable modifications, the non-harmful and easy to handle plant gene transfer system was generated (Lee and Gelvin, 2008).

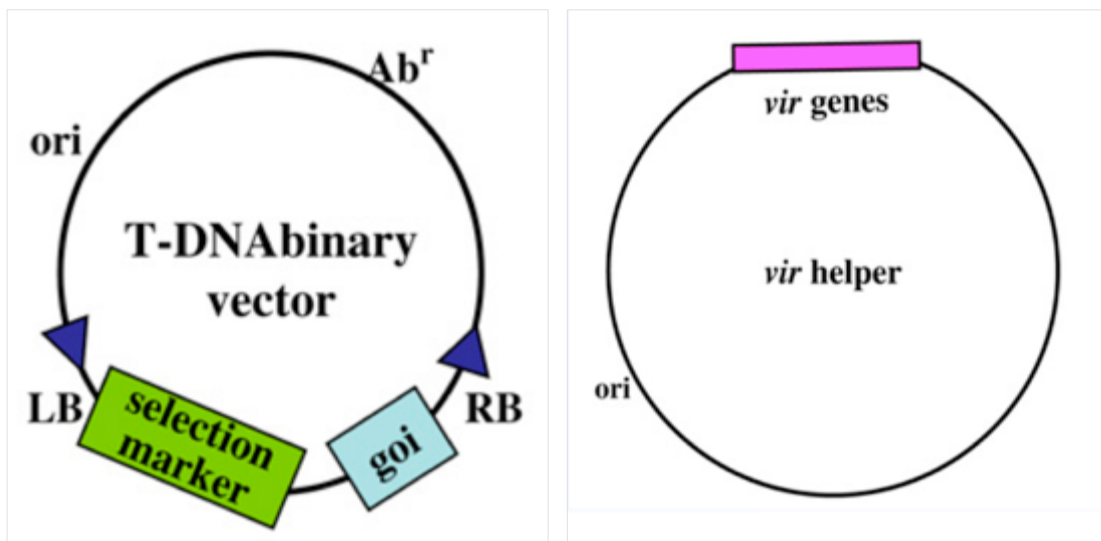


Figure 1.2 T-DNA binary vectors. On T-DNA vector, antibiotic resistance (Ab^r) for both *E. coli* and *Agrobacterium* and origin of replication (ori) for amplification of plasmid are found. The right border (RB) and the left border (LB) are the boundary of T-DNA. Target gene (or ‘goi’) is integrated into the vector. In plant, the ‘selective marker’ is designed to select the putative transformed cells. On *Vir* helper plasmid, *Vir* genes encode proteins that function to insert T-DNA into plant genome (Lee and Gelvin, 2008).

1.6.1 *Tobacco mosaic virus* derived pTRBO vector

Tobacco mosaic virus (TMV), which is one of the most well studied model systems in biology, is a rod-shaped virus containing a single-stranded plus-sense RNA genome. There are many TMV-based vectors such as pJL24, pJL36 and pJL43 for transient expression of gene of interest (GOI) in plants. These vectors have ability to express target protein in high amount in plants. But the delivery system agro-infiltration had not been very effective. The main reason for this outcome was reported as capsid protein (CP) expression from TMV (Marillonnet *et al.*, 2005), which is responsible for systematical movement of virus in plants. In general, this can be solved by increased amount of the *A. tumefaciens* inoculation concentration; however, high exposure of the bacteria can activate hypersensitive response (HR) in

some plants (Wroblewski et al., 2005). Lindbo (2007) developed the TMV-based vector called TMV RNA-based overexpression (TRBO) that lacks CP gene (Figure 1.3). So, as compared to full length TMV, pTRBO provided much more efficient agro-infection and higher amount of target protein expression with low concentration of *A. tumefaciens* inoculation. In addition, CP deletion ceased the virus systematic movement in tissue. The virus with insert has much slower motion than the virus with no insert, so it has tendency to lose the insert during the movement (Toth *et al.*, 2002; Lindbo, 2007). Therefore, pTRBO is more favorable to express the recombinant protein. Moreover, the deletion made in this vector reduced the size that gives advantage in cloning and handling the vector *in vitro*. This improved vector has better agro-infection efficiency, higher level of recombinant protein expressions and is more reliable for purification of the protein than full length TMV (Lindbo, 2007).

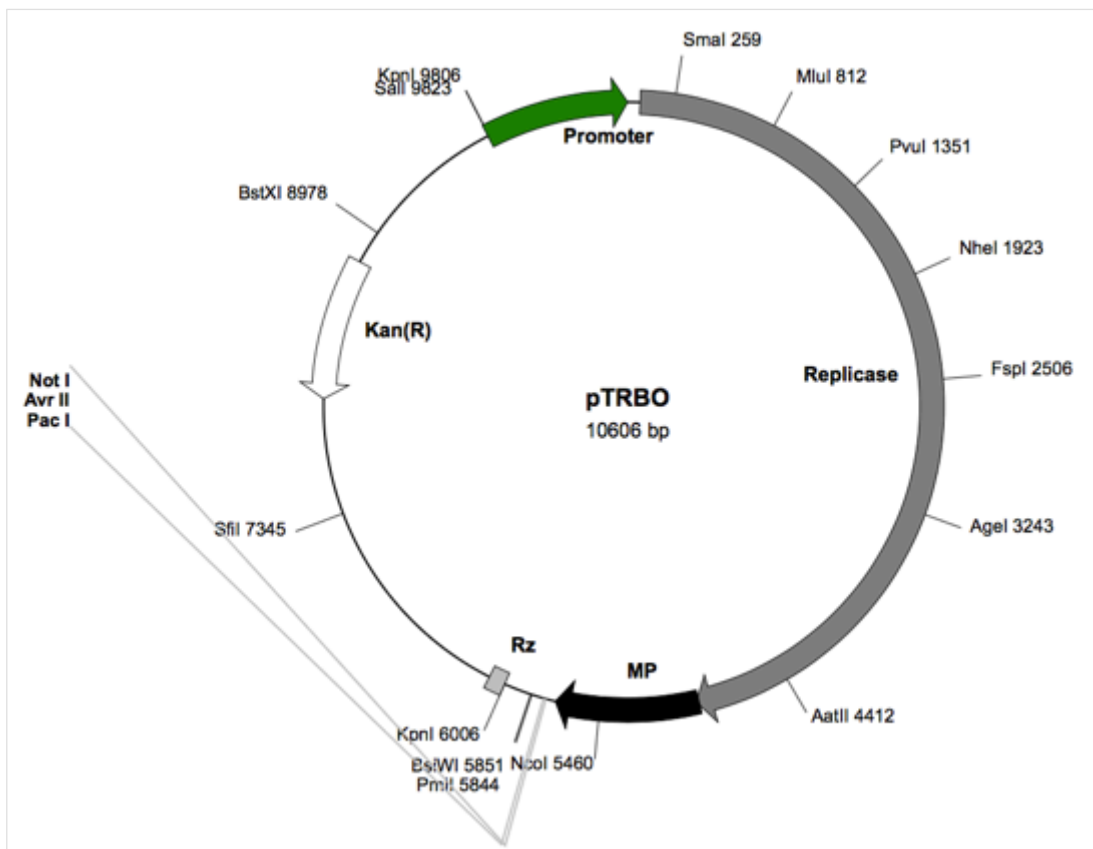


Figure 1.3 pTRBO (or pJL48) vector map. The vector contains replicase and movement protein (MP), ribozyme (Rz), kanamycin resistance (Kan(R)) gene, and CaMV-35S promoter sequence, originated from TMV. The GOI cloning site shown as *PacI* and *NotI*. The vector can operate both in *E. coli* and in *Agrobacterium*. The left and right borders of T-DNA are not indicated (Lindbo, 2007).

1.7 Gateway cloning

In general, to define a function of DNA element, it involves achievement of various practices such as cloning and expression of the gene, protein purification, and subcellular localization. Each procedure requires its gene expression system. Thus, the GOI needs to be inserted into distinct specific vectors for a particular purpose. This become laborious and prolonged task when conventional molecular cloning method is practiced.

Thanks to Gateway® Cloning System, this hurdle solved by the combination of precise and site-specific recombination system of λ phage, and topoisomerase-mediated cloning. In this system, target DNA element is cloned into Gateway® Entry vector (such as pENTR/D-TOPO) possessing specific recognition sites (*attL1* and *attL2*) flanking the insert DNA for following recombination reaction. From entry vector, the DNA element can easily be recombined with multiple destination vectors carrying *attR* recombination sites (Hartley, 2000; Earley *et al.*, 2006) (Figure 1.4).

In short, PCR is used to adding CACC at its 5' and amplification of the DNA. The CACC sequence contributes to insertion of the PCR product into the entry plasmid by topoisomerase, site-specific recombinase (Earley *et al.*, 2006). The topoisomerase cuts and ligates the DNA into entry vector with great accuracy (Shuman, 1994).

From entry plasmid, the gene of interest is recombined into expression vector by LR reaction, which allows recombination between *attL* and *attR* sites (Figure 1.4). For obtaining of the desired vector, the reaction product is transformed into *E. coli*, and the colonies are selected by *ccdb* gene product and antibiotic. Non-recombined destination vector possessing *ccdb* gene, of its product is toxic to the *E. coli* strains, except engineered ones. Thus, the colonies with recombined destination vector meaning with GOI will be persisted. Moreover, selection with the antibiotic excludes colony with entry vector or non-transformed ones (Hartley *et al.*, 2000).

Topoisomerase-mediated capture and Gateway recombination

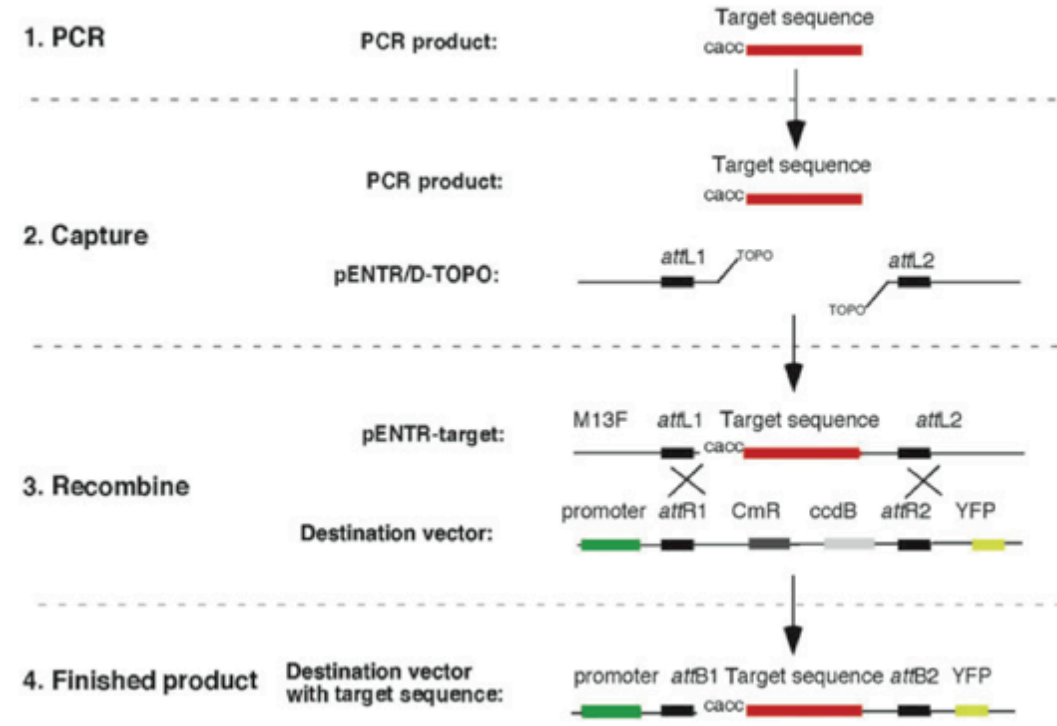


Figure 1.4 Gateway cloning. The GOI is combined CACC at 5' by PCR. This is vital for directional cloning (1). The amplified DNA is integrated into pENTR/D-TOPO by topoisomerase-mediated cloning (2). The Entry vector with GOI recombined with destination vector by LR clonase reaction (3). In non-recombined vector, *ccdB* gene encodes gyrase inhibitor resulting in bacterial cell death. Therefore, the cells containing expression vectors recombined with GOI will be viable (4) (Earley *et al.*, 2006).

1.7.1 Gateway destination vectors

In this study, destination vectors including pK7FWG2 (Karimi *et al.*, 2002) and pGWB445 (Nakagawa *et al.*, 2007) were used to study subcellular localization of the target gene product *in vivo*. Destination vectors are T-DNA plasmids that are used agrobacterium-mediated transformation for gene delivery. Because of Gateway cloning system, cloning of a target DNA in destination vector has become quick and

straightforward. The target gene exchange occurs from entry to destination vector through LR recombination that takes place between *attL* and *attR* sites (Karimi *et al.*, 2002).

These vectors are commonly practiced in a protein subcellular localization because of its fluorescent tag fusion to the target protein (Karimi *et al.*, 2002; Nakagawa *et al.*, 2007). Both of the vectors have spectinomycin (Sm) resistance for selection in *E. coli* and in *Agrobacterium*, and kanamycin (Kan) resistance for selection in plants. The *ccdB* gene is flanked between *attR* sites. Thus, desired transformants are negatively selected for colonies possessing the vector with GOI. The pK7FWG2 (Figure 1.5) and pGWB445 vectors introduce eGFP and mRFP fusion, respectively, at the C-terminal of the target protein.

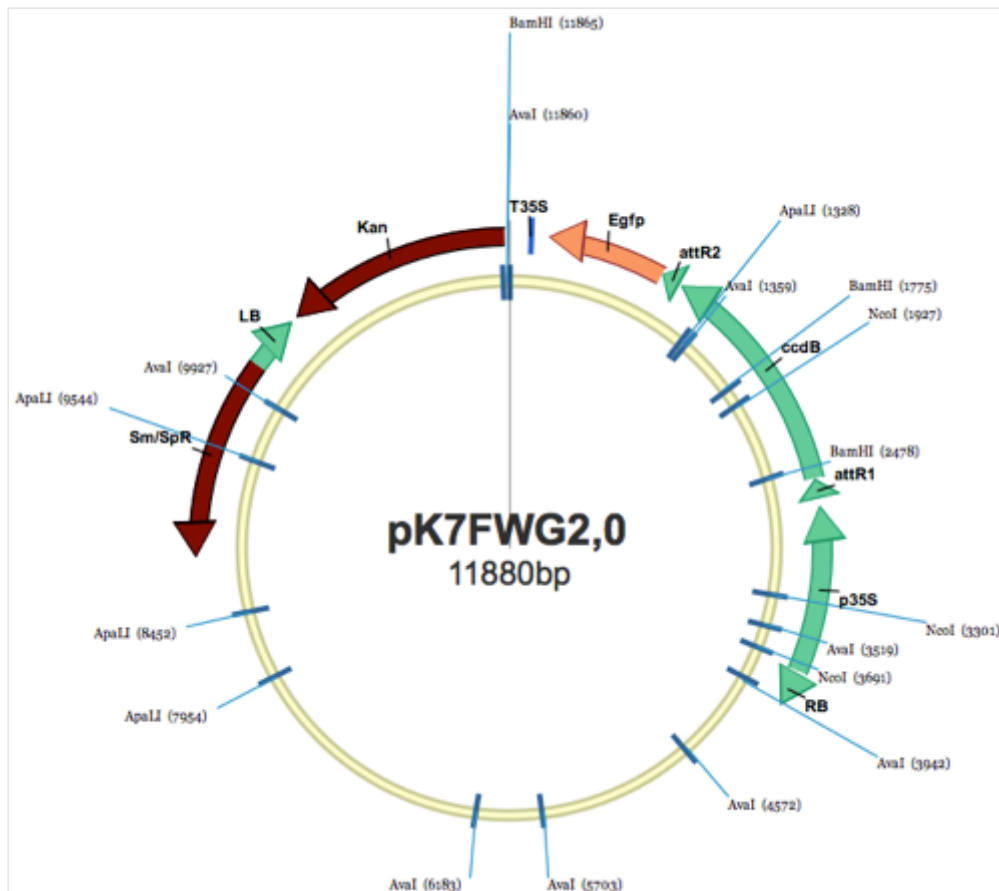


Figure 1.5 Destination vector pK7FWG2 map (Karimi *et al.*, 2002).

1.8 Subcellular localization

Accumulation of pathogen effector in specific cell compartment(s) possesses particular significance for its proper functioning (Dowen *et al.*, 2009) and it might imply the mode of action of the effector in modifying the host immunity (Bozkurt *et al.*, 2014). To detect the subcellular localization of a particular pathogen protein with fluorescence tag (i.e. GFP) might be the one of the methods. However, in obligate biotroph plant pathogens, it has been known that stable gene transformation of the pathogens is troublesome (Caillaud *et al.*, 2012). Moreover, transformed effector's fluorescence is not readily perceptible due its dilute form in cytoplasm of the plant cell (Whisson *et al.*, 2007, Boevink *et al.*, 2011; Bozkurt *et al.*, 2012). Therefore, to visualize subcellular localization, effectors fused with the fluorescent protein such as GFP, RFP and YFP are practiced for expression, especially through Agrobacterium-mediated gene expression system in *planta* (Rafiqi *et al.*, 2010; Bozkurt *et al.*, 2014). Fluorescent-tagged protein is fast and amenable approach to identify the pathogen candidate effectors. But it cannot be ignored that the chance of any side-effect or interference by the fluorescence tag could affect effector function. In subcellular localization experiment, naked GFP has its own localization, nucleo-cytoplasmic, in the model plant *N. benthamiana*, as well as many host-translocated effectors show same localization signals (Win *et al.*, 2012). So, the localization of these effectors might be considered as non-informative since they imitate the experimental control (Petre *et al.*, 2015).

The plant proteins can be used in subcellular localization experiment as markers. For instance, the plasma membrane targeting plant protein Remorin (Raffaele *et al.*, 2009), which was successfully used as a marker when confirming the AVR2 effector localization on the plasma membrane (Saunders *et al.*, 2012). In addition to this, REM1.3 from *Solanum tuberosum* localizes around haustoria when expressed in *N. benthamiana* infected by *P. infestans* (Bozkurt *et al.*, 2014), which makes it a potential *P. infestans* haustorial marker. Another example is secreted plant defense protease C14, which is accumulated in apoplast and vacuole of the plant. The C14

was found to be expressed during the biotic stress for defense (Kaschani *et al.*, 2010). The C14 can be used as an apoplastic marker in subcellular localization experiments.

1.9 Gene silencing

Tobacco rattle virus (TRV) based system is broadly used in virus induced gene silencing (VIGS) (Velasquez *et al.*, 2009). The TRV vectors (Figure 1.6), each T-DNA vector and replicate in different *Agrobacterium*, are used in gene silencing. One, functioning in virus movement and replication is pTRV1 and other carrying the coat protein and the target gene is pTRV2 (Liu *et al.*, 2002; MacFarlane, 1999). Co-infiltration of both agrobacterium strains causes the target gene silencing in inoculated plants such as *N. benthamiana* and *Solanum lycopersicum* (Velasquez *et al.*, 2009).

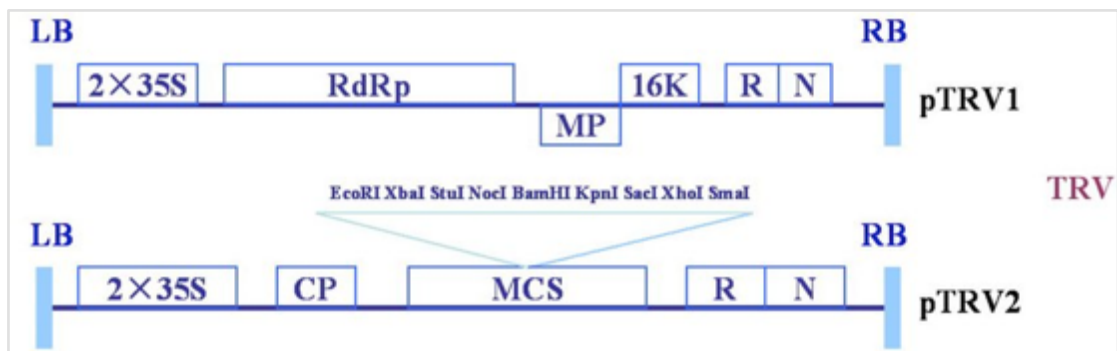


Figure 1.6 *Tobacco Rattle Virus* (TRV) vectors schematic view. T-DNA borders are left border (LB) and right border (RB). Double CaMV 35S promoters (2X35S), RNA-dependent RNA polymerase (RdRp), movement protein (MP), 16 kDa cysteine-rich protein (16K), coat protein (CP), multiple cloning sites (MCS), self-cleaving ribozyme, and nopaline synthase terminator (N) are illustrated in the drawing.

1.10 Immunoprecipitation

Immunoprecipitation (IP) allows purifying a protein or protein complexes from protein mixture by antibody-antigen affinity purification methods. In protein study, the approach has advantage to concentrate a protein that is not feasible to study in cellular concentration due to its minute amount. During IP, interacting complexes such as protein, DNA, and RNA can be immunoprecipitated together, which is important for determining the possible interactions. Simply, a total protein extract or mixture with the target protein is incubated in a solution with specific antibody immobilized to beads. Then, the protein of interest will be specifically recognized and bound to the antibodies. The beads can be pelleted so the antibody with target protein can be collected by centrifugation. Finally, the protein of interest (POI) can be eluted with buffer containing dissociating molecules, competing with the POI (antigen) for immobilized antibody (Hall, 2004).

One factor determining the successful IP is specificity and quality of antibody against the protein of interest. In each target protein, specific and high quality antibody must be produced, which is often challenging and troublesome procedure. This is one limitation in the method. For this reason, the target protein is fused to commercial peptide tag to be purified by IP. This method has several advantages over classic IP including reduced contamination in background, cost-effective, simple, specific and effective in comparison to normal IP method. In addition, it is not necessary to modify the experiment for different protein isolates. However, the selection of the tag and the position where it is fused in the target protein might affect the protein structure and function. The commercially used tags are FLAG, His, Strep, GST, and HA. (Rigaut *et al.*, 1999; Seraphin and Puig, 2002).

1.11 Objective of the research

Cereal grains including corn, rice, wheat, and barley are the basic food source for human consumption. But abiotic (environmental) and biotic (pathogens and pests) stresses result in massive yield damage of these crops on earth. Starting from the beginning of the 20th century, the chemicals controlling the diseases on these crops were heavily used in agronomy, which has been the active solution against biotic stress. However, often these substances are toxic to the ecosystem. Furthermore, cost of manufacture and storage space is made the application overpriced. On the other hand, one promising answer might be producing genetically improved crops. To do this, initial and crucial step is to understand the infection and the development of the pathogen at a level that allows generating best possible strategies for crop protection.

A number of candidate effectors of *Puccinica striiformis* f. sp. *tritici* (*Pst*) are predicted as secreted to the host cell. One of which is a small cysteine-rich effector of *Pst* (*PstSCR1*) identified as EST was chosen to study. The objective of the thesis is to characterize the function of *PstSCR1* effector in plant cell.

The knowledge on the functions, cellular localizations, structures and the other factors or interacting proteins of candidate effectors of *Puccinica striiformis* f. sp. *tritici* (*Pst*) are very limited. This is due to insufficient capability of functional genetic methodologies for crop species (Petre *et al.*, 2014; Upadhyaya *et al.*, 2014). As a substitute to the limitations, *N. benthamiana* has been one of the best plant model organisms to study molecular plant-microbe interactions (Bombarely *et al.*, 2012). Recently, Petre *et al.* (2016) have reported that *N. benthamiana* is a practicable experimental tool to functionally examine candidate effectors from *Pst*. In this study, *PstSCR1* effector was studied on model plant, *N. benthamiana*.

To investigate the subcellular localization of the protein, *PstSCR1* (with or without SP) was cloned into pK7FWG2 and pGWB445 subcellular localization vector,

which generate the protein product fused with C-terminal RFP and GFP, respectively. As a control, naked GFP was expressed. The proteins were expressed in *N. benthamiana* plants, which were recorded under microscope afterwards. Then, to observe the effect of PstSCR1 during the infection, we inoculated the plants expressing the effector constructs with two pathogens namely *Phytophthora infestans* and *Peronospora tabacina*.

Secondly, to purify the PstSCR1, the gene was fused FLAG tag and cloned into pTRBO overexpression vector; then expressed in *planta*. This construct was also used to reveal the phenotype changes in the plant when effector is overexpressed. The overexpressed tagged-effector was conducted with immunoprecipitation. The purified effector molecules were injected in *N. benthamiana* leaves to confirm whether the phenotype change on plant is dependent solely on the effector or not.

Thirdly, we suspected that PstSCR1 might be involved in innate immunity of the non-host plant. To test this hypothesis, the *BAK1/SERK3* gene, key regulator in PTI, was silenced in *N. benthamiana*. Then, the apoplastic fluid with PstSCR1, which was isolated from *N. benthamiana* expressing PstSCR1 with SP, was infiltrated into silenced plants. The GFP with SP expressed plants were used as control. The phenotypes were observed after 3dpi. We also purified the SCR1 from apoplast of *N. benthamiana* expressing the effector. Then, purified SCR1 was infiltrated into *N. benthamiana* leaves and defense gene expression level was recorded after 2- and 4-dpi.

CHAPTER II

EXPERIMENTAL PROCEDURES

2.1 Plants and pathogen materials

2.1.1 Plants used in the study

Tobacco plants, *Nicotiana benthamiana* were grown, sub-cultured and maintained in plant growth room with 16h-light/8h-dark cycle at 22-25 °C. For agro-infiltration, 4-6 week old plant middle leaves were used in the experiment. Wheat line Avocet-S was grown and incubated in growth chamber with conditions: 16h-light and 8h-dark at 18° C and 15 °C, respectively. After 15-day post seed plantation, plants were used for infection with *Pst*.

2.1.2 Pathogen

Puccinia striiformis f. sp. *tritici* *Pst*-78 strain was obtained from Dr. Xianming Chen, Washington State University, USA. Wheat strain Avoset-S (susceptible) was used for maintenance of the *Pst*-78. Approximately 50 seeds were planted in a pot (volume of 700 cm³) with soil and placed in plant growth chamber with regular conditions: 16-h/light at 22 °C, 8-h/dark at 18 °C and 60% humidity. The plants were grown until two-leaf stage, which normally takes 10-15 days. Then, the plants were inoculated with *Pst*-78 spores. The spores were taken from -80 °C and incubated at 42 °C for 10 minutes for germination activation. Avocet-S plant leaves were infected with *Pst*-78 spores with mineral oil spraying by the compressed air (Figure 2.1). Afterwards, for germination, the infected plants were incubated at 10 °C with high humidity in dark for overnight. The next morning growth chamber was set to the

regular working condition. Finally, 24-hour, 72-hour, 8-day and 10-day post inoculated leaves were harvested, instantly frozen in liquid N₂, and kept in -80 °C freezer until the total RNA isolations.



Figure 2.1 Inoculation of wheat with yellow rust *Pst-78* spores.

2.2 Isolation of total RNA

2.2.1 Preparation steps prior to isolation

Mortars, grinders, spatulas and microfuge tubes were incubated in 0.1 % diethylpyrocarbonate for overnight and followed by autoclave sterilization. Afterwards utensils were kept in 80 °C over at least a day prior to use. All pipette tips were RNase free and with filtering (Thermo Scientific) during the RNA isolation. Working bench was wiped with ethanol and, then, RNase inhibitor spray. Gloves were worn all time when handing the RNA samples and changed several times with new ones in order to minimize possible contamination.

2.2.2 Total RNA purification from plant tissue

For RNA isolation, Qiagen RNeasy Mini Kit was used and the manufactures instructions were followed. Plant samples were collected and immediately frozen in liquid N₂ and stored in -80 °C until purification step. The plant tissue was crushed into powder in liquid N₂ by mortar and pestle. The powder was transferred into fresh 2 mL microfuge and kept in liquid N₂. Upto 100 mg plant material was measured by weighing and added 450 µL RLT buffer with β-Mercaptoethanol to lysate the plant cells. The tube was vortexed vigorously. After that the lysate was transferred into a QIAshredder spin column with collection tube and centrifuged for 2 min at maximum speed. From the collection tube, supernatant was transferred to a fresh microfuge without touching the pellet in flow-through. The collected supernatant was added 500 µL ethanol (99.5%) and mixed by pipetting. The solution was transferred to an RNeasy spin column placed in a collection tube and centrifuged for 15 seconds at 13,000 rpm. The flow-through was removed from collection tube and 700 µL RW1 buffer was added into the RNeasy spin column followed by centrifugation for 15 seconds at 13,000 rpm. Then, the membrane was washed twice by adding 500 µL RPE buffer followed by centrifugation, first 15 seconds and final 2 minutes at 13,000 rpm. Lastly, the RNeasy spin column is placed in a new Microfuge tube and 30-50 µL RNase-free water to the middle of the membrane column. The centrifugation was 1 minute at 13,000 rpm. The collected RNA sample was kept on ice for further use or stored at -80 °C in deep freezer.

2.2.3 RNA sample integrity check

The concentration of isolated RNA samples were measured by NanoDrop. Then, all the samples were adjusted to same amount of total RNA (100-200ng/µL) and separated on 1% agarose gel with ethidium bromide at 70 volts for RNA quality test. Tris-acetate EDTA buffer was used in agarose gel preparation and as a running buffer.

2.3 First strand cDNA synthesis

2.3.1 Genomic DNA removal

Before cDNA synthesis from total RNA samples, genomic DNA contamination was removed by treating the sample with DNase I (#EN0521, Fermentas). The reaction contents were summarized in Table 2.1. The contents were mixed by pipetting and was incubated at 37 °C for half an hour. The reaction was stopped by incubating at 65 °C with addition of 1 µL 50mM EDTA to prevent RNA hydrolysis in elevated temperatures.

Table 2.1 Genomic DNA elimination from RNA sample

In an RNase free tube	Amount
Total RNA	1 µg
10X Reaction Buffer	1 µL
DNase I (#EN0521, Fermentas)	1 unit
H ₂ O, nuclease free	variable
Total	10 µL

2.3.2 cDNA synthesis

For cDNA synthesis, Transcriptor First Strand cDNA Synthesis Kit (Cat# 04379012001, Roche) was used and manufacture's protocol was followed with minor changes. The components and amounts of the mixture for cDNA synthesis are illustrated in Table 2.2. The solution was mixed carefully. The mixture was incubated at 25 °C for 10 minutes followed by at 55 °C for 30 minutes. To deactivate the reaction, the solution was heated to 85 °C for 5 minutes and transferred onto ice. The cDNA was directly used for qPCR or kept in -20 °C for further usage.

Table 2.2 cDNA synthesis mix

In a RNase free tube	Amount
Total RNA	1 µg
Anchored-oligo(dT) ₁₈ primer (1.25 µM final)	0.5 µL
Random hexamer primer (30 µM)	1 µL
H ₂ O, PCR-grade	up to 13
Transcriptor Reverse Transcriptase Reaction Buffer (5X)	4 µL
Protector RNase Inhibitor (40 u/µL)	0.5 µL
Deoxynucleotide Mix (10mM each)	2 µL
Reverse Transcriptase (20 u/µL) (Cat# 04379012001,	0.5 µL
Total	20 µL

2.4 qPCR

The gene expression level analysis was conducted in a Stratagene® Mx3005P™ thermocycler instrument using AccuPower GreenStar™ qPCR Premix (Cat#: K-6212, BIONEER). qPCR with each cDNA and primer combination was conducted as three replicates in all the amplifications. To normalize the amounts of RNA samples, endogenous control Elongation factor 1 alpha (EF1 α) was used as constitutively expressed gene (Liu *et al.*, 2012; Ma *et al.*, 2015). The AccuPower GreenStar™ qPCR Premix tubes were transferred from -20 °C to Room Temperature (RT) and kept in RT for at least 5 minutes. Then, the tubes were spun; the cover was removed carefully and placed on ice. Appropriate amount of cDNA (e.g. diluted 1:20) and 10 pmol primers of both forward and reverse directions were mixed in dH₂O with total volume of 20 µL for each qPCR premix tube. The replicates prepared as master mix and divided into corresponding tubes. For the endogenous control of *N. benthamiana* (EF1 α), EF1 α -qRT-F and EF1 α -qRT-R were used as forward and reverse primers, respectively (Liu *et al.*, 2012; Ma *et al.*, 2015; Segonzac *et al.*, 2011). To quantitative analysis of *BAK1/SERK3*, *NbCYP71D20* and *NbACRE31*, combinations of NbSerk3-qRT-F and NbSerk3-qRT-R, NbCYP71D20-F and NbCYP71D20-R, and NbACRE31-F and NbACRE31-R primers were used, respectively (Ma *et al.*, 2015; Segonzac *et al.*, 2011). The primer sequences used in qPCR amplifications are illustrated in Table 2.3.

Table 2.3 The primers used in qPCR amplifications

Names	5'-3' sequence	Length
PstSCR1-TM-5-	gacctcttgactaaggcagctcatg	25
PstSCR1-SP-5-	tatttgtttagaattacacaagatg	25
PstSCR1-Rev	ctaagatgcttggagcagttgttgc	27
PstEF1 α -F	ttcgccgtccgtgatatgagacaa	24
PstEF1 α -R	atgcgttatcatgggtggagtgaa	24
Actin-1-F	aatggtaaggctgggttcgc	21
Actin-1-R	ctgcgcctcatcaccaacata	21
NbEF1 α -F	ctacctaagaagggtggatac	22
NbEF1 α -R	aacatcctgaagtggaaagac	20
NbSerk3-F	gcttcctgaggctgaataata	21
NbSerk3-R	gaagaagaagatgagggtgtag	22
NbCYP71D20-F	accgcaccatgtcccttagag	20
NbCYP71D20-R	cttggcccttgagttacttgc	20
NbACRE31-F	cgtcttcgtcgatcttcg	19
NbACRE31-R	ggccatcgtgatctggtc	19

2.5 Calculation of $\Delta\Delta Ct$ and fold change of treated sample

There are two most commonly practiced methods, absolute and relative quantifications for qPCR data analysis. In here, we used relative quantification to analyze the qPCR data, where the PCR signal of a gene of interest in a treated sample compared to that of untreated control group (Livak and Schmittgen, 2001) (Figure 2.2). To determine the difference between treated and untreated samples, the $\Delta\Delta Ct$ value should be calculated to find the target gene expression fold change, which equals to $2^{-\Delta\Delta Ct}$. The Ct is the number of cycles where the fluorescence produced in a reaction passes the threshold or baseline.

$$1) \Delta Ct = Ct_{\text{target}} - Ct_{\text{reference}}$$

$$2) \Delta\Delta Ct = \Delta Ct_{\text{test sample}} - \Delta Ct_{\text{reference sample}}$$

$$\text{Standard deviation of } \Delta Ct \text{ value: } s = (s^2_{\text{target}} + s^2_{\text{reference}})^{1/2}$$

Figure 2.2 $\Delta\Delta Ct$ calculation.

To obtain accurate and legitimate results of qPCR, the target gene value from qPCR is normalized using chosen reference gene (Figure 2.2). The reference genes must have stable expression level under variable conditions. The housekeeping or endogenous control genes are used as reference in normalization of qPCR values. The well-known reference genes are elongation factor (EF), actin, ubiquitin and ribosomal RNA subunits genes (Abbal *et al.*, 2008; Lund *et al.*, 2008; Olsen *et al.*, 2010; Wang *et al.*, 2010; Xue *et al.*, 2010). Generally, the reference genes should be validated in each experiment since their expression level might differ in altered conditions (Gamm *et al.*, 2011). However, in this study, we chose previously validated housekeeping genes in same experiment conditions. *NbEF1 α* was used to normalize the amount of mRNA level of *NbBAK1/SERK3* (Liu *et al.*, 2012; Ma *et al.*, 2015), *NbCYP71D20* and *NbACRE31* (Segonzac *et al.*, 2011) genes in *N. benthamiana* plants.

2.6 The PstSCR1 sequence analysis

The EST sequence of the candidate effector, PstSCR1, was attained from NCBI (accession no: GH737102). The open reading frame of the EST was detected by ORF-Finder (NCBI). The signal peptide (SP) of PstSCR1 was predicted by SignalP 4.1 web tool (Petersen *et al.*, 2011). The amino acid sequence was analyzed *via* blastp at the NCBI to detect the closely related sequences. The promoter predictions

were carried out on 348811-345691 bp regions of the supercontig using Neural Network Promoter Prediction (version 2.2) in the Berkeley Drosophila Genome Project (BDGP; http://www.fruitfly.org/seq_tools/promoter.html) (Reese and Eeckman, 1995; last update 2015) which had been applied to predict other promoters (Filichkin *et al.*, 2004; Wang *et al.*, 2007; Witte *et al.*, 2005; Zhao *et al.*, 2010). Recognition of Regulatory Motifs with Statistics in the Softberry software (<http://www.softberry.ru/berry.phtml>, subgroups as CpG Finder and FPROM) (Solovyev *et al.*, 2010) were used to detect Promoter upstream GC islands and TATA box.

2.7 PstSCR1 gene constructs

The primers designed and in the experiments are presented in Table 2.4. The plasmids pTRV1, pTRBO, pTRBO/GFP and pTRBO/FLAG-RFP were obtained from Dr. S. Kamoun, The Sainsbury laboratory, Norwich, UK. The vector constructs 35S-RFP:C14 (pGWB554/C14), and 35S-YFP:REM1.3 (pK7WFY2/REM1.3) were the same as in Bozkurt *et al.*, 2011; Raffaele *et al.*, 2009 (Bozkurt *et al.*, 2014). The PstSCR1 gene had made synthesized inclusive with SP and extension of *PacI* and *NotI* restriction sites corresponding to 5' and 3' ends, respectively, and retrieved as pBSK/PstSCR1 (GeneScript). For subcellular localization experiments, the gene, PstSCR1, was amplified from pBSK/PstSCR1 using CACC-SP or CACC-ATG-SCR1 (with no SP) as forward primer and SCR1-noSTP as reverse primer and inserted into pENTR/D-TOPO plasmid (Invitrogen), then it was recombined in two destination vectors; pK7FWG2 (Karimi *et al.*, 2002) and pGWB454 (Nakagawa *et al.*, 2007) via LR clonase reaction (Invitrogen). For overexpression of the effector with and without SP, and FLAG-Tag (on the C-terminus) was constructed by PCR using forward primers, *PacI*-SP-SCR1-F or *PacI*-noSP-SCR1-F and reverse primers, SCR1-C-FLAG-R2 and SCR1-C-FLAG-R1. The final PCR product was obtained with *PacI* restriction site on the 5'-end and FLAG-Tag and *NotI* restriction site on the 3'-end. The PCR product was cloned into pTRBO (pJL48) vector (Lindbo *et al.*,

2007) and labeled as pTRBO/SP-SCR1-FLAG. To express secreted GFP (SP-GFP), SP was amplified using CACC-SP, SP-noSTP primers on pBSK-PstSCR1 as a template; then, cloned into pENTR/D-TOPO, and followed by LR recombination (Invitrogen) into pK7FWG2 (Karimi *et al.*, 2002); labeled as pK7FWG2/SP-GFP. For cloning of SP-GFP-FLAG; SP-GFP was first amplified with PacI-SP-SCR1-F and GFP-FLAG-Rev primers using pK7FWG2/SP-GFP as a template. SP-GFP-FLAG was generated using the amplified product as a template with the primers PacI-SP-SCR1-F forward and SCR1-C-FLAG-R1 as reverse primers. The SP-GFP-FLAG was cloned into pTRBO (pJL48) (Lindbo *et al.*, 2007) and denoted as pTRBO/SP-GFP-FLAG. For cloning and amplification of the plasmids, the constructs were maintained in *E. coli* Top10 strain. For Agro-infiltration experiments, constructs were introduced into *Agrobacterium tumefaciens* GV3101 strain by electroporation (Win *et al.*, 2011).

Table 2.4 The primers used in the cloning of gene constructs

2.8 PCR amplifications

The PCR components and volumes in reactions are presented in the Table 2.5 and 2.7. A template DNA was amplified by one of two DNA polymerases: *Taq* DNA Polymerase (M0320, NEB) in standard usage, and Q5 DNA Polymerase (M0478G, NEB) in molecular cloning. For all PCR: master mixes were prepared to ensure reproducibility.

Table 2.5 Components and their amounts used in PCR for *Taq* DNA polymerase.

In 0.2 mL microfuge tube	Amount
Template DNA	variable
10X PCR buffer	2.5 µL
dNTPs (10mM)	0.5 µL
Forward primer (10 pmol/µL)	0.5 µL
Reverse primer (10 pmol/µL)	0.5 µL
<i>Taq</i> DNA polymerase (5 unit/µL) (M0320, ddH ₂ O	0.125 variable
Total	25 µL

Thermo-cycling conditions for *Taq* DNA polymerase are the followings: initial denaturation 95 °C for 30 sec, 35 cycles: denaturation at 95 °C for 15-30 sec, annealing at 50-58 °C (Table 2.6) for 15-60 sec and extension at 68 °C for 1 min/kb, and final extension at 68 °C for 5 min.

Table 2.6 Annealing temperatures applied for *Taq* DNA polymerase amplifications

Names	Ta (°C)
PstSCR1-SP-5-	54
PstSCR1-TM-5-	55
PstSCR1-Rev	55
PstEF1α-F	55
PstEF1α-R	55
Actin-1-F	55
Actin-1-R	55
NbEF1α-F	55
NbEF1α-R	55
NbSerk3-F	55
NbSerk3-R	55
NbCYP71D20-F	52
NbCYP71D20-R	52
NbACRE31-F	52
NbACRE31-R	52

Table 2.7 Components and their amounts used in PCR for Q5 DNA polymerase.

In 0.2 mL Microfuge	Amount
Template DNA	50 pg-
5X Q5 Reaction buffer	5 μL
dNTPs (10mM)	0.5 μL
Forward primer (10 pmol/μL)	1.25 μL
Reverse primer (10 pmol/μL)	1.25 μL
Q5 DNA polymerase (2 unit/μL),	0.25 μL
5X Q5 High GC Enhancer	5 μL
ddH ₂ O	Variable
Total volume	25 μL

Thermo-cycling conditions for Q5 DNA polymerase: initial denaturation 98 °C for 30 sec, 35 cycles: denaturation at 98 °C for 5-10 sec, annealing at 50-58 °C (Table 2.8) for 10-20 sec and extension at 72 °C for 20-30 sec/kb, and final extension at 72 °C for 2 min. The amplification products were sent for sequencing as purified PCR products.

Table 2.8 Annealing temperatures applied for *Q5* DNA polymerase amplifications

Names	T _a (°C)
CACC-	67
CACC-SCR1SP	67
SCR1-noSTP	67
PacI-SP-SCR1-	67
PacI-noSP-	67
SCR1-C-Flag-	67
SCR1-C-Flag-	67
TRBO seqF	65
TRBO seqR	65
PstSCR1-NotI-	67
SCR1SP-noSTP	60
GFP-FLAG-R	67
GFP-STP-NotI	67

The amplified DNA was run on the agarose (1%) gel for imaging, and the purification or band isolation of PCR products was carried out for further usage.

2.9 Cloning of a gene construct in pTRBO vector

2.9.1 pTRBO plasmid and insert DNA digestion

An insert DNA digestion and pTRBO vector linearization to generate sticky ends with *NotI* HF (NEB) and *PacI* (NEB) restriction endonucleases (REs) was performed. The digestion components were mixed as in Table 2.9.

Table 2.9 Contents and amounts for rerestriction enzyme digestions

In 0.2 mL Microfuge	Amount
Vector or insert DNA	500ng-
<i>PacI</i> (10,000unit/mL, #R0547S, NEB)	0.5µL
<i>NotI</i> HF (20,000unit/mL, #R3189S, NEB)	0.25µL
Cut Smart™ Buffer (10x, #B7204S, NEB)	1.5µL
ddH ₂ O	variable
Total	15 µL

Digestion tube was kept for overnight at 37 °C. Digestion products were electrophoresed on agarose (1%) gel for size confirmation and/or gel extraction.

2.9.2 DNA purification

QIAprep® Spin Miniprep Kit (Qiagen), QIAquick® PCR purification Kit (Qiagen), and QIAquick® Gel Extraction Kit (Qiagen) were used in plasmid purification, PCR purification, and DNA isolation from an agarose gel, respectively. Manufacturer's protocols were applied for purification procedures.

2.9.3 Ligation reaction

After extraction of DNA, reaction of ligation was carried out by mixture of the contents in Table 2.10.

Table 2.10 Components of ligation reactions

In 0.2 mL Microfuge	Amount
10X T4 ligase buffer	2 µL
Vector	'x' mol
Insert DNA	'5x' mol
T4 ligase (400u/µL, #M0202,	1 µL
ddH ₂ O	variable
Total	20 µL

The mixture was incubated at room temperature for 10 min. For transformation, 1-5 μ L of ligation product was used.

2.10 Gateway cloning

First, the gene of interest (GOI) was cloned in gateway entry vector (pENTRTM/D-TOPO) via topoisomerase-mediated cloning. Then, it was transferred from entry vector to a destination vector, which allows expression the construct in host organism, by LR recombination reaction.

2.10.1 pENTR/D-TOPO cloning

The CACC nucleotide was added to the 5' end of the gene construct by PCR. Invitrogen pENTRTM Directional TOPO^R cloning kit and its instructions were applied in cloning. Combination of 0.5 μ L fresh amplified DNA by PCR, 1 μ L salt solution provided by kit, 1 μ L pENTR/D-TOPO vector and nuclease free H₂O filled upto 6 μ L were in 0.2 mL tube. The reaction mixture was rested for 30 minutes at 25 °C. Then, reaction products were transformed into *E.coli Top10* competent cells. Transformants were grown on agar plate containing 50 μ g/mL kanamycin. Successful transformed colonies were controlled by PCR, and the plasmids were purified for further usage.

2.10.2 LR clonase reaction

In LR clonase reaction, GOI is recombined from the entry vector (pENTR/GOI) to destination vector (pK7WGF2 or pGWB454). In this reaction, Invitrogen Gateway^R LR ClonaseTM II Enzyme Mix kit was used. In table 2.11, the components and their amounts used in LR reaction were given. In room temperature, reaction mixture was added in 0.2 mL microfuge tube. Then, 2 μ L of LR Clonase Enzyme mix was added to each tube and mixed shortly by vortex. The tube was incubated for an hour at 25

°C. To stop the reaction, 1 µL Proteinase K solution was added to the tube and incubated for 10 minutes at 37 °C.

One-five µL of LR reaction products were used for transformation, and transformants were selected on 100 µg/mL spectinomycin agar plates.

Table 2.11 LR clonase reaction components

Component	Amount
pENTR-GOI (100-150 ng/µL)	1-2 µL
Destination vector (150-200	1-2 µL
TE buffer (Invitrogen)	variable
LR Clonase Enzyme mix	2 µL
Total	10 µL

2.11 Bacterial transformation of plasmids

2.11.1 *E.coli* competent cell preparation

A single colony *E. coli* Top10 was inoculated in 2-5 mL of LB (1 % w/v tryptone, 0.5 % w/v yeast extract, 1 % w/v NaCl, 1.6 mM NaOH) with no antibiotic. Cells were let grow overnight at 37 °C in shaker with 250 rpm. The next morning, 0.5 mL of overnight culture was added into fresh 50 mL of LB in 100 mL Erlenmeyer flask. The culture was grown approximately 2 hours until OD₆₀₀ absorbance reached 0.375-0.4 nm at 37 °C, 250 rpm. Bacterial culture was poured into a pre-chilled sterile 50 mL falcon tube and incubated on ice for 10 min. The tube was centrifuged at 5000 rpm for 3 minutes, 4 °C and supernatant was discarded. Pellet was re-suspended in 10 mL cold 50 mM CaCl₂ solution by gentle shaking. The tube was centrifuged with 5000 rpm for 3 min, at 4 °C. Supernatant was removed and re-suspended again in 10 mL cold 50mM CaCl₂. Tube was rested on ice for 30 min. The cells were pelleted as mentioned above. After removal of supernatant, pellet was dissolved in 2 mL cold CaCl₂ solution. The competent cells were set on ice until use.

2.11.2 Transformation of *E. coli* Top10 competent cell

Five-ten μ L of a ligation product or 1-2 μ L of a plasmid was added to 50 μ L of *E. coli* Top10 competent cells in 1.5 mL Microfuge tube. The tube was incubated on ice for 10 min. To apply heat-shock, the tube was placed in water bath at 42 °C for 45 sec. Immediately, the tube was transferred and set on ice for 3-5 minutes. Then, 300 μ L LB was added and the tube was shaken with 150 rpm at 37 °C for 1-2 hours. LB agar (1 % w/v tryptone, 0.5 % w/v yeast extract, 1 % w/v NaCl, 1.5 % w/v agar, 1.6 mM NaOH) plates with desired antibiotics (Table 2.12) were spread with transformed cells. Cells were grown on plates at 37 °C, overnight. Then, several colonies were chosen for colony PCR.

Table 2.12 Selection of recombinant plasmids

Vector	Antibiotic	Antibiotic usage
pTRBO	Kanamycin	50
pK7FWG2	Spectinomycin	100
pGWB454	Spectinomycin	100

2.11.3 Preparation Agrobacterium GV3101 electro-competent cells

From stock, GV3101 cells were streak plated on LB-tetracycline 2.5 μ g/mL and let grow for 2 days at 28 °C. A single colony was added in fresh 5 mL LB having 5 μ g/mL tetracycline and grown overnight at 28 °C with 250 rpm. The overnight culture of 1 mL was inoculated in fresh 100 mL LB-Tet (5 μ g/mL) media, incubated overnight at 28 °C with shaking. Next day, absorbance OD₆₀₀ of bacterial culture was measured whether it is in desired OD range 0.5-0.7. The medium was poured into two 50 mL Falcon tubes and rested on ice for 30 min. The cells were pelleted by centrifuging for 15 min at 3500 rpm, 4 °C and then supernatant was removed. Then, pellet was re-suspended in 50 mL ice-cold 10 % glycerol solution. The cells were centrifuged for 15 minutes at 3500 rpm, 4 °C. Pellet was re-suspended once more

and centrifuged. Supernatant was discarded and 200 μ L GYT (10 % v/v glycerol, 0.125 % w/v yeast extract, 0.25 % w/v tryptone) medium was added to suspend the pellet. The culture was divided into 50 μ L aliquots in 1.5 mL microfuge tubes. The tube containing electro-competent *Agrobacteria* cells were frozen in liquid nitrogen and stored at -80 °C.

2.11.4 Agrobacterium GV3101 transformation

For Agrobacterium transformation, 1-2 μ L-purified plasmid was mixed in 50 μ L GV3101 electro-competent cell in 1.5 ml microfuge. The tube was chilled on ice for 10 min. Then, the mixture was taken into a pre-chilled 1 mm pulser cuvette. The cuvette was electrocuted at 2200 V (Cellject duo, Thermo corporation). Next, 1 mL of LB medium was added on the cuvette with transformed cells and the mixture was transferred into fresh 1.5 ml microfuge tube. The medium was incubated at 28 °C for 1.5 hour at 200 rpm shaking. LB agar plate with antibiotic(s) was spread with 10-30 μ L of medium and grown at 28 °C for 2 days. Randomly, 3-5 single colonies were selected for colony PCR.

2.12 Agro-infiltration of plant leaves

Agrobacterium GV3101 colonies were grown on plate with appropriate antibiotic(s) (Table 2.12) by streak plating from single colony or stock. After one or two days, colonies were scratched out and suspended in 1 mL of dH₂O in 1.5 mL microfuge tube. The tube was shaken thoroughly until cells were suspended completely, and centrifuged for 5 min at 4000 rpm in tabletop centrifuge. The wash was discarded without disturbing the pellet. Then, 1 mL of dH₂O added into the tube, and it was shaken and centrifuged as mentioned above. The pellet was washed with Agro-infiltration (10mM MES, 10mM MgCl₂, pH 5.7) buffer and the cell pellet was re-suspended with 1 mL Agro-infiltration buffer. For infiltration, the cell concentration was adjusted to 0.2 A₆₀₀. The infiltrated leaves were collected after 2-3 days post

infiltration (dpi) for microscopic imaging, apoplastic fluid isolation and total protein extraction.

2.13 Apoplastic fluid isolation

Agrobacterium infiltrated *N. benthamiana* leaves of 2-3 dpi were used to obtain apoplastic fluid as in the method previously described (O’Leary *et al.*, 2014). Briefly, the leaves were detached, rinsed with distilled water, carefully folded, placed in 60 mL syringe filled with distilled water, vacuum was applied for 5-15 seconds repeatedly until the leaves appeared as dark translucent. The leaves were wiped with clean tissue or filter paper, and sandwiched in parafilm sheets, rolled and placed in 20 mL syringe, centrifuged in 50 mL falcon tubes for 10 min at 1,000 g, at 4°C. The collected apoplastic fluid (400-500 µL/1.0-1.5 g leaf sample) was centrifuged at 15,000 g for 5 min and supernatant, having 600-700 µg/µL total protein concentration, transferred into a fresh tube.

2.14 Apoplastic fluid infiltration

Apoplastic fluid samples obtained from various constructs containing agrobacterim infiltrated *N. benthamiana* were infiltrated until the infiltration area reaches to the size of a penny. The samples and controls were infiltrated side by side on the same leaf with non- or various dilutions (1, 1:3, 1:10, 1:30) in sterilized ddH₂O. The presence of or the level of hypersensitive response (HR) was examined in 4-5 dpi by eye or DAB staining (Thordal-Christensen *et al.*, 1997)

2.15 Virus induced gene silencing of *BAK1*

To test the role of the effector in PTI, *BAK1/SERK3* gene of *N. benthamiana* was silenced using agrobacterium-mediated co-infiltration of the clones containing *Tobacco Rattle Virus* (TRV) genome as pTRV2/*BAK1* and pTRV1 with A₆₀₀ ratio of 2:1 (0.4:0.2, respectively). As a viral control, Agro-pTRV2/GFP:pTRV1 (2:1) were co-infiltrated (Chaparro-Garcia *et al.*, 2011). Newly emerged leaves of three weeks post-silenced tobacco were used for the injection of apoplastic fluid obtained from PstSCR1 effector expressing leaves.

2.16 Infection assay

The effect of PstSCR1 expression during pathogen growth was assayed by transiently expressing pK7FWG2/SP-SCR1-GFP on one half and pK7FWG2/SP-GFP on the other half of *N. benthamiana* leaves. Following after 4-5 hour post infiltration (hpi), leaves were detached and either *P. infestans* 88069 or *P. tabacina* were inoculated as 3 spots of 10 µL of cultures of each, on each half of the infiltrated area of the leaves (Dagdas *et al.*, 2016; Giannakopoulou *et al.*, 2015; Lee *et al.*, 2014). The lesion diameter of *P. infestans* growth and the number of spores of *P. tabacina* were recorded at 8 dpi. The infection assay experiments were repeated on at least three independent *N. benthamiana* leaves.

2.17 Confocal microscopy

N. benthamiana leaves infiltrated with fluorescently tagged proteins at 3 dpi were cut in small pieces, immersed in distilled water and imaged on Leica 385 TCS SP5 confocal microscope (Leica Microsystems, Germany). The GFP and RFP probes were excited by 488 and 561 nm by laser diodes and fluorescent emissions were detected at 495 – 550 and 570 – 620 nm, respectively. For chloroplast autofluorescence, far infrared over 800 nm excitation and emission were applied for excitation and emission.

2.18 Protein extraction and immunoprecipitation

2.18.1 Total protein extraction

At two-three dpi, fully infiltrated *N. benthamiana* leaves with Agrobacterium containing the GOI were removed, dipped in mortar with liquid nitrogen and crushed into powder by grinding. During the grinding, the leaf powder was kept frozen in liquid nitrogen all the time. Then, 1 g grinded leaf sample was mixed with 2 mL of ice-cold fresh extraction buffer (GTEN (10 % glycerol; 25 mM Tris pH 7.5; 1 mM EDTA; and 150 mM NaCl), 2 % (w/v) PVPP, 10 mM β -mercaptoethanol, 1X Protease inhibitor (Thermo, #88666) and 0.1 % Tween-20) in 15 mL centrifuge tube. The tube contents were completely homogenized by vortex and leaf debris was pelleted at centrifuging at 3000 g for 10 min, at 4 °C. The supernatant was transferred into a 2 mL microfuge tube and remaining solid parts were pelleted by centrifuging at maximum speed (20,000 g) for 10 min, at 4 °C. The supernatant was placed into fresh tube again, and centrifugation was repeated until supernatant was completely cleared from leaf remnants. The total protein extract can be kept on ice for the next step or stored at -80 °C for later use.

2.18.2 Tagged-protein immunoprecipitation

Anti-FLAG M2 affinity gel (Sigma, A2220) was mixed gently by pipetting with a cut tip. After resin completely suspended, 50 μ L of it was placed into a 1.5 mL tube containing protein extract in IP buffer (250 μ L total extract). The tube was mixed turning end-over-end at 4 °C for 1-3 hour. After the incubation, resin was pelleted at 800 g for 30 sec, and supernatant was removed; then pellet was re-suspended in 1 mL IP buffer. This wash was repeated four times. After last wash, the remnant liquid was removed very carefully by using syringe with needle not to remove the beads. Immobilized proteins were eluted from the beads in re-suspension solution of 100 μ L IP buffer containing 150 ng/ μ L FLAG tag peptide and the tube was gently shaken in

horizontal position for 30 minutes, at 4 °C. Eluted proteins (supernatants) were transferred into fresh tubes.

2.19 SDS-PAGE

2.19.1 Materials and preparation of the SDS-PAGE gel

In SDS-PAGE, separating buffer (1.5 M Tris HCl, pH 8.8), stacking buffer (0.5 M Tris HCl, pH 6.8), 10 % SDS, 40 % acrylamide/bisacrylamide (37.5 g acrylamide and 1 g bisacrylamide in 100mL ddH₂O), 10 % ammonium persulfate (APS) prepared fresh, NNNN-Tetramethylethylenediamine (TEMED), SDS running buffer 1X (3.3 g Tris base, 1 g SDS and 14.4 g glycine dissolved; then volume brought up to 1 L ddH₂O), Lane Marker Sample Buffer 5X protein loading dye (Thermo, #39001), 1M DTT and PageRuler™ Prestained Protein Ladder (Thermo, #26616). For the SDS-PAGE experiment, Thermo *Owl* P8DS electrophoresis system was used. The manufacturer's manual was applied for gel casting and running. For separating gel, the contents were mixed as illustrated in Table 2.13. APS and TEMED were added last and immediately the solution was poured between the glass plates. The gel was let stand for at least 30 minutes to polymerize before adding stacking gel. Stacking gel was prepared by mixing contents in Table 2.13. The stacking gel was added to cover up onto the separating gel and comb was positioned. The gel was rested for at least an hour to completely solidify.

Table 2.13 SDS gel casting contents

Separating gel	Amount
Separating buffer (4X), 1.5 M Tris, pH	2.5 mL
SDS, 10 % (w/v)	100 μ L
Acrylamide, 40 % (w/v)	3 mL
ddH ₂ O	4.35 mL
APS, 10 % (w/v)	50 μ L
TEMED	6 μ L
Stacking gel	Amount
Stacking buffer (4X), 0.5 M Tris, pH 8.8	1.25 mL
SDS, 10 % (w/v)	40 μ L
Acrylamide, 40 % (w/v)	0.45 mL
ddH ₂ O	3.25 mL
APS, 10 % (w/v)	20 μ L
TEMED	8 μ L

2.19.2 SDS-PAGE

Prepared gel with glass plates was placed in Thermo *Owl* P8DS gel tank. The running buffer (section 2.19.1) was used to fill up the inner and outer chambers of the gel and comb was replaced. In PCR tube, a protein sample mixed with Lane Marker Sample Buffer (1X) and DTT (100mM). The tube was incubated at 95 °C for 5-10 min. Protein samples were loaded and electrophoresis was conducted at 100 V until the samples reached to the separating gel (\approx 20 min), and the voltage was increased to 200 V until loading dye reached to the bottom of the gel (\approx 1.5 h).

2.18 Western Blot

After electrophoresis, the gel was rinsed in dH₂O and incubated in Transfer Buffer (Thermo, #84731) for 15 min for equilibration by gentle shaking. PVDF membrane (Thermo, #88520, 0.2 μ m pore size) and Western Blotting Filter Paper (Thermo, #84783) were soaked in Transfer Buffer for 10 min for equilibration. The blot was performed on PierceG2 Fast Blotter (Thermo) at constant current of 1.3 A for 10

min. The membrane was incubated in blocking solution (3% BSA in TBS-T (25mM Tris-HCl, pH 7.4, 0.137 M NaCl, 2.7 mM KCl, 0.1% Tween 20)) with shaking for an hour at RT. Then, the membrane was taken into primary antibody solution (primary antibody diluted 1/5000 in blocking solution) and shaken gently for 1 hour. Anti-FLAG (Thermo MA1-91878) and anti-GFP (Thermo MA5-15256) antibodies were used as the primary antibodies. After primary antibody incubation, the membrane was washed 5 times with TBS-T for 3 min each time, on shaking platform. Anti-mouse Alkaline Phosphatase conjugated antibody (Chemicon International #AP308A) was diluted 1/10000 in blocking buffer and the membrane was incubated in this solution for 1 hour. Then, the membrane was washed 5 times with TBS-T for 3 min each time. For visualization, 1-StepTM NBT/BCIP Substrate Solution (Thermo #34042) was added to the blot and incubated (\approx 5-15 min) until desired development of color obtained. To stop the reaction, the membrane was rinsed with dH₂O.

CHAPTER III

RESULTS and DISCUSSION

3.1 PstSCR1 homologs

The earliest candidate effector gene sequences of *Pst* (race *Pst-78*) were reported in Yin *et al.* (2009). The study predicted fifteen genes, one of which is Pstha2a5 (we refer to it as PstSCR1 in the entirety of this thesis) to be secreted from *Pst* haustoria. This secreted candidate was chosen in this study since it has i) putative signal peptide at N-terminus, ii) high cysteine content, iii) conserved motif W/Y/F(x)C found in rusts (Cantu *et al.*, 2011; Duplessis *et al.*, 2011; Godfrey *et al.*, 2010; Hacquard *et al.*, 2012; Morais do Amaral *et al.*, 2012) and iv) it is a small protein as expected for secreted effectors. It is one of few EST sequences identified with the full-length the gene when searched for ORF.

NCBI database search of the protein sequence of PstSCR1 produced 11 possible homologs, all of which were predicted protein sequences of the genome of *Pst-78* and *Puccinia graminis* f. sp. *tritici* (*Pgt*) (Figure 3.1). Furthermore, multiple sequence alignment of these homologs including PstSCR1 revealed that the FKC corresponding to the W/Y/F(x)C conserved motif found in rust candidate effectors at N-terminus is adjacent to signal peptide cleavage site, two other (F/Y)x C motifs were present in an internal and C-terminal regions were found to be highly conserved. Among the homologs, the six-cysteine residues conserved to each other, two of which are adjacent cysteine amino acids (Figure 3.1). This preliminary information indicates that the candidate effector is specific to *Pucciniaceae* family. Interestingly, one homolog was annotated as a gene (BioProject: PRJNA41279 (of *Pst-78*); GenBank acc: AJIL01000081.1) defines a hypothetical protein. We noticed

that it has two predicted transmembrane domains, composed of 4 exons, where PstSCR1 was found as a part of the latter three exons combined. The second transmembrane domain of this denoted hypothetical protein is actually corresponding to the SP of PstSCR1 with L (tta) to F (ttc) substitution in the middle of SP (Figure S1A). Note that, *Pst*-78 stripe rust race is the same as the one from which protein sequence of PstSCR1 from EST was predicted (Figure 3.1 and 3.2). When we investigated AJIL01000081.1 super-contig; between the sequences of 3488811-345691 bp, in which the hypothetical protein having two transmembrane regions was annotated, we found three possible promoters, one of which is on the exon 1. Additionally, the only TATA box, GC islands, and the most probable transcription start site also coincided in the exon 1, suggesting the EST sequence, which is composed of the last three exons, is the most likely transcript that is expressed. A pilot computational analysis was conducted and presented at Figure 3.2. On the other hand, if the expression of this hypothetical transmembrane protein is also generated, further analyses will be needed to find out in what condition and at what developmental stages of the pathogen that it is expressed and whether it functions with a consorted manner with PstSCR1.

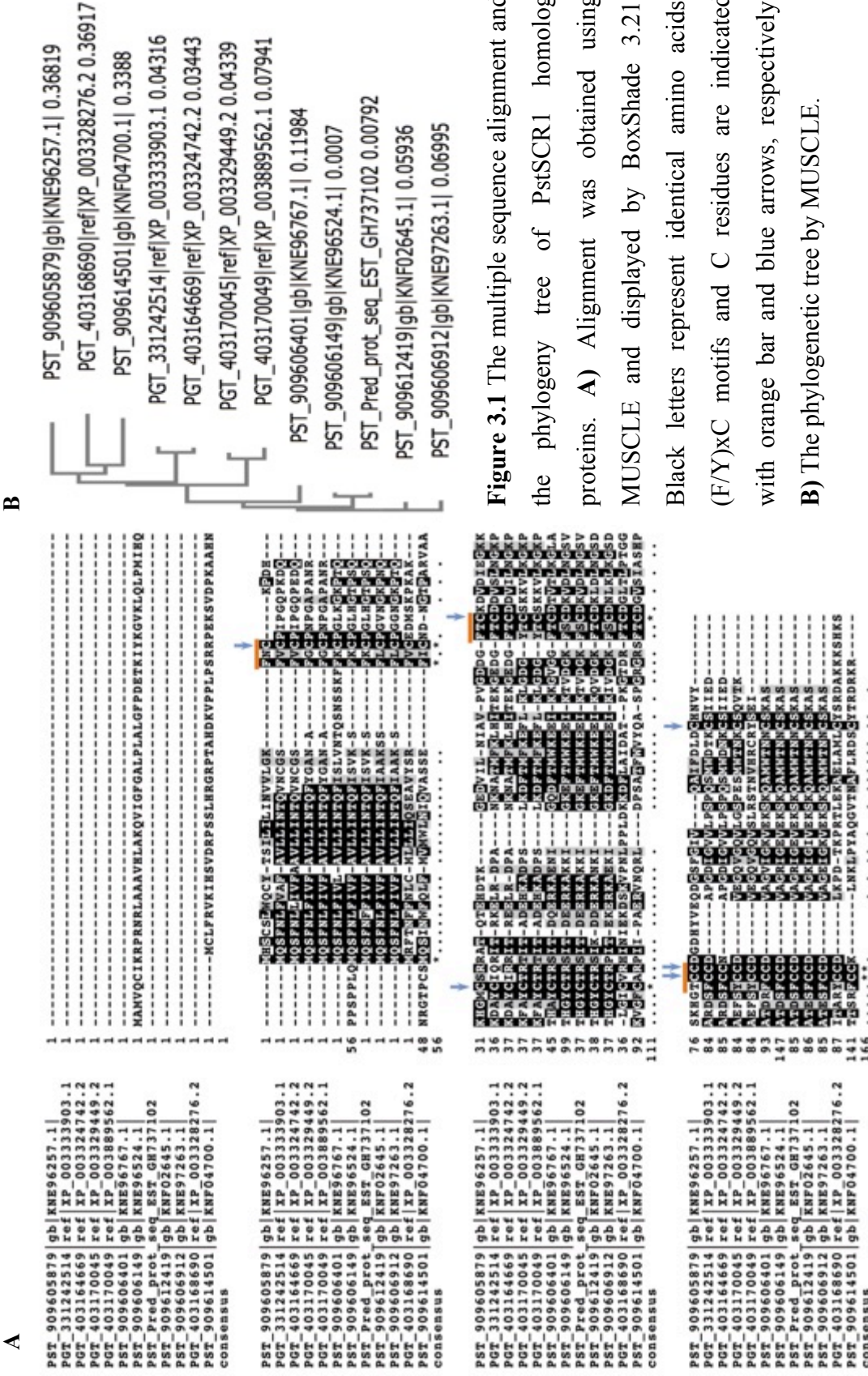


Figure 3.1 The multiple sequence alignment and the phylogeny tree of PstSCR1 homolog proteins. **A)** Alignment was obtained using MUSCLE and displayed by BoxShade 3.21.

(F/Y)xC motifs and C residues are indicated. Black letters represent identical amino acids.

with orange bar and blue arrows, respectively.

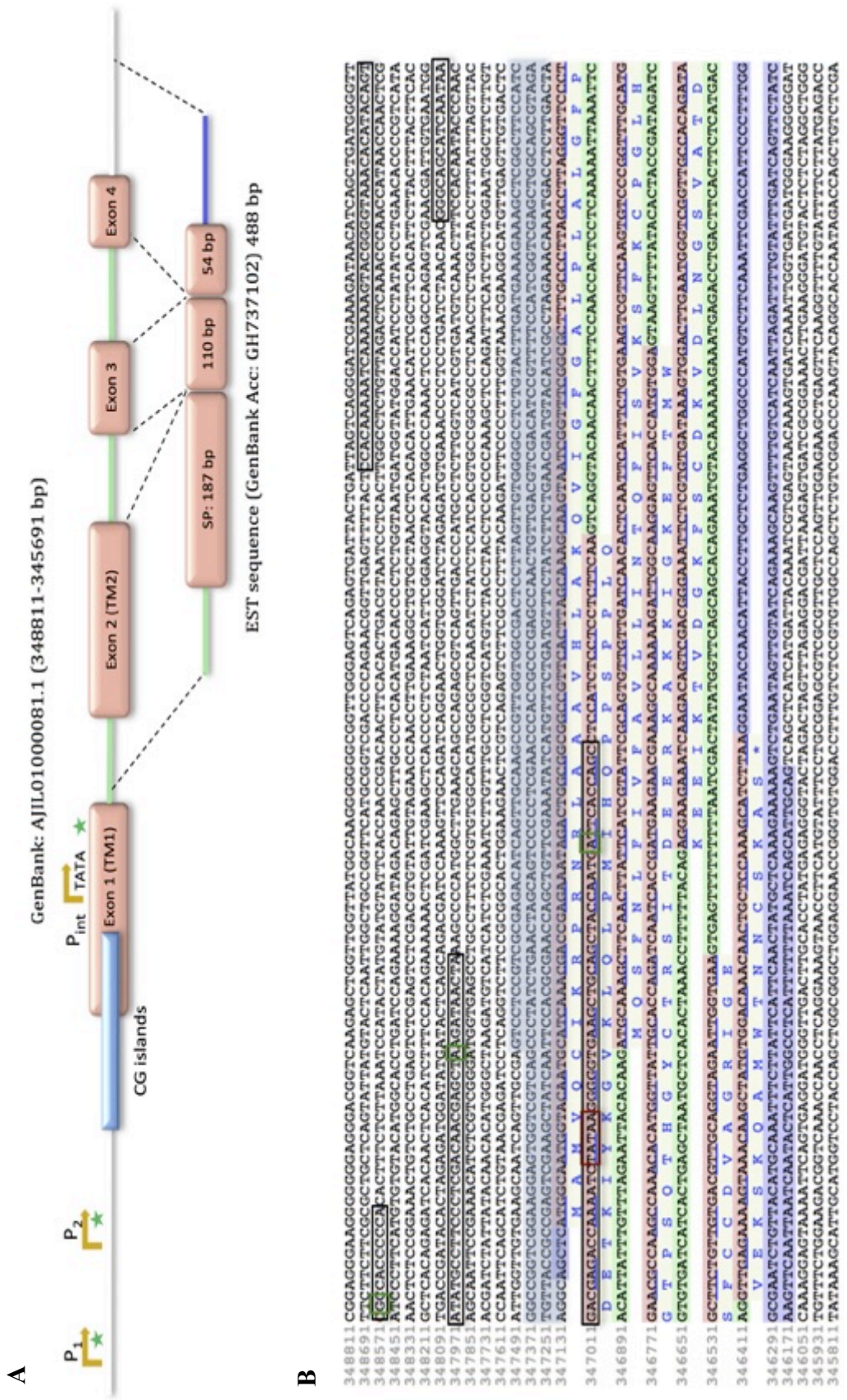


Figure 3.2 (*Continued in next page*)

Figure 3.2 (*Continued from previous page*) The sequence comparisons of AJIL01000081.1 and GH737102 (PstSCR1). Predicted gene structure with putative gene regulatory regions. The EST: GH737102 shared the part of the super-contig of the AJIL01000081.1 of *Pst-78* race genome sequence **A)** Schematic view and **B)** Sequence view: the sequence with upstream (1689 bp) and downstream (644 bp) of the hypothetical gene. Predicted promoter sequences and transcription start sites are indicated in black and green boxes, respectively. The exons and the introns of the annotated hypothetical gene are highlighted in green and light purple, respectively. The predicted TATA box is presented in red box and the putative GC islands on the upstream of the predicted internal-promoter (P_{int}) is highlighted as blue.

3.2 Expression levels of PstSCR1 and its closest homolog during *Pst*-78 infection

In order to test whether PstSCR1 is expressed in *Pst* infection, in the qPCR its expression was determined at different time points (24-h, 72-h, 8-d and 10-d) after the inoculation with *Pst*-78 strain on the leaves of wheat Avoset-S (susceptible line) (Section 2.1.2). The integrity of the isolated RNA samples is presented in Figure 3.3.

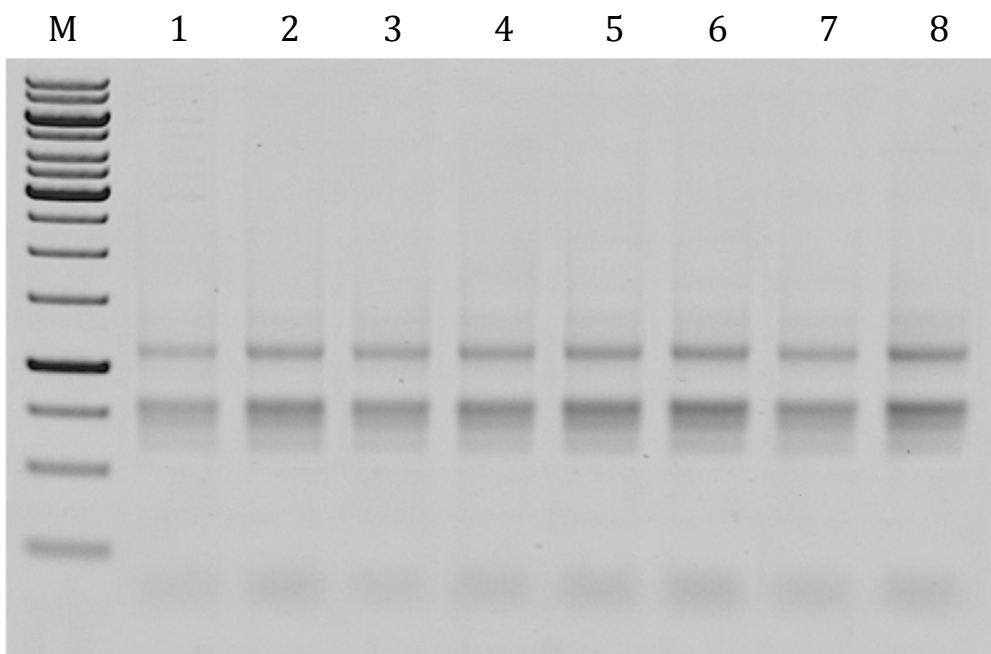


Figure 3.3 The quality of RNA from *Pst*-78 infected wheat samples. **M**) 1 kb ladder (Fermentas #SM0311). **1-4** lanes are total RNA isolated from wheat infected with *Pst*-78 collected at 24-hour, 72-hour, 8-day, and 10-day post infection, respectively. **5-8** lanes are total RNA of wheat mock infected samples correspondent to 24-hour, 72-hour, 8-day, and 10-day post infection, respectively. After DNase I treatment, 1 μ L of RNA samples (\approx 100 ng/lane) were loaded on 1% agarose RNA gel for RNA quality check.

For expression level analysis, the forward primer of PstSCR1 was designed to amplify the 5' UTR region of the PstSCR1, which is predicted as the intron region in the closest homolog of PstSCR1 (Figure 3.4). As controls, we used pathogen

endogenous control gene *PstEF1α* (Yin *et al.*, 2009) and as wheat endogenous gene control, *Actin-1* of wheat (Bozkurt *et al.*, 2007).

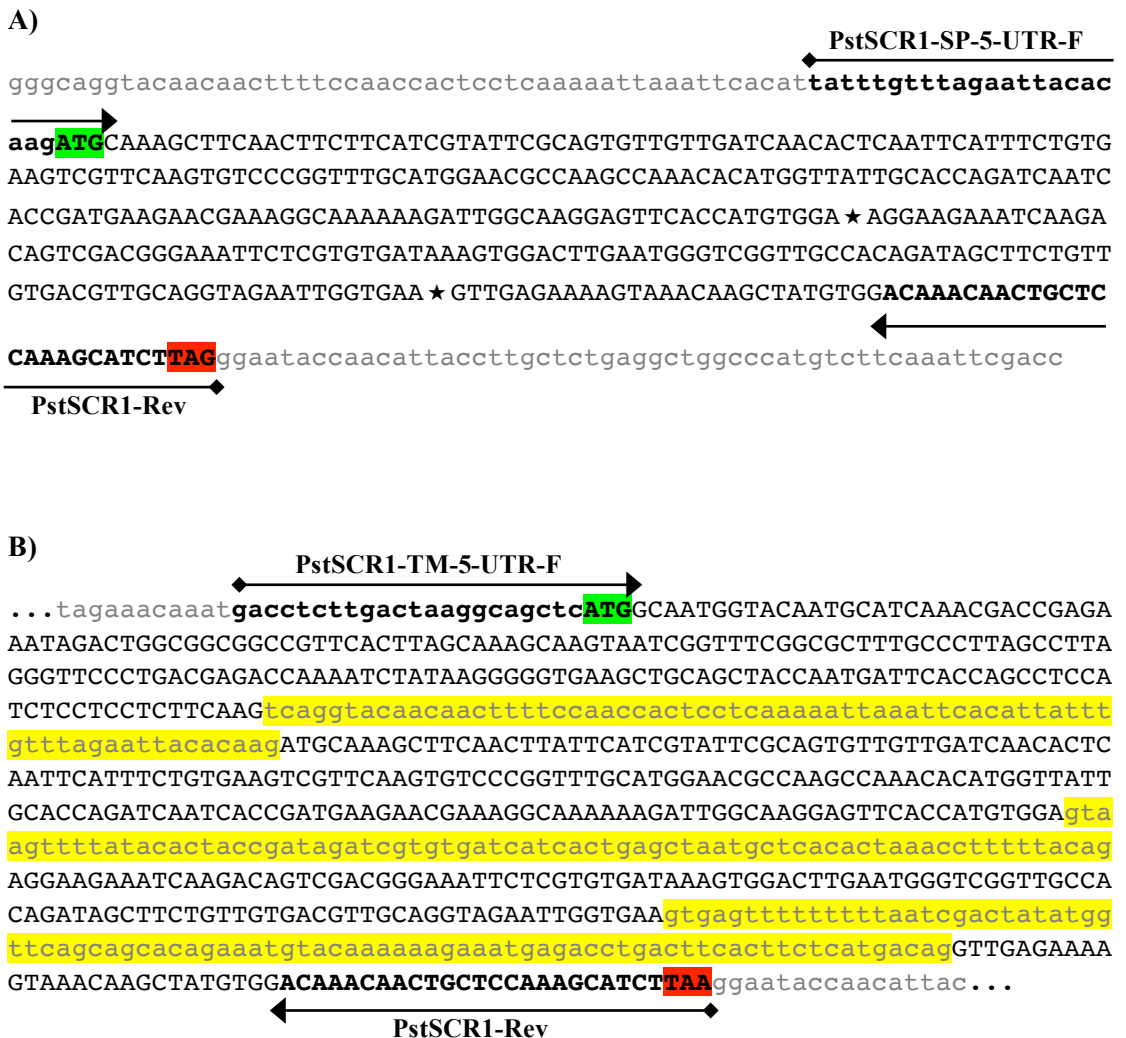


Figure 3.4 PCR primer design strategy to detect the presence of PstSCR1 expression in *Pst* infected wheat samples. **A)** PstSCR1 EST sequence; arrows indicate primers annealing regions and expected amplification size is 375 bp. Stars indicate the exon joints. **B)** The genome region of predicted transcript sequence of PstSCR1 homolog and introns are highlighted in yellow. Expected spliced product amplification size is 560 bp when all introns are removed (Table 2.3).

The qPCR showed that both of the putative transcripts are present at different levels and at different time points (Figure 3.5). The PstSCR1 (PstSCR1-SP-5-UTR-F and PstSCR1-Rev primers) is expressed in high amount in 72-hpi and 8-dpi but it was reduced in 10-dpi. The closest homolog gene (AJIL01000081.1 super-contig; between the sequences of 3488811-345691 bp, NCBI) when putative transcript expression was targeted (with PstSCR1-TM-5-UTR-F and PstSCR1-Rev primers, Figure 3.5-B), we observed three amplification products (a, b, c) and the band intensities appeared a gradual increase from 72-hpi to 10-dpi. So, in order to obtain more conclusive results, the bands were isolated and have made sequenced.

Direct sequencing reactions of the isolated PCR product (sample of 8th dpi PCR) presented in the Figure 3.5A from both directions showed perfect match with the EST sequence of PstSCR1. In its putative homolog, based on the designed primers the expected PCR product is 559 bp, if the gene is transcribed with all the exons. But we have observed longer product –band **a**- in that PCR was above 600 bp (Figure 3.5B/product **a**). The sequence information of that band (**a**) revealed that the putative intron between putative exon 1 and exon 2 was not spliced. So it can be concluded that indeed the sequence between the exons 1 and 2 is not an intron it is indeed the 5' UTR of PstSCR1. Thus, the result confirms the computationally detected TATA box, promoter, and GC islands on exon 1 are indeed biologically relevant and it is the 5' UTR of PstSCR1. Another explanation can be the alternative splicing.

Interestingly, based on the sequencing of the PCR product, band (**b**) of the Figure 3.5B appeared as it an alternative splicing took place. The putative exon 1 was retained completely, but intron 1 was removed except first three nucleotides "GTC" and it was joined with the last 5 nucleotides of the signal peptide transcript in exon 2, which produced a frame-shift on PstSCR1 orginal sequence. Although the part of the exon 3, and exon 4 sequences were missing in our sequence readings, it is highly possible that they retained in the rest of the sequence based on the observed band size (\approx 500 bp) (Figure 3.5B). The expected size of the band (**b**) is 491 bp if the

exon 3 and exon 4 included fully in the rest of the transcript. As a result, this putative transcript produce 49 amino acid protein product with no predicted secretion signal, no conserved motif like W/Y/F(x)C, and no high cysteine content, which were important features of known predicted effector candidates. Thus, fungus may be using alternative splicing to express a short peptide having a different function than that of an effector.

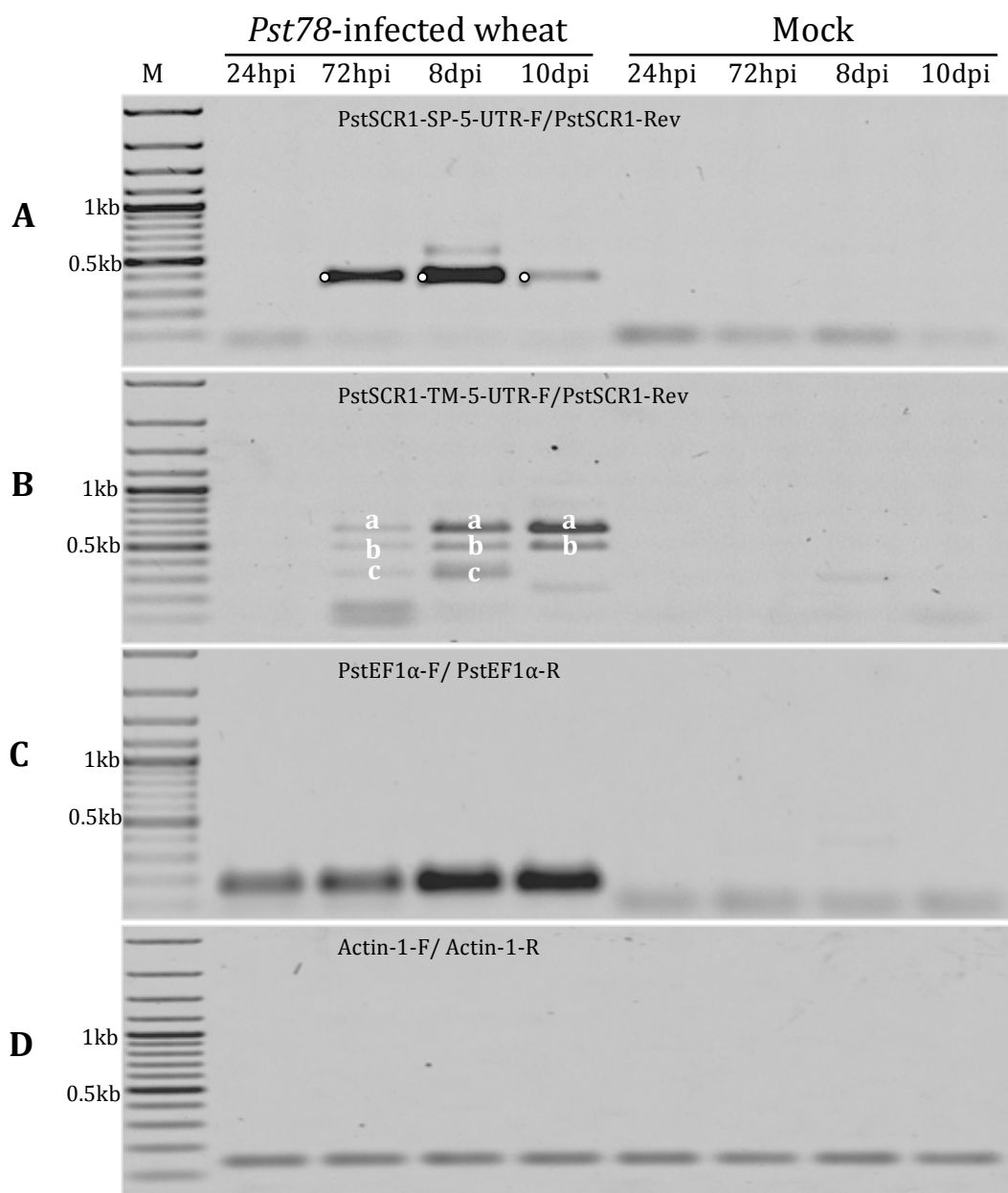


Figure 3.5 The PstSCR1 and its closest homolog gene expression comparisons in different time points during *Pst-78* infection. **M:** 100 bp ladder (Fermentas SM#0321). **A, B, C** and **D** are PstSCR1 (exp: 375 bp), homolog of PstSCR1 (exp: 560 bp, if all introns were removed), *Pst* Elongation factor 1 alpha (*PstEF1 α*), and wheat *Actin-1* genes amplifications, respectively. qPCR products of 10 μ L were loaded on 1% agarose gel.

3.3 Subcellular localization of PstSCR1

To determine the subcellular localization of the PstSCR1, we constructed expression vectors with insert of PstSCR1 (with or without SP) fused with a C-terminal fluorescent tag, either RFP or GFP. The PstSCR1 was amplified with CACC-SCR1noSP and CACC-SCR1SP as forward primers to generate with SP and without SP, respectively. The primer SCR1-noSTP was used as reverse primer in both amplifications. The PCR products were introduced into pENTR-D/TOPO vector by topoisomerase cloning. Then, pENTR-D/TOPO/SCR1 and pENTR-D/TOPO/SP-SCR1 was used to recombine with pK7FWG2, and pGWB454 to produce C-terminal GFP, and RFP fusions, respectively (Section 2.10). The *Agrobacterium* GV3101 strain was transformed with constructs and the genes were transiently expressed in *N. benthamiana* (Section 2.11 and 2.12).

According to subcellular localization results, the overlayed images of the co-expressed SP-SCR1-RFP (red) and EV-GFP (green) in Figure 3.6A shows that GFP was directed to cytoplasm and nucleus, where plastids were seen clearly. However, we were able to detect that PstSCR1 was secreted into apoplast when it was expressed with SP. In Figure 3.6B and 3.7, when SP-SCR1-RFP and SP-SCR1-GFP were co-expressed, they were both observed to be secreted to apoplastic region. It should be noted that the clearly visible endoplasmic reticulum (ER) network in Figure 3.7 is indicative of the effector targeting to the apoplast *via* ER. As a control, when the protein was expressed with no SP (SCR1-GFP), it appeared in cytoplasm and nucleus instead of apoplast (Figure 3.6C), similar to a typical GFP expression images obtained in *N. benthamiana* (Petre *et al.*, 2015).

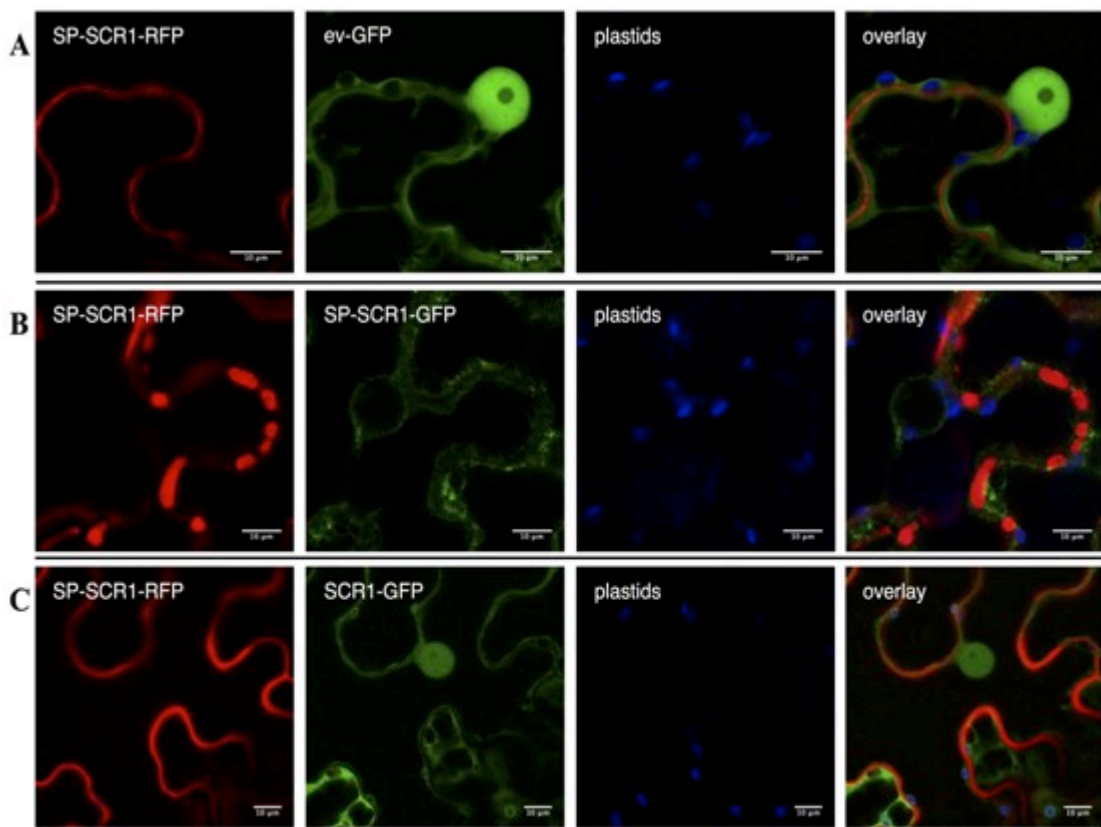


Figure 3.6 The subcellular localization of PstSCR1. *N. benthamiana* plants were co-expressed by agro-infiltration using the following constructs: **A)** pGWB454/SP-SCR1-RFP and pK7FWG2/ev-GFP, (ev: Empty vector), as nucleo-cytoplasmic marker; **B)** pGWB454/SP-SCR1-RFP and pK7FWG2/SP-SCR1-GFP; **C)** pGWB454/SP-SCR1-RFP and pK7FWG2/SCR1-GFP. The GFP and RFP probes were excited using 488 and 561 nm laser diodes and their fluorescent emissions collected at 495–550 and 570–620 nm, respectively. For chloroplast auto-fluorescence detection, far infrared (>800 nm) excitation and emission were used. Scale bars are 10 μ m.

To substantiate that the protein is apoplast-secreted, SP-SCR1-RFP was co-expressed with plasma membrane marker REM1.3 (Bozkurt *et al.*, 2014; Pike, 2006; Simons and Gerl, 2010) in comparison with the co-expression of an apoplastic marker, Papain like protease (Plp) C14 (Bozkurt *et al.*, 2011), also known as vacuole membrane tonoplast targeting protein, and REM1.3. The co-localizations of co-

expressed SP-SCR1-RFP and YFP-REM1.3 (Figure 3.8B) appeared identical to the overlay picture in Figure 3.8A (RFP-C14/YFP-REM1.3 overlay) with one exception of RFP-C14 also being targeted to tonoplast as predicted. This comparison suggests that the protein is accumulating solely in apoplastic region. If there is an interaction with the outer membrane, it must be a weak one or it is not noticeable in the microscopic observations.

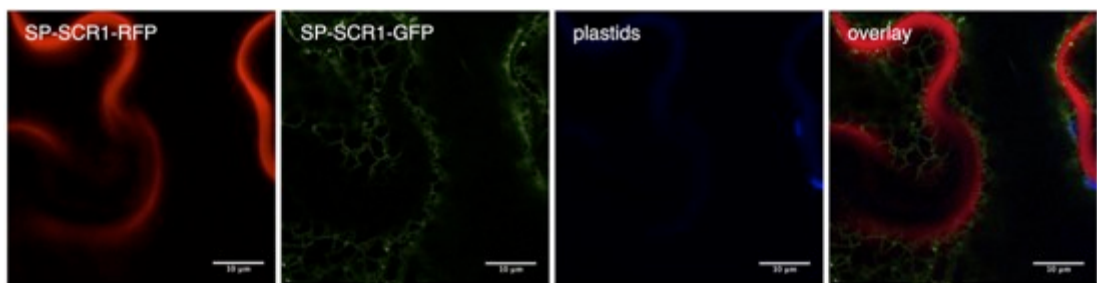


Figure 3.7 The co-localization of PstSCR1-RFP and PstSCR1-GFP. *N. benthamiana* leaves were agro-infiltrated with the constructs of pGWB454/SP-SCR1-RFP and pK7FWG2/SP-SCR1-GFP both expressing with the signal peptide of the effector. The GFP and RFP probes were excited using 488 and 561 nm laser diodes and their fluorescent emissions collected at 495–550 and 570–620 nm, respectively. For chloroplast auto-fluorescence detection, far infrared (>800 nm) excitation and emission were used (Leica SP40). Scale bars are 10 μm.

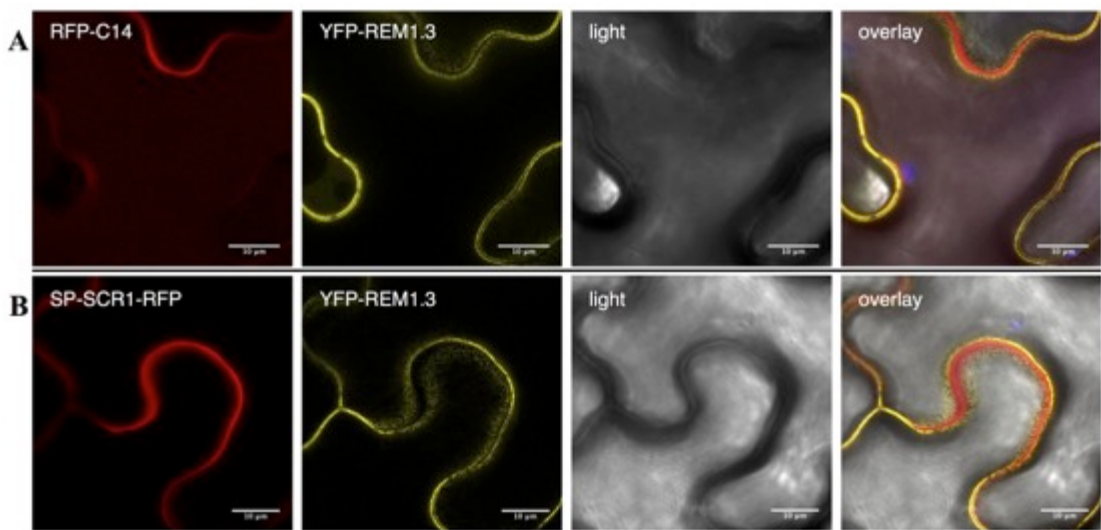


Figure 3.8 Pictures of representative *N. benthamiana* leaf samples co-expressing **A)** pGWB554/C14 and pK7WGY2/REM1.3, and **B)** pGWB454/SP-SCR1-RFP and pK7WGY2/YFP-REM1.3. The comparisons (A and B) are indicating PstSCR1 expressed with SP accumulates in apoplastic space but not on the outer plasma membrane. The YFP and RFP probes were excited using 514 and 561 nm laser diodes and their fluorescent emissions collected at 495 – 550 and 570 – 620 nm, respectively. Scale bars are 10 μ m.

3.4 PstSCR1 lowers pathogen infections

To investigate the role of PstSCR1 as an effector in response to pathogen infection, host-pathogen interaction assays were conducted on the plant samples with agro-infiltrated leaves expressing the effector. *N. benthamiana* leaves expressing the effector with SP (SP-SCR1-GFP) and without SP (SCR1-GFP) were infected with *Phytophthora infestans* and *Peronospora tabacina* (Section 2.16). At 8 dpi, lesion growth of hemibiotrophic *P. infestans* was measured and spores of *P. tabacina* on *N. benthamiana* were counted.

Based on the results (Figure 3.9 and 3.10), the protein expressed without SP (SCR1-GFP) showed no significant change in the pathogen developments (lesion growth

and spore count) when inoculated with a hemibiotrophic *P. infestans* and an obligate biotroph, *P. tabacina*. However, SP intact-protein, which accumulates in apoplast, reduced the pathogen growth and development of *P. infestans* and *P. tabacina*. These findings suggest that PstSCR1 is functional in apoplast, but not in cytosol.

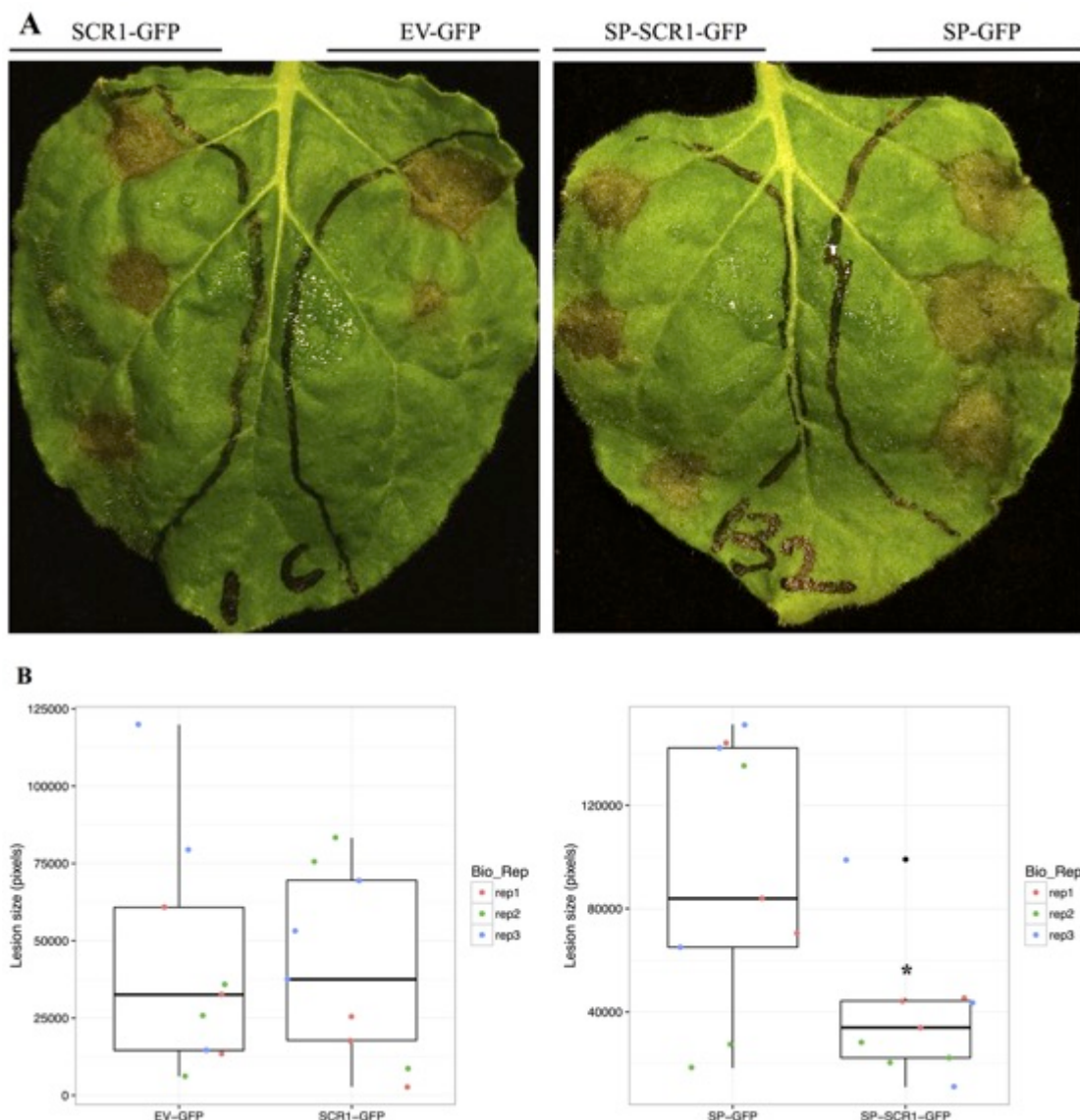


Figure 3.9 The assessment of the level of lesions by *P. infestans* in effector expressed samples. **A)** The infection of *N. benthamiana* (4-5 week old) leaf with *P. infestans* after expressing SCR1-GFP and SP-SCR1-GFP constructs. Photographs were taken after an 8-day post inoculation (dpi). **B)** Infected areas in the leaf were measured in pixels (by ImageJ tool) and plotted into the graph. EV-GFP and SP-GFP were used as the controls of SCR1-GFP and SP-SCR1-GFP, respectively. Asterisks indicate significant differences by ttest (*P = 0.0121 ≤ 0.05).

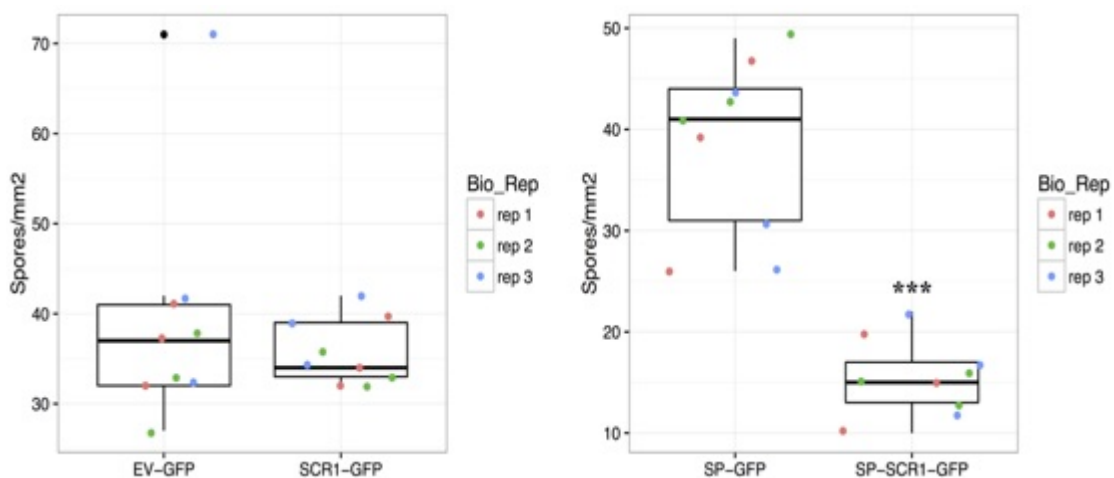


Figure 3.10 The evaluation of the level of *P. tabacina* spore formation in effector expressed samples. *N. benthamiana* (4-5 week old) leaves were infected with *P. tabacina* after expressing SCR1-GFP and SP-SCR1-GFP constructs and collected after 8-dpi. Spores from the leaf disks were suspended in water and counted under the microscope. EV-GFP and SP-GFP were used as the controls of SCR1-GFP, and SP-SCR1-GFP, respectively. Asterisks indicate significant differences by ttest ($***P = 2.0232 \times 10^{-6} \leq 0.001$).

3.5 Overexpression of PstSCR1 in *N. benthamiana*

3.5.1 PstSCR1 cloning in TRBO vector

The PstSCR1 gene construct was inserted into pTRBO (pJL48) (Lindbo, 2007) vector for overexpression. The FLAG tag was introduced by PCR in C-terminus of the gene. Since the nucleotide sequence of FLAG tag with linker is too long for one primer, it was separated into two primers with overlapping regions. First PCR was carried out with PacI-noSP-SCR1-F as forward and SCR1-C-Flag-R2 as reverse primers to generate PstSCR1 with no SP (Figure 3.10). For PstSCR1 with SP, PacI-SP-SCR1-F as forward and SCR1-C-Flag-R2 as reverse primers were used (Figure 3.11). Second PCR was amplified using the first PCR product as template. The primers PacI-noSP-SCR1-F as forward and SCR1-C-Flag-R1 as reverse, and PacI-noSP-SCR1-F as forward and SCR1-C-Flag-R1 as reverse are used to complete the

FLAG tag fusion, and 5' *PacI* and 3' *NotI* restriction site extensions in PstSCR1 without SP (Figure 3.11A and Figure E-1 in Appendix-E), and with SP (Figure 3.11B and Figure E-2 in Appendix-E), respectively. All four PCR products were purified and run on gel to confirm the quality and size control (Figure 3.12).

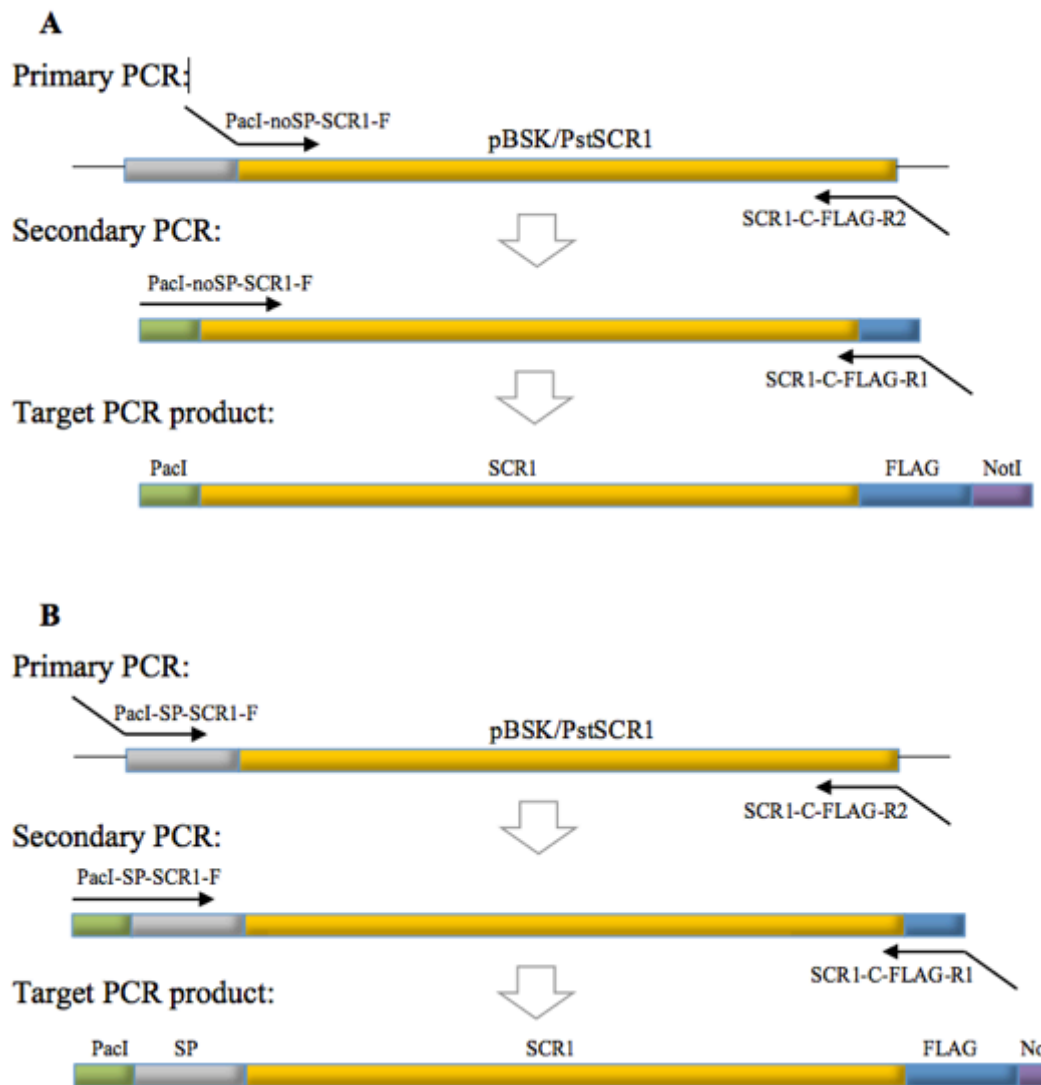


Figure 3.11 Schematic view of the positions of PCR primers on **A)** SCR1-FLAG and **B)** SP-SCR1-FLAG constructs.

The purified PCR products and pTRBO-empty vector were digested with *PacI* and *NotI-HF* for directional cloning (Section 2.9.1). Digested products were separated on an agarose gel and the bands were isolated (Section 2.9.2). The isolated bands were separated again on a gel for concentration control (Figure 3.13) and used for ligation (Section 2.9.3).

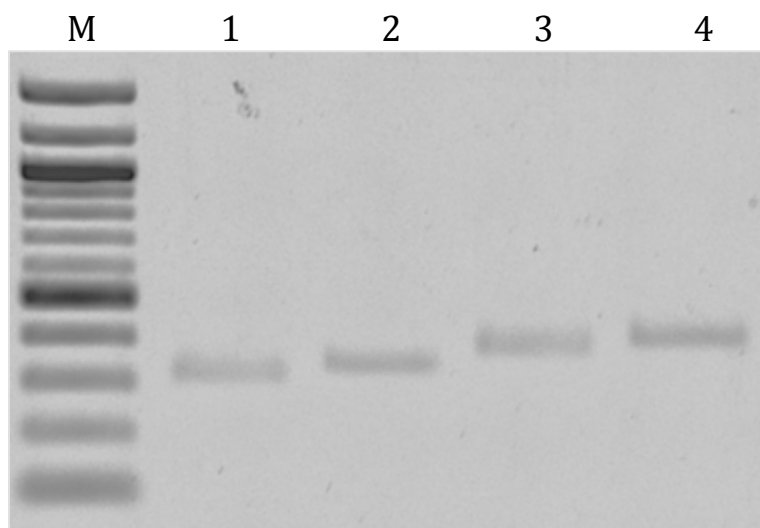


Figure 3.12 PstSCR1 with C-term FLAG amplification for cloning in pTRBO vector. **M**-100 bp ladder (Fermentas #SM0321). **1)** and **3)** are first PCR amplification of PstSCR1 exclusive (321 bp) and inclusive (390 bp) SP, respectively. **2)** and **4)** are second amplification to complete the FLAG tag fusion by using **1** and **3** as a template, respectively. The final SCR1-FLAG and SP-SCR1-FLAG PCR products sizes are 349 bp and 418 bp, respectively.

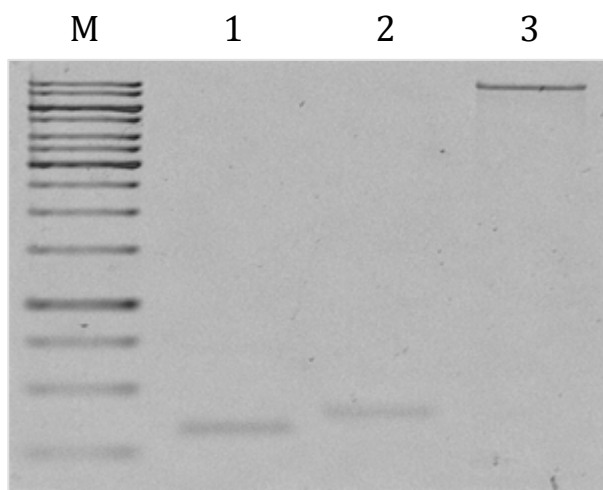


Figure 3.13 Restriction enzyme digestions followed by gel extraction of PstSCR1 PCR products and pTRBO vector agarose gel analysis. **M)** 1kb ladder (Fermentas #SM0311). **1)** PstSCR1 without SP and with C-terminus FLAG fused PCR product was digested and gel extracted. **2)** PstSCR1 with SP and C-terminus FLAG fused PCR product was digested and gel extracted. **3)** pTRBO-empty vector was digested and gel extracted. Digestions were carried out with *PacI* and *NotI*-HF restriction enzymes (NEB).

The ligation products were transformed into *E.coli Top10* competent cells. The putative colonies were amplified by colony PCR by TRBO seq-F and TRBO seq-R primers (TRBO sequencing primers), which amplify flanking regions of the insert of the target DNA (Figure 3.14).

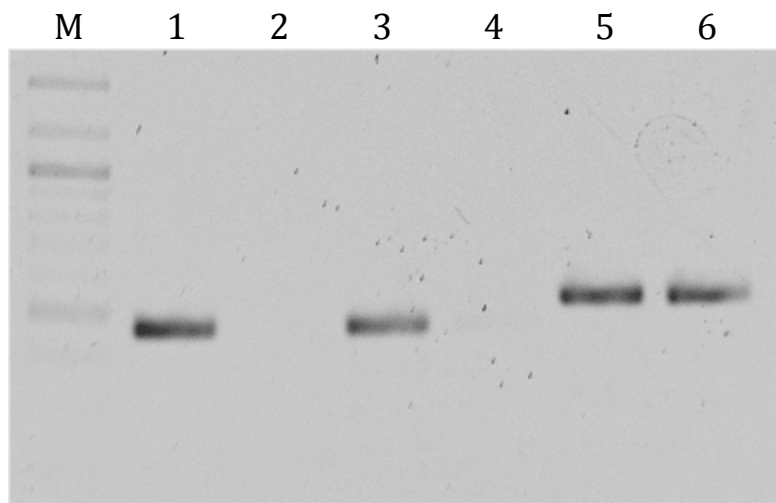


Figure 3.14 Colony PCR after cloning of PstSCR1 in pTRBO vector. **M)** 100 bp ladder (Fermentas #SM0321). **1-3)** Putative *E.coli* colonies possessing PstSCR1 without SP and with C-terminus FLAG fused construct in pTRBO were used in PCR amplification. **4-6)** Putative *E.coli* colonies possessing PstSCR1 with SP and C-terminus FLAG fused construct in pTRBO were used in PCR amplification. PCR was carried out with TRBO sequencing primers. SCR1-FLAG and SP-SCR1-FLAG expected sizes are 479 bp and 548 bp, respectively, by sequencing primers.

The colonies belong to 3rd and 6th lanes (Figure 3.14) were chosen for plasmid isolation (Section 2.9.2). The plasmids were isolated and controlled for PCR amplification with TRBO sequencing primers. Both plasmids and PCR products were separated on a gel for control. The bands of the PCR products were in expected size ranges.

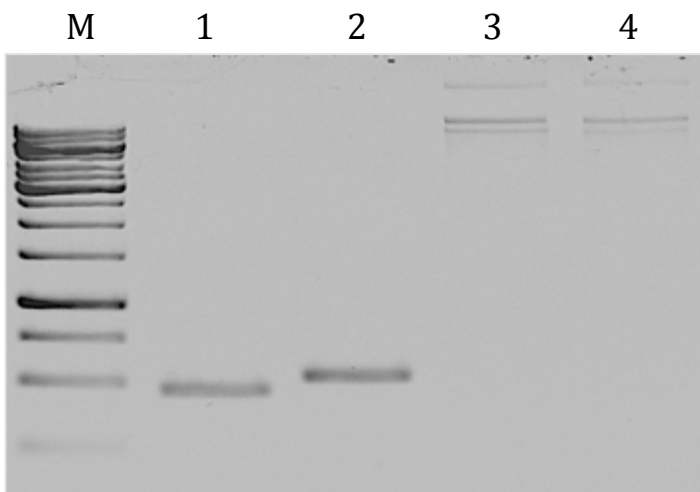


Figure 3.15 Plasmid isolation and PCR of pTRBO/SCR1-FLAG and pTRBO/SP-SCR1-FLAG. **M)** 1 kb ladder (Fermentas #SM0311). **1)** PCR amplification of pTRBO/SCR1-FLAG. **2)** PCR amplification of pTRBO/SP-SCR1-FLAG. **3)** and **4)** are pTRBO/SCR1-FLAG and pTRBO/SP-SCR1-FLAG vectors, respectively, after plasmid isolation. The PCR was carried out with TRBO sequencing primers. SCR1-FLAG and SP-SCR1-FLAG expected sizes are 479 bp and 548 bp, respectively, by TRBO sequencing primers.

The plasmids pTRBO/SCR1-FLAG and pTRBO/SP-SCR1-FLAG have made sequenced by TRBO seq-R primer. The sequencing the construct was confirmed 100% hit when it was compared with theoretical sequence. The sequences of chromatogram are presented in Appendix-E. After these confirmations, the plasmids were transferred into *Agrobacterium* GV3101 strain by electroporation (Section 2.11.4). These transformants were taken into stock in -80 °C and used for effector overexpression experiments.

The constructs pTRBO/SP-SCR1, pTRBO/SP-GFP and pTRBO/SP-GFP-FLAG were generated likewise as cloning strategy was illustrated above. For SP-SCR1 amplification, PacI-SP-SCR1-F and PstSCR1-NotI-R primers were used. The SP was fused with GFP by introducing the SP sequence into pK7FWG2 vector by

Gateway Cloning with amplification with CACC-SCR1SP as forward and SCR1SP-noSTP. For SP-GFP, PacI-SP-SCR1-F as a forward and, GFP-STP-NotI as reverse primers were used. For SP-GFP-FLAG, PacI-SP-SCR1-F as a forward and, GFP-FLAG-R and SCR1-C-Flag-R1 as reverse primers were used.

3.5.2 Overexpression of PstSCR1 cause cell death in *N. benthamiana*

For overexpression and purification of the effector, the pTRBO/SCR1-FLAG and pTRBO/SP-SCR1-FLAG constructs were expressed in *N. benthamiana* by Agrobacterium-mediated gene transfer (Section 2.12). After 3-4 dpi, the phenotypical changes were recorded.

Interestingly, the overexpression of PstSCR1 consistently showed cell death (hypersensitive response, HR) only when it was expressed with the SP, but regardless of the presence of FLAG-Tag attachment to the C-terminus. In order to assess the cell death caused by PstSCR1 in apoplast, we substituted the effector with GFP as a control; however, we kept the SP on the N-terminus of GFP so that it can target to apoplast. Moreover, we tested the possible effect of the fusion of FLAG-Tag at the C-terminus of PstSCR1, and it was noticed that the FLAG-Tag did not interfere with the outcome. Thus, we were able to use tag-fused effector (no SP) as a negative control (Figure 3.17A). Regardless of the presence of the FLAG-Tag fusion, when the SP-SCR1 and SP-SCR1-FLAG constructs were let expressed, we observed cell death in the leaves, but SCR1-FLAG and SP-GFP presented no cell death (Figure 3.17B). This result is suggesting that PstSCR1 needs to be secreted to the apoplast of *N. benthamiana* to trigger the cell death, but SP itself does not stimulate the cell death (Figure 3.17B). Recently, it has been reported that the secretion signal of the apoplastic effectors is indispensable for their cell death-inducing activity (Fang *et al.*, 2016; Ma *et al.*, 2015).

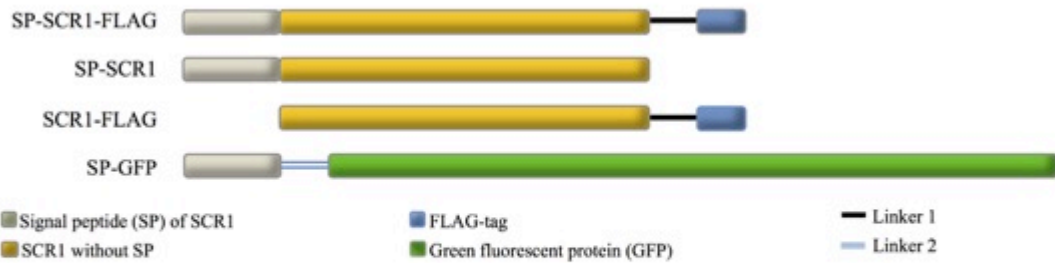
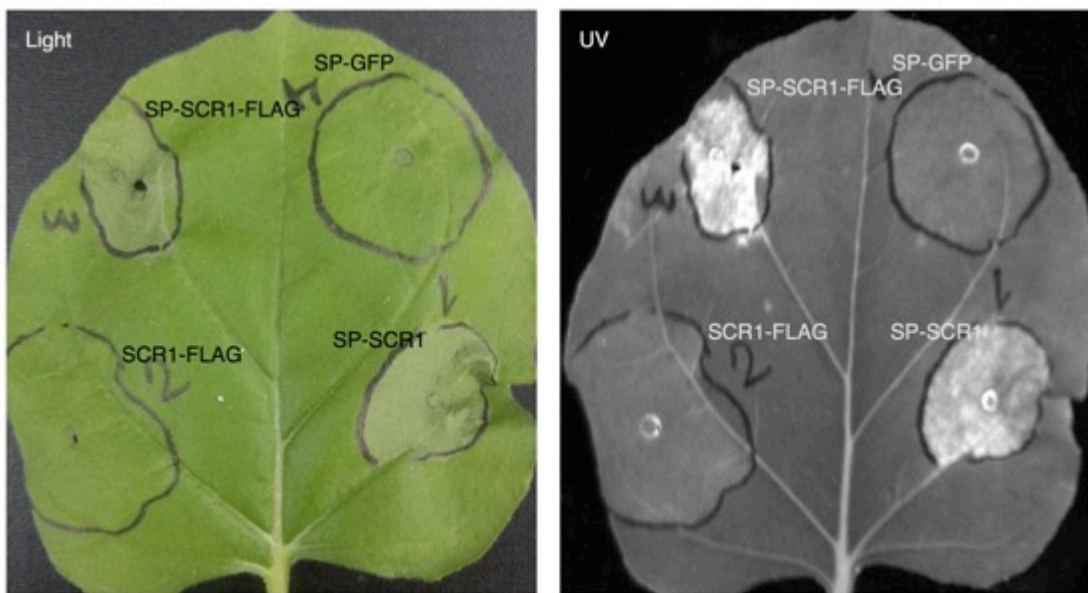
A**B**

Figure 3.16 The effector needs to be secreted to induce cell death in *N. benthamiana*. The effect of SP and FLAG was tested. **A)** The schematic view of constructs used in the experiment. **B)** Representative *N. benthamiana* leaf expressing pTRBO/SP-SCR1, pTRBO/SP-SCR1-FLAG, pTRBO/SCR1-FLAG and pTRBO/SP-GFP after 4dpi.

3.6 Apoplastic extracts of PstSCR1 expressing leaves triggered cell death in a dose dependent manner

Although our subcellular localization experiments were confidently conclusive (Figure 3.6, 3.7 and 3.8) in which the PstSCR1 is secreted to apoplast where causing reduced pathogen development (Figure 3.9 and 3.10), to further investigate the cell

death by PstSCR1, apoplastic fluid infiltration assays were conducted (Figure 3.17A). The infiltration of apoplastic fluid extracted (Section 2.13) from *N. benthamiana* leaves expressing SP-SCR1-FLAG or SP-GFP-FLAG (negative control) at differing amounts (no dilution = 1 (\approx 600 ng/ μ L), 1:3 and 1:10 dilutions with ddH₂O) on fresh *N. benthamiana* leaves (Figure 3.17A) allowed us to test cell death (Section 2.14). We observed cell death in a dose dependent manner on the plant surface infiltrated with apoplastic fluid samples possessing SCR1-FLAG, but not with the secreted GFP control,. Interestingly, the infiltration of total protein extracted into new leaves did not show any indication of cell death (Appendix L).

3.7 Stability of PstSCR1 in apoplast

The samples of apoplastic fluid, which were investigated on western blotting were the same as the one used to test cell death (Figure 3.17B). Apoplastic fluid and extracted total protein were from the very same leave samples of which apoplastic fluid were removed of the leaves expressing SP-SCR1-FLAG (14.75 kDa expected size with SP) and SP-GFP-FLAG (33.2 kDa expected with SP). In the control samples, the anti-GFP western blotting revealed that GFP is present both in apoplast and total protein extract. However, anti-FLAG antibody did not detect GFP-FLAG in apoplast. It was concluded that FLAG tag was cleaved, suggesting that tagged GFP is prone to proteolysis in apoplast (Badel *et al.*, 2013; van Esse *et al.*, 2006), which can also be deducted from the size differences of the pre-stained protein bands on WB:GFP (Figure 3.17B). In case of SP-SCR1-FLAG expressed samples, anti-FLAG antibody detected the FLAG-tagged effector both in apoplast and in the total protein extract (after apoplastic fluid removal). Double bands were detected in the protein total extract, but in apoplastic fluid mostly PstSCR1 appeared as SP-cleaved. Theoretical size of the SCR1-FLAG is smaller than that of the size observed on blots, which implies post-translational modification. The identical FLAG tag was cleaved from the SP-GFP-FLAG expressing *N. benthamiana* but not from SP-SCR1-

FLAG. This result suggests that PstSCR1 protein is stable in apoplast and thereby it is functional.

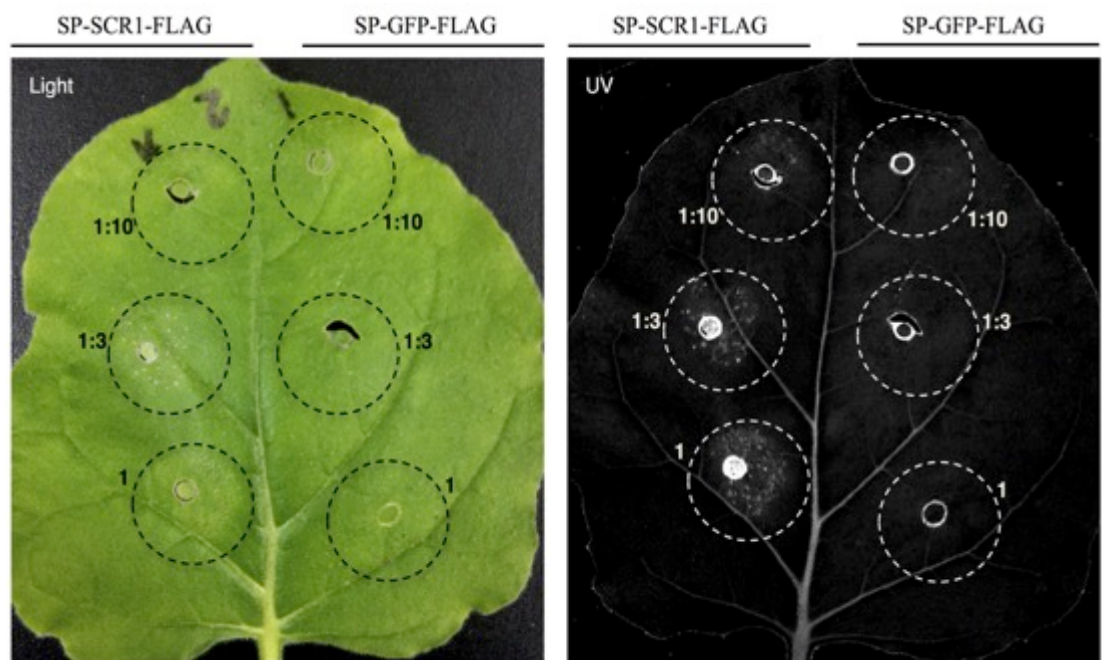
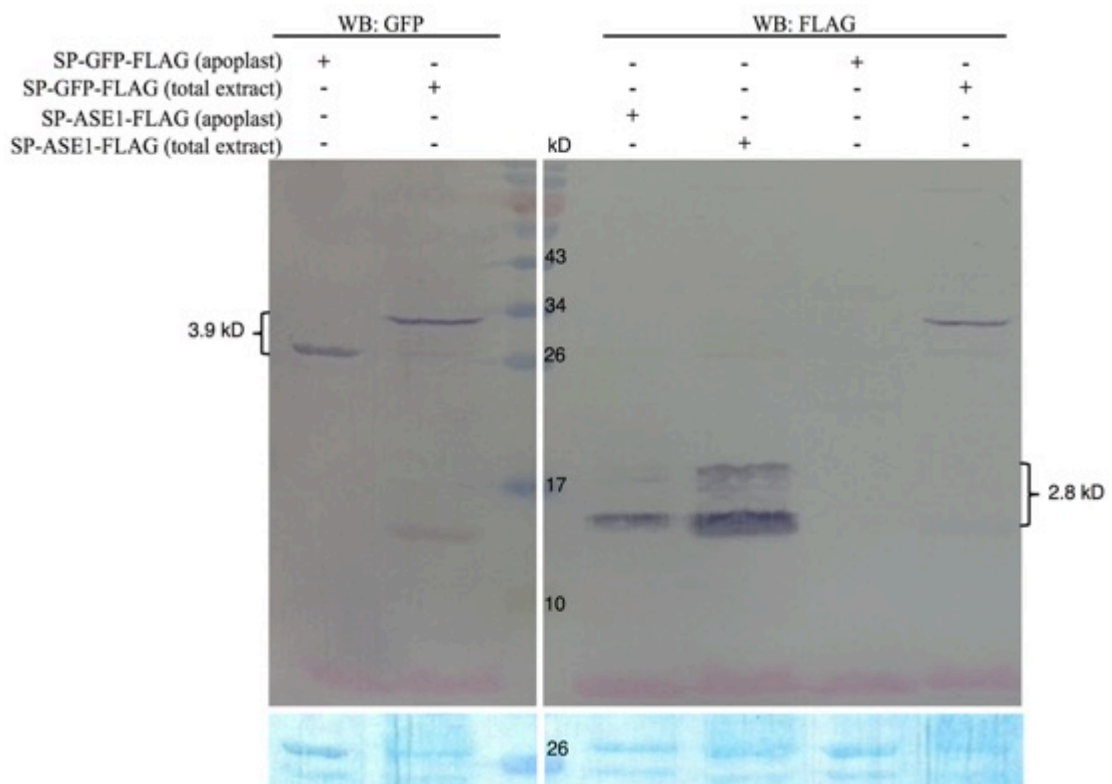
A**B**

Figure 3.17 (Continued in next page)

Figure 3.17 (Continued from previous page) Apoplastic fluid with secreted effector triggers cell death in *N. benthamiana*. The infiltration of *N. benthamiana* was conducted with apoplastic fluid containing processed PstSCR1. A) The representative leaf of *N. benthamiana* infiltrated with apoplastic fluid from *N. benthamiana* expressing SP-SCR1-FLAG and SP-GFP-FLAG. After 4-5 days of apoplastic fluid infiltration, the leaves were examined under normal light and UV exposure. B) Apoplastic fluid and total protein extract, from leaves after removal of apoplastic fluid, (10 µL) was loaded on SDS-PAGE gel and Western blotting was carried out with anti-FLAG (Thermo) or anti-GFP (Thermo) antibodies; total protein was detected by Reversible Protein Stain on PVDF membrane (Thermo). As a control, SP-GFP-FLAG was used. The theoretical sizes of the bands; SP-GFP-FLAG is 33.2 kD; SP-GFP-FLAG (SP and FLAG cleaved) is 29.4 kD; SP-SCR1-FLAG is 14.74 kD and SCR1-FLAG is 11.96kD.

3.9 PstSCR1 reducing the level of cell death in BAK1 silenced plants

It is established that Brassinosteroid Insensitive 1-Associated Kinase 1 (*BAK1/SERK3*) in plants is involved in response to PAMP molecules and it is a key participant of PTI response (Chaparro-Garcia *et al.*, 2011; Heese *et al.*, 2007; Shan *et al.*, 2008; Zipfel, 2008). To check whether *BAK1/SERK3* is modulating the cell death by PstSCR1, we tested *BAK1/SERK3* silenced *N. benthamiana* plants with apoplastic fluid extracted from *N. benthamiana* overexpressing the secreted effector. The *NbBAK1/SERK3* silenced *N. benthamiana* plants showed phenotype of darkened green color and semi-dwarfism with comparison to the control pTRV2/GFP treated plants (Figure 3.18). This is because, beside, plant defense related roles of *BAK1*, the gene product possibly also is involved in optimum development and growth of plants, (He *et al.*, 2007).

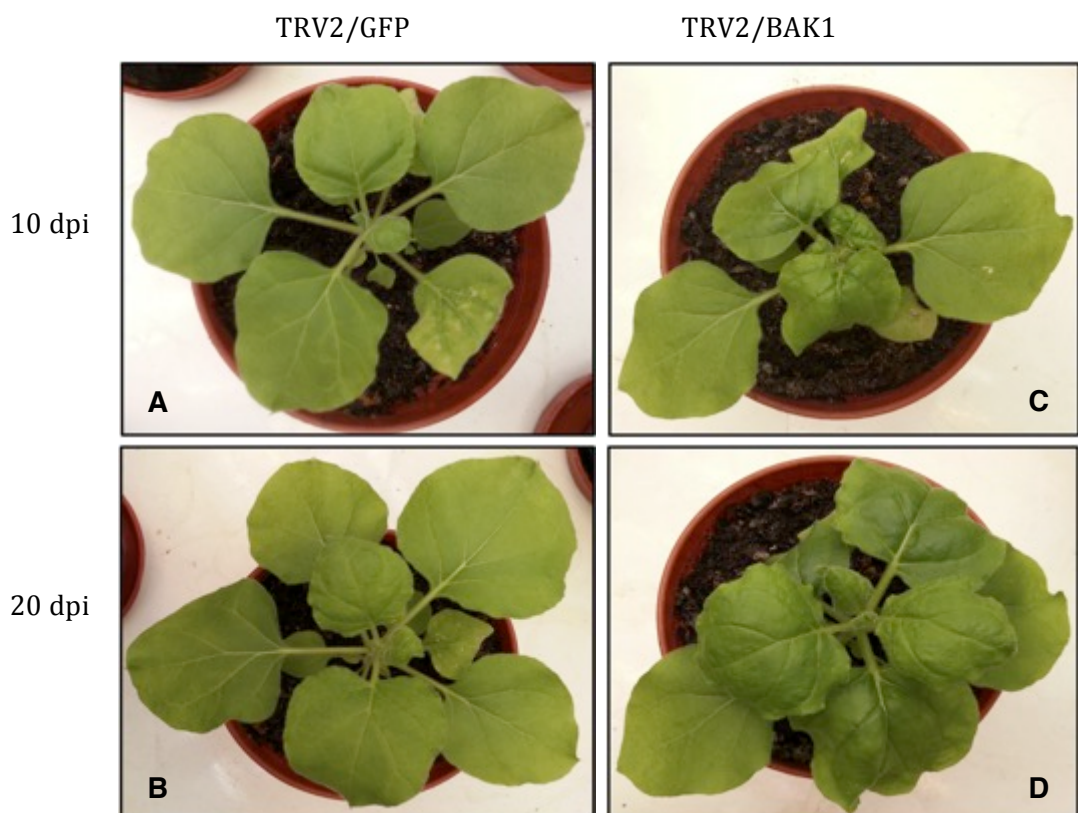


Figure 3.18 Appearance of *N. benthamiana* plants expressing pTRV2/GFP or pTRV2/BAK1 construct. **A** and **B** illustrate representative plants of 10- and 20-day post infection (dpi), respectively, with TRV2/GFP construct which used as control. **C** and **D** illustrate representative plants of 10- and 20-dpi, respectively, with TRV2/BAK1 construct.

The leaf samples were collected for total RNA isolation to quantify the level of silencing by qPCR. The RNA integrity was tested by agarose gel electrophoresis after DNase I treatment (Figure 3.19 and Section 2.3.1). Then, first strand cDNA was synthesized (Section 2.3.2).

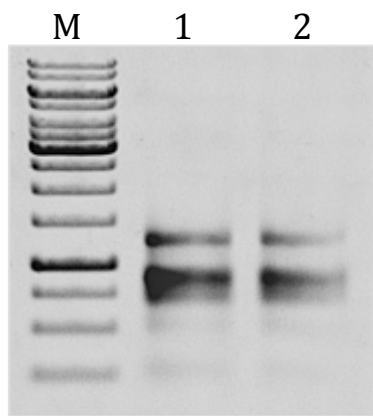


Figure 3.19 The RNA quality of *NbBAK1/SERK3* and *GFP* silenced *N. benthamiana* plants. **M)** 1 kb ladder (Fermentas #SM0311). **1)** Total RNA of *N. benthamiana* infiltrated with pTRV2/*GFP*. **2)** Total RNA of *N. benthamiana* infiltrated with pTRV2/*BAK1-SERK3*. After DNase I treatment, 1 μ L of sample was loaded on 1% agarose gel.

The qPCR was conducted with primers NbSerk3-F and NbSerk3-R for *NbBAK1/SERK3*, and NbEF1 α -F and NbEF1 α -R for *NbEF1 α* as endogenous control by using the cDNA samples (Section 2.4). The qPCR product profiles and the appearance on agarose gel are shown in Figure 3.20 and 3.21, respectively. The controls including all contents except template or primers did not produce any Ct value on profiles or bands on gel (data not shown).

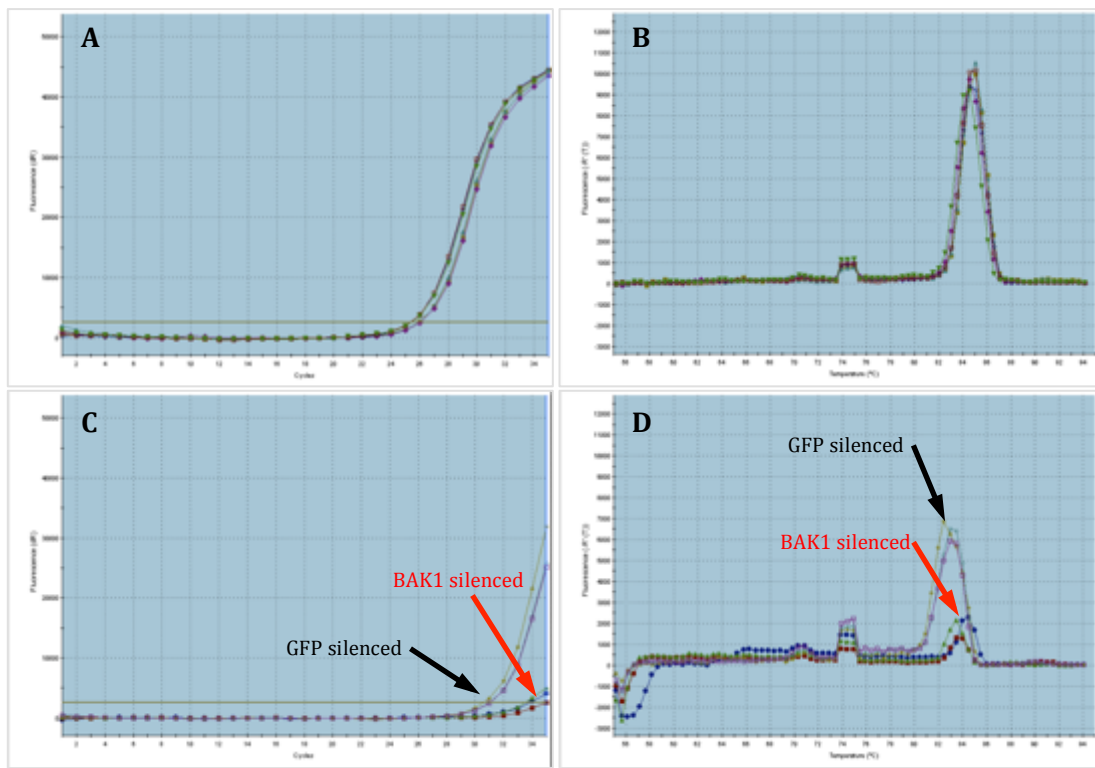


Figure 3.20 The qPCR profiles for *NbEF1 α* and *NbBAK1/SERK3* gene expressions in *BAK1* and *GFP* silenced plants. The silencing was carried out with pTRV1 and pTRV2 systems. **A)** The endogenous control *NbEF1 α* expression levels with 3 replicates in both *BAK1* and *GFP* silenced plants. **B)** Dissociation curve for *NbEF1 α* amplification in both *BAK1* and *GFP* silenced plants. **C)** The expression levels of *NbBAK1/SERK3* gene with 3 replicates in *BAK1* and *GFP* silenced plants. **D)** Dissociation curve for *NbBAK1/SERK3* amplification in both *BAK1* and *GFP* silenced plants.

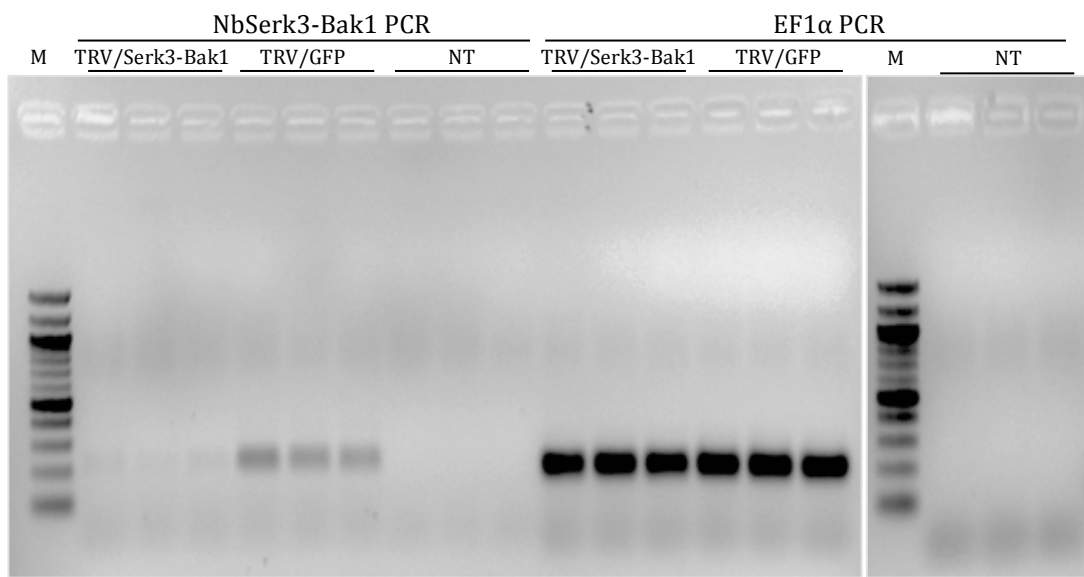


Figure 3.21 *NbBAK1/SERK3* was silenced by TRV2/*BAK1* silencing construct. qPCRs were carried out on *BAK1/SERK3* or control silenced leaf (TRV2/*GFP*). Total cDNA were subjected to PCR using endogenous control *EF1 α* primers or *NbSerk3* specific primers and visualized in an agarose gel.

The $\Delta\Delta Ct$ value was calculated using Ct values shown in Appendix-I (Section 2.5). First, average Ct value of the replicates and its standard deviation were calculated for qPCR amplifications Table J (in Appendix-J). Then, the Ct values from *NbBAK1/SERK3* amplification were normalized using the corresponding Ct values from *NbEF1 α* amplification. The normalized ΔCt value differences resulted in $\Delta\Delta Ct$ (Table 3.1 and Figure-J in Appendix-J). The fold change was calculated by the following formula $RQ = 2^{-\Delta\Delta Ct} = 0.23$ with standard deviation of 0.04 (Table 3.2).

Our results suggest that the *NbBAK1/SERK3* gene was 77 % silenced in *N. benthamiana* leaves with comparison to the control plants (Table 3.2 and Figure 3.22).

Table 3.1 The ΔCt , $\Delta\Delta Ct$, fold difference calculations.

Sample	CtBAK1 average	CtEF1 α average	$\Delta Ct = CtBAK1 - CtEF1\alpha$	$\Delta\Delta Ct = \Delta CtBAK1 - \Delta CtGFP$	Fold difference in BAK1 relative to GFP
GFP-silenced	31.07 \pm 0.042	25.42 \pm 0.07	5.65 \pm 0.082	0 \pm 0.082	1 (0.87-1.17)
BAK1-silenced	33.735 \pm 0.205	25.976 \pm 0.055	7.758 \pm 0.212	2.108 \pm 0.212	0.234 (0.200-0.268)

Table 3.2 Relative quantification and its standard deviation of *BAK1* silencing experiment.

	TRV- <i>BAK1</i>	TRV- <i>GFP</i>
RQ mean	0.23	1.00
RQ stdev	0.04	0.08

*RQ = relative quantification

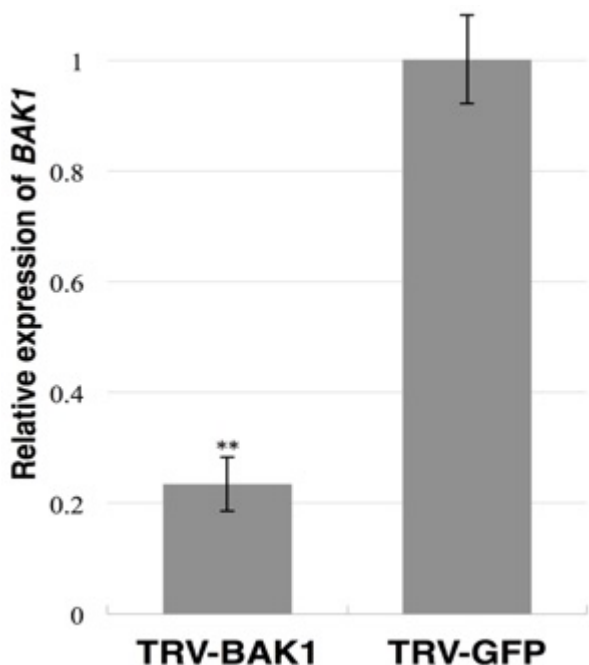


Figure 3.22 *BAK1* silencing. In *N. benthamiana* plant leaves, *BAK1* was silenced using TRV-*BAK1* construct in comparison with TRV/GFP infected plants (Chaparro-Garcia *et al.*, 2011). The expression levels of *BAK1* were determined by qPCR in both plant sets. *EF1α* was used as an endogenous gene control. Means and standard deviations from biological replicates are illustrated. Asterisks indicate significant differences by ttest (**P = 0.007386 ≤ 0.01).

The *NbBAK1/SERK3* silenced plants were infiltrated with apoplastic fluid from *N. benthamiana* expressing SP-SCR1-FLAG and SP-GFP-FLAG. The cell death was diminished with comparison to the control *GFP* silenced plants. On the other hand, in the *GFP* silenced *N. benthamiana* plants, which served as control, no change was observed (Figure 3.23).

The silencing of *BAK1/SERK3* showed reduction in HR by the candidate effector thereby concluded that *BAK1/SERK3* was required for cell death triggered by PstSCR1 in the apoplast. This might indicate that PstSCR1 may be recognized by the plant surface receptors in which the immune response strength appeared to be concentration dependent (Figure 3.16, 3.17 and 3.23). It is difficult to rule out the involvement of other factors of apoplast in cell death in addition to the PstSCR1

since we introduced PstSCR1 as in apoplastic fluid, not as the purified protein. However, as a mean of control, the same construct where effector was substituted with GFP (SP-GFP-FLAG) did not cause any observable phenotypical changes suggesting that the effector is the source of cell death either directly or indirectly, such as, by inducing some elicitors or interacting with other pathogen secreted proteins.

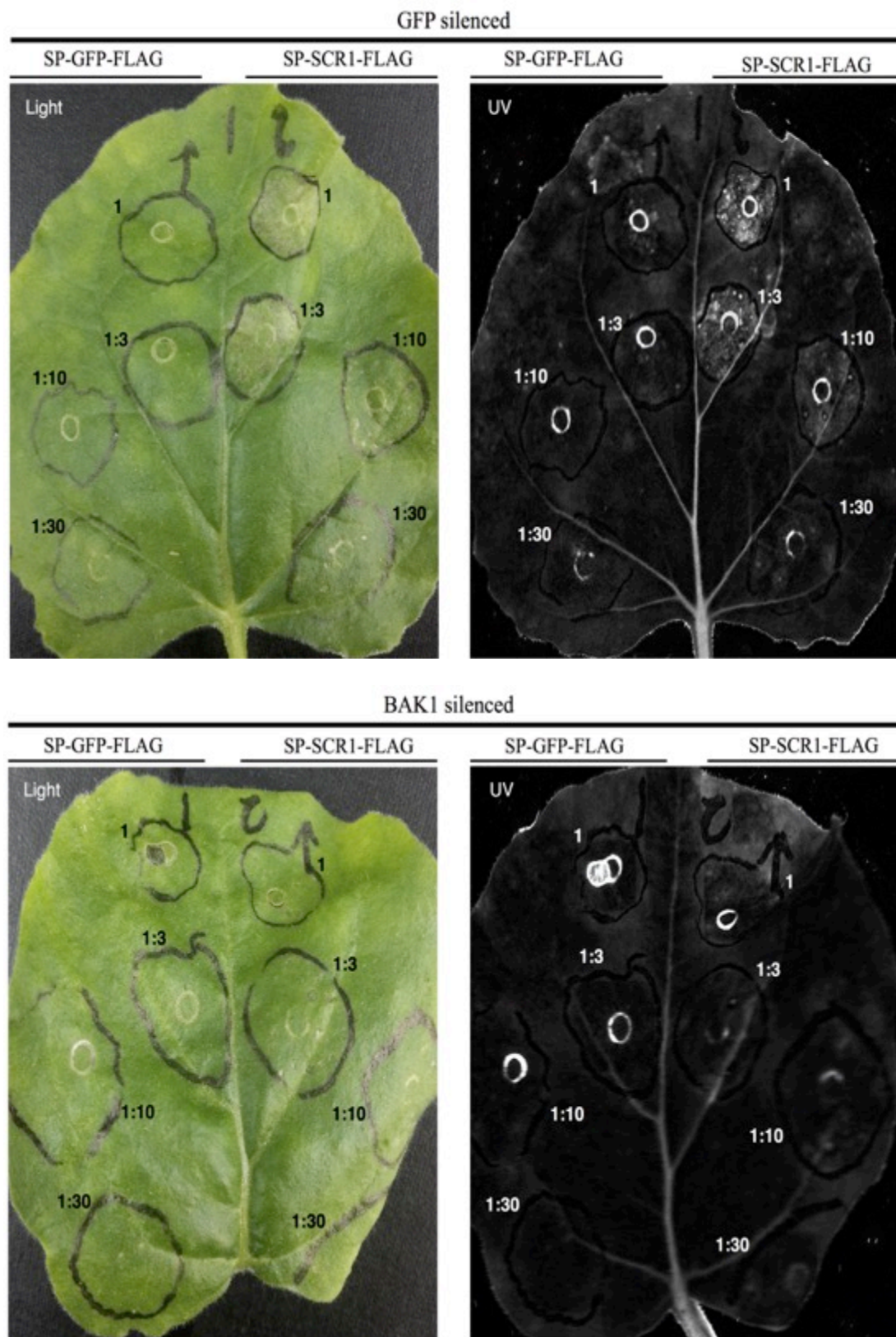


Figure 3.23 (Continued in next page)

Figure 3.23 (Continued from previous page) PstSCR1 triggered cell death reduced in the BAK1 silenced *N. benthamiana*. Infiltration of BAK1 and GFP silenced *N. benthamiana* with apoplastic fluid from *N. benthamiana* expressing SP-SCR1-FLAG and SP-GFP-FLAG. Apoplastic fluid was diluted as 1 (no dilution), 1:3, 1:10 and 1:30 dilution with distilled water before infiltration. After 4-5 days of apoplastic fluid infiltration, the leaves were examined under normal light and UV exposure.

3.10 Activation of *NbCYP71D20* and *NbACRE31* genes upon SCR1 treatment

In BAK1 silenced plants, cell death was significantly reduced, so we wanted to further analyze the SCR1 role on defense related gene activations in *N. benthamiana*. We chose two *N. benthamiana* genes namely *NbCYP71D20* (a putative cytochrome P450) and *NbACRE31* (a putative calcium-binding protein), which were reported that their expression levels were increased dramatically after treatment of PAMP molecules, such flg22 (Chaparro-Garcia *et al.*, 2015; Xin *et al.*, 2012).

We isolated 40 mL of apoplastic fluid from *N. benthamiana* leaves expressing pTRBO/SP-SCR1-FLAG. Then, the apoplastic fluid was used for immunoprecipitation to purify the SCR1 protein using Anti-FLAG affinity beads (Sigma). The purified SCR1 was separated on SDS-PAGE and western blotted to assess purification quality and protein concentration determination (Figure 3.24). The purified SCR1 was diluted 1:10 and infiltrated into *N. benthamiana* leaves.

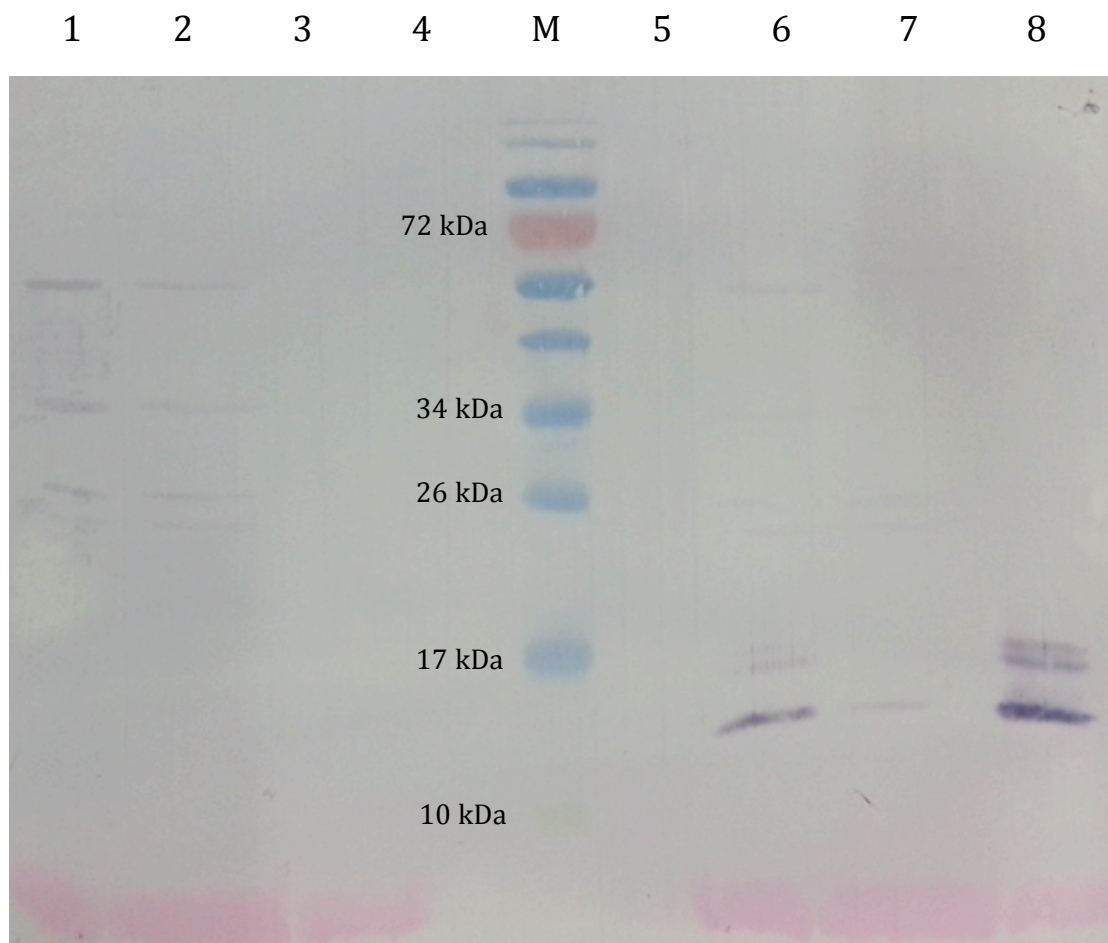


Figure 3.24 Western blot analysis of purified SCR1 from *planta*. **M**) Pre-stained protein ladder (Thermo, #26616). **1)** and **6)** Apoplastic fluid with GFP and SCR1, respectively. **2)** and **7)** Apoplastic fluid with GFP and SCR1, respectively, after immunoprecipitation. **3)** and **8)** immunoprecipitated or purified GFP and SCR1, respectively, by anti-FLAG beads. **4)** and **5)** no load **2)**. As a control, SP-GFP-FLAG was used. Theoretical size of SCR1-FLAG is 11.96kD.

The infiltrated leaves were collected and total RNA were isolated. The integrity of RNA was tested on an RNA agarose gel after DNase I treatment (Figure 3.25). The first strand cDNA was synthesized for qPCR.

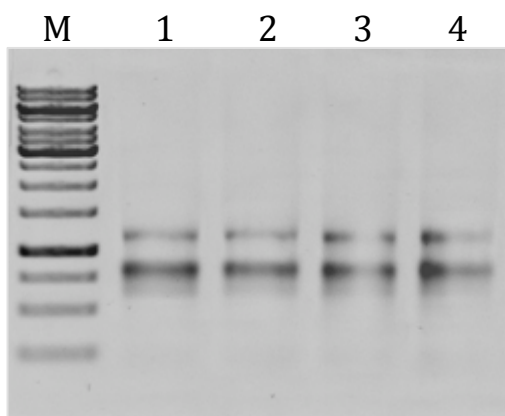


Figure 3.25 The RNA isolated from *N. benthamiana* leaves injected with isolated PstSCR1 protein. **M**) 1 kb ladder (Fermentas #SM0311). **1** and **2** Total RNA of *N. benthamiana* treated with control sample after 2 dpi and 4 dpi, respectively. **3** and **4** Total RNA of *N. benthamiana* treated with purified PstSCR1 after 2 dpi and 4 dpi, respectively. After DNase I treatment, 1 µL of RNA samples (\approx 100 ng/lane) was loaded on 1 % agarose gel for RNA quality check.

The cDNA was used for amplifications of the *NbCYP71D20* and *NbACRE31*. The qPCR profiles are shown in Figure 3.26.

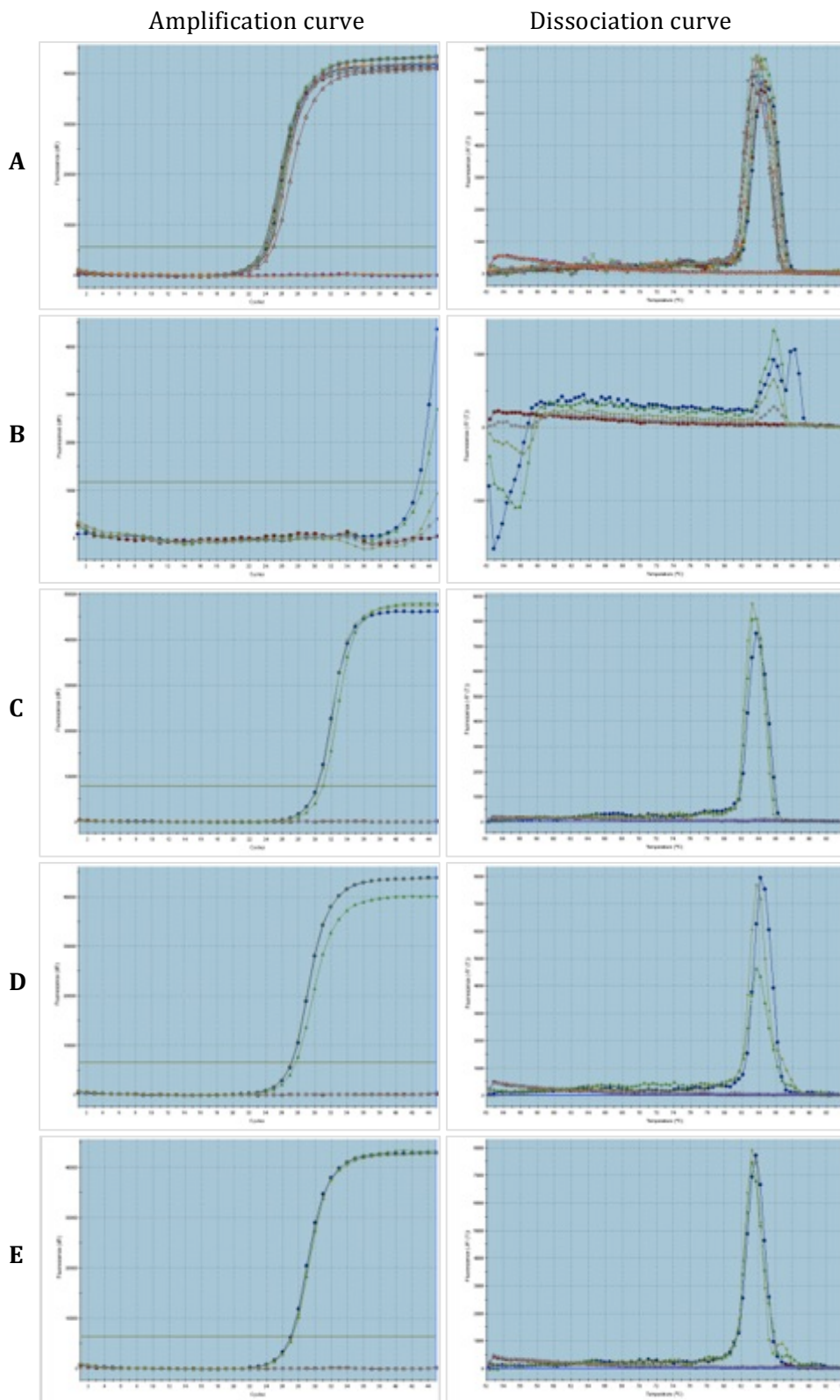


Figure 3.26 (Continued in next page)

Figure 3.26 (Continued from previous page) The qPCR profiles for *NbCYP71D20* and *NbACRE31* gene expressions in SCR1 and GFP treated plants. The qPCR was carried out 2nd and 4th day after treatment. **A)** The endogenous control *NbEF1α* expression levels with 3 replicates in all four samples including negative control with no template. **B** and **C** are the expression level of *NbCYP71D20* gene with 3 replicates in 2dpi and 4dpi plants, respectively. **D** and **E** are the expression level of *NbACRE31* gene with 3 replicates in 2-dpi and 4-dpi plants, respectively

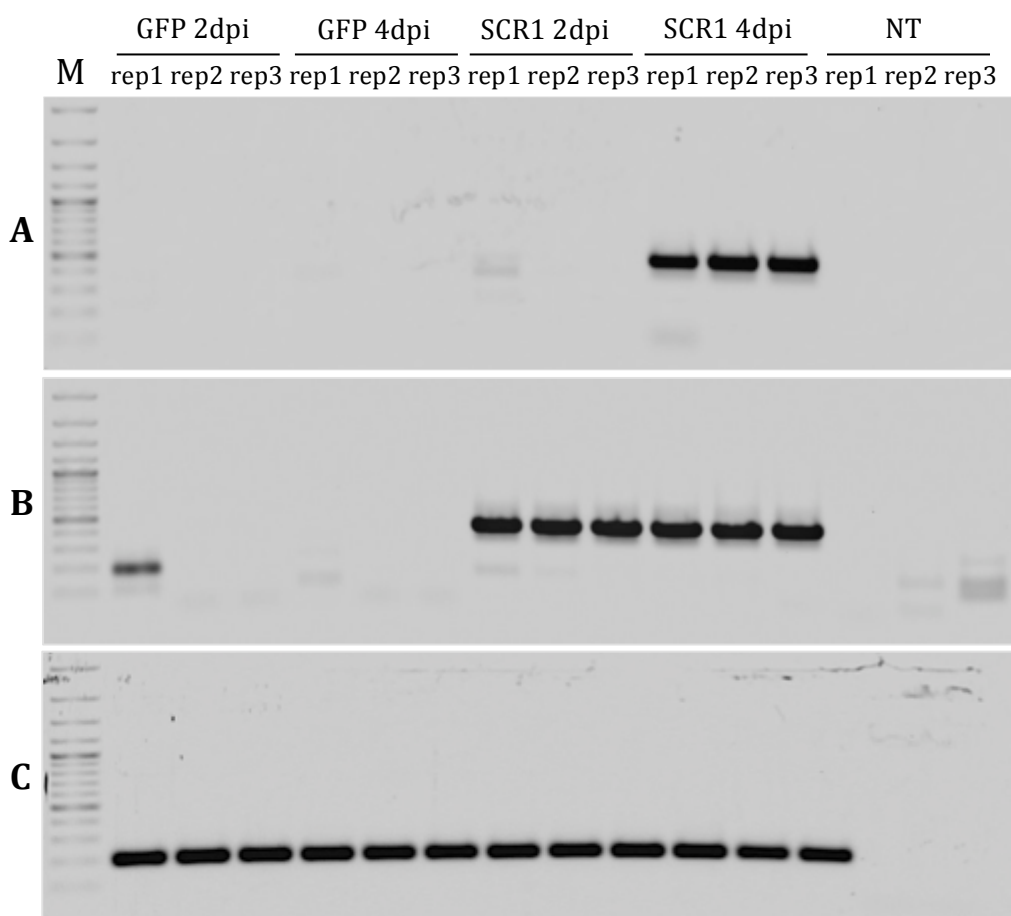


Figure 3.27 The SCR1 treated plants were analyzed by qPCR for defense related genes of *N. benthamiana*. Total RNA was isolated after 2-dpi and 4-dpi. The synthesized cDNAs were subjected to PCR using **A)** *NbCYP71D20*, **B)** *NbACRE31* or **C)** housekeeping *EF1α* gene specific primers and visualized in an agarose gel.

As it is observed in the Figure 3.26 and 3.27, the defense gene *NbCYP71D20* was expressed in the 4-dpi but not in the 2-dpi in SCR1 protein injected leaves. However, *NbACRE31* gene expression was observed both in 2- and 4-dpi (Figure 3.26 and 3.27). The *NbACRE31* was activated stably after the treatment of the effector but *NbCYP71D20* took place later. The SCR1 protein activated these two genes at different time point, independent from each other. In control leaves treated with GFP, there were no expressions of these defense genes.

In contrast to the expectation of HR when the leaves were injected with isolated SCR1 (Appendix K) or total protein with SCR1 (Appendix L) into the leaves of *N. benthamiana*, we observed no HR. This is obviously not due to the limited amount of protein injected, since the apoplastic fluid possesses a lesser amount of PstSCR1 than in pure and total protein samples (Figure 3.24). Therefore, it may be possible that the content of apoplastic fluid; other factors such as pH, reducing or oxidizing environment of the apoplast are required for the effector to stimulate HR. Alternatively, presence of DTT in the total protein extract and the purified PstSCR1 may be changing the atmosphere of the apoplast for the effector to function to stimulate HR. However, to trigger the immune response by purified PstSCR1 injection suffices the PTI with no HR, since it induces the BAK1 dependent defense genes (Figure 3.26 and 3.27).

3.11 Limitations of conducting expression of proteins in wheat

Ideally, it is the most appropriate to conduct the experiments for investigating the function of effectors in their own host plants. However, Agrobacterium-mediated transient expression a foreign protein on the leaves of wheat is not efficient, since studied strains of *Agrobacterium* are not infective to deliver T-DNA. Nevertheless, we tried the expression of PstSCR1 and GFP on wheat leaves by Agrobacterium-mediated gene transfer; GFP fluorescence was not detectable (data not shown) in spite of using different combinations of vector constructs (pTRBO/GFP,

pK7FWG2/effectector candidate constructs) and *Agrobacterium* strains (GV3101, LBA4404 and COR308). In addition to this, Akkaya lab group applied type III secretion system (T3SS) for protein delivery using *Pseudomonas fluorescens* (Ethan) to express *Pst* effector candidates, including PstSCR1, which were cloned in pEDV6 vector on various differential wheat lines of yellow rust. However, the results were inconsistent in the biological replicates for assessing cell death. The naked bacteria (no effector) treatments were not consistent either. We are suspecting that *Pseudomonas fluorescens* requires very narrow margin of optimum conditions for infection and effective protein delivery, which are difficult to attain for reproducible data.

We also treated wheat strains, *Avoset-S*, *Siete Cerros* and *Super Kauz*, with apoplastic fluid with SCR1 and purified SCR1. Interestingly, the wheat leaves showed no indication of cell death as observed in *N. benthamiana* (Figure 3.17). This is because the amount of SCR1 in the samples was not enough to trigger cell death in host plant wheat. Another explanation might be SCR1 interaction with *N. benthamiana* being non-host induced cell death.

CHAPTER IV

CONCLUSION

Although, there are remarkable efforts on the identification of cytoplasmic and apoplastic pathogen effectors (Djamei *et al.*, 2011; Dou and Zhou, 2012; Fernandez *et al.*, 2012), the information on their biochemical and biological roles in plant defense are limited (Doehlemann and Hemetsberger, 2013; van Esse *et al.*, 2006). Apoplast is important for plants to activate initial defense responses upon pathogen invasions. A large number of apoplastic effectors are found to be small cysteine-rich proteins (Kamoun, 2006). Most often, they have multiple disulfide bonds, possibly for maintaining the stability in protease-abundant apoplast. They are also known to induce plant defenses such as cell death (Kamoun, 2006; Chen *et al.*, 2015).

The search in identification of effectors of wheat yellow rust disease causing agent, *Puccinia striiformis* f. sp. *tritici*, is intensified in recent years. Although a number of candidate effectors of *Pst* has been predicted, very recently a few of them were experimentally studied for subcellular localizations (Petre *et al.*, 2016). An effector of *Pst* identified as EST was selected for investigation in this thesis. The aim was functionally analyze the small cysteine rich secreted effector, PstSCR1, from wheat pathogen *Pst*, on the model plant *N. benthamiana*.

The candidate effector was shown i) to be expressed in a most appropriate model plant *N. benthamiana* as a fusion construct with red and green fluorescent proteins in apoplast; ii) This observation was also confirmed by western blotting with the apoplastic fluid of the samples collected from the PstSCR1 expressing plants; iii) when the PstSCR1 was expressed up on the inoculation with the host pathogens of *N.*

benthamiana, it was shown that the symptoms of disease were significantly reduced; iv) overexpression of PstSCR1 in *N. benthamiana* was resulted in cell death, suggesting the effector is likely to function in PAMP-triggered immunity (PTI); v) functioning of the effector as PTI agent was tested by means of two approaches. First, in *BAK1/SERK3* silenced *N. benthamiana*, cell death was remarkably abated after treatment of apoplastic fluid extracted from *N. benthamiana* expressing PstSCR1. Secondly; purified SCR1 injection resulted in activation of defense genes *NbCYP71D20* and *NbACRE31* on *N. benthamiana*. Based on the results conducted in *N. benthamiana*, we concluded that PstSCR1, as a small cysteine-rich effector of *Pst*, is secreted to apoplast causing cell death in defense as a PTI dependent manner.

Since PstSCR1 awakes plant defense response, it can be utilized for plant improvement as an elicitor. Transgenic plants expressing elicitors are found to be a good strategy to stimulate plant resistance against to broad-spectrum of pathogens (Cai *et al.*, 2007; Choi *et al.*, 2004; Keller *et al.*, 1999; Vidhyasakaran, 2016). For example, transgenic tobacco expressing the elicitor cryptogein gene from *Phytophthora cryptogea*, under the control of tobacco pathogen-inducible promoter, demonstrated resistance against several pathogens without any harmful effect on the plants (Keller *et al.*, 1999). In another study, the pemG1 elicitor from rice blast pathogen constitutively expressed by maize ubiquitin 1 promoter in rice transgenic plant showed elevated resistance to *Magnaporthe oryzae* (Qui *et al.*, 2009).

In this study, we demonstrated that the biological role of PstSCR1, secreted to apoplast is causing cell death *via* PTI response, however, until a biochemical function, its structure, modifications, and interactions with other factors (self or host) are determined, precise molecular mechanism of how it facilitates cell death awaits to be fully understood. Unfortunately, our attempts to obtain the X-ray structure of the effector expressed in *E. coli* was not realized since the crystallization failed, most likely due to the improper folding. Although it can be proposed that disulfide bonds may form solely to sustain the stability or cysteine amino acids may be involved in metal coordination bonds of apoplastic effectors, they may also regulate redox

(Khalimonchuk and Winge, 2008; Rodinovich and Weiss, 2010). This is especially probable for an effector secreted and causing HR in apoplast, where the fluctuation of pH and the formation of reactive oxygen species take place upon biotic stress (Bolwell *et al.*, 2002; Jashni *et al.*, 2015). Interestingly, the adjacent cysteine amino acids (-CC-) have been shown that they can form an eight membered ring by disulfide bond formation to each other, which is found to be less stable than interrupted cysteines (CxC-) (Maiorino *et al.*, 2005; Miller *et al.*, 1989; Park and Raines, 2001). Thus, it can be speculated that the effector may assume in an active or inactive forms pH and/or redox dependent manner by the oxidation and the reduction of the adjacent -CC- with each other or other intra-cysteines, leading to switching back and forth as a dimer or a monomer.

This study revealed that PstSCR1 is an apoplastic effector, a first from *Pst* that activates immune response by being dependent on plant surface receptor or by inducing formation of other cellular elicitors. It should be noted that this study was carried out on the model plant *N. benthamiana*, therefore further research is required on broad host range to confirm its role as an effector in PTI.

REFERENCES

- Abbal, P., Pradal, M., Muniz, L., Sauvage, F.X., Chatelet, P., Ueda, T. and Tesniere, C. (2008) Molecular characterization and expression analysis of the Rab GTPase family in *Vitis vinifera* reveal the specific expression of a VvRabA protein. *J Exp Bot.*, 59, 2403–2416.
- Albrecht, M. and Takken, F.L.W. (2006) Update on the domain architectures of NLRs and R proteins. *Biochemical and Biophysical Research Communications*, 339, 459-462.
- Badel, J.L., Piquerez, S.J., Greenshields, D., Rallapalli, G., Fabro, G., Ishaque, N. and Jones, J.D.G. (2013) In planta effector competition assays detect *Hyaloperonospora arabidopsis* effectors that contribute to virulence and localize to different plant subcellular compartments. *Mol. Plant-Microbe Interact.*, 26, 745–757.
- Bigeard, J., Colcombet, J. and Hirt H. (2015) Signaling mechanisms in pattern-triggered immunity (PTI). *Mol. Plant*, 8, 521–539.
- Bittner-Eddy, P.D., Allen, R.L., Rehmany, A.P., Birch, P., Beynon, J.L. (2003) Use of suppression subtractive hybridization to identify downy mildew genes expressed during infection of *Arabidopsis thaliana*. *Mol. Plant Pathol.*, 4, 501–507.
- Boevink, P.C., Birch, P.R. and Whisson, S.C. (2011) Imaging fluorescently tagged Phytophthora effector proteins inside infected plant tissue. *Methods Mol. Biol.*, 712, 195–209.
- Bohnert, H.U., Fudal, I., Dioh, W., Tharreau, D., Notteghem, J-L., and Lebrun, M.H. (2004) A putative polyketide synthase/peptide synthetase from *Magnaporthe grisea* signals pathogen attack to resistant rice. *Plant Cell*, 16, 2499–2513.

Bolton, M.D., van Esse, H.P., Vossen, J.H., De Jonge, R., Stergiopoulos, I., et al. (2008) The novel *Cladosporium fulvum* lysin motif effector Ecp6 is a virulence factor with orthologues in other fungal species. *Mol. Microbiol.*, 69, 119–136.

Bolwell, G.P., Bindschedler, L.V., Blee, K.A., Butt, V.S., Davies, D.R., Gardner, S.L., Gerrish, C. and Minibayeva, F. (2002) The apoplastic oxidative burst in response to biotic stress in plants: a three-component system. *J. Exp. Bot.*, 53, 1367–1376.

Bombarely, A., Rosli, H.G., Vrebalov, J., Moffett, P., Mueller, L.A. and Martin, G.B. (2012) A draft genome sequence of *Nicotiana benthamiana* to enhance molecular plant-microbe biology research. *Mol. Plant-Microbe Interact.*, 25, 1523–1530.

Bos, J. I. B., Armstrong, M. R., Gilroy, E. M., Boevink, P. C., Hein, I., Taylor, R. M., Zhendong, T., et al. (2010) Phytophthora infestans effector AVR3a is essential for virulence and manipulates plant immunity by stabilizing host E3 ligase CMPG1. *Proceedings of the National Academy of Sciences, USA*, 107, 9909-9914.

Bos, J.I.B., Armstrong, M., Whisson, S.C., Torto, T., Ochwo, M., et al. (2003) Intraspecific comparative genomics to identify avirulence genes from *Phytophthora*. *New Phytol.*, 159, 63–72.

Bozkurt, O. (2007) Determination of genes involved in the yellow rust disease of wheat (Doctoral dissertation). Retrieved from <http://etd.lib.metu.edu.tr/upload/12608246/index.pdf>.

Bozkurt, T.O., Richardson, a., Dagdas, Y.F., Mongrand, S., Kamoun, S. and Raffaele, S. (2014) The Plant Membrane-Associated REMORIN1.3 Accumulates in Discrete Perihastorial Domains and Enhances Susceptibility to *Phytophthora infestans*. *Plant Physiol.*, 165, 1005–1018.

Bozkurt, T.O., Schornack, S., Banfield, M.J. and Kamoun, S. (2012) Oomycetes, effectors, and all that jazz. *Curr. Opin. Plant Biol.*, 15, 483–492.

Bozkurt, T.O., Schornack, S., Win, J., Shindo, T., Ilyas, M., Oliva, R. Cano, L.M., Jones, A.M., Huitema E, van der Hoorn, R.A. and Kamoun, S. (2011) *Phytophthora infestans* effector AVRblb2 prevents secretion of a plant immune protease at the haustorial interface. *Proc. Natl. Acad. Sci. U.S.A.*, 108, 20832–208327.

Brown, J. F., & Sharp, E. L. (1969) Interactions of minor host genes for resistance to *Puccinia striiformis* with changing temperatures. *Phytopathology*, 59, 999–1001.

Cai, X.Z., Zhou, X., Xu, Y.P., Joosten, M.H., and de Wit, P.J. (2007) *Cladosporium fulvum* CfHNNI1 induces hypersensitive necrosis, defence gene expression and disease resistance in both host and nonhost plants. *Plant Mol. Biol.*, 64, 89–101.

Caillaud, M.C., Piquerez, S.J., Fabro, G., Steinbrenner, J., Ishaque, N., Beynon, J., and Jones, J.D. (2012) Subcellular localization of the Hpa RxLR effector repertoire identifies a tonoplast-associated protein HaRxL17 that confers enhanced plant susceptibility. *Plant J.*, 69, 252-65.

Cantu, D., Govindarajulu, M., Kozik, A., Wang, M., Chen, X., Kojima, K.K., Jurka, J., Michelmore, R.W. and Dubcovsky, J. (2011) Next generation sequencing provides rapid access to the genome of *Puccinia striiformis* f. sp. *tritici*, the causal agent of wheat stripe rust. *PLoS ONE*, 6, e24230.

Cantu, D., Segovia, V., MacLean, D., Bayles, R., Chen, X., Kamoun, S., Dubcovsky, J., Saunders, D.G. and Uauy, C. (2013) Genome analyses of the wheat yellow (stripe) rust pathogen *Puccinia striiformis* f. sp. *tritici* reveal polymorphic and haustorial expressed secreted proteins as candidate effectors. *BMC Genomics*, 14, 270.

Catanzariti AM, Dodds PN, Lawrence GJ, Ayliffe MA, Ellis JG. 2006. Haustorially expressed secreted proteins from flax rust are highly enriched for avirulence elicitors. *Plant Cell*, 18, 243–56.

Chaparro-Garcia A, Schwizer S, Sklenar J, Yoshida K, Petre B, Bos JIB, Schornack S, Jones AME, Bozkurt TO, Kamoun S et al., (2015) Phytophthora infestans RXLR-WY Effector AVR3a Associates with Dynamin-Related Protein 2 Required for Endocytosis of the Plant Pattern Recognition Receptor FLS2, *PLOS ONE*, 10, 1932-6203.

Chaparro-Garcia, A., Wilkinson, R.C., Gimenez-Ibanez, S., Findlay, K., Coffey M.D., Zipfel, C., Rathjen, J.P., Kamoun, S. and Schornack, S. (2011) The Receptor-Like Kinase SERK3/BAK1 Is Required for Basal Resistance against the Late Blight Pathogen *Phytophthora infestans* in *Nicotiana benthamiana*. *PLoS ONE*, 6, e16608.

Chen XL, Shi T, Yang J, Shi W, Gao X, Chen D, Xu X, Xu JR, Talbot NJ, Peng YL. 2014. N-Glycosylation of effector proteins by an alpha-1,3-mannosyltransferase is required for the rice blast fungus to evade host innate immunity. *Plant Cell*, 26, 1360–1376.

Chen, X. M. (2005) Review / Synthèse Epidemiology and control of stripe rust [Puccinia striiformis f. sp . tritici] on wheat, *Canadian Journal of Plant Pathology*, 27, 314-337.

Chen, X-R., Li, Y-P., Li, Q-Y., Xing, Y-P., Liu, B-B., Tong, Y-H. and Xu, J-Y. (2015) SCR96, a small cysteine-rich secretory protein of *Phytophthora cactorum*, can trigger cell death in the Solanaceae and is important for pathogenicity and oxidative stress tolerance. *Mol. Plant Pathol.*, [Epub ahead of print].
10.1111/mpp.12303

Chinchilla, D., Zipfel, C., Robatzek, S., Kemmerling, B., Nürnberger, T., Jones, J.D.G., Felix, G. and Bolle, T. (2007) A flagellin-induced complex of the receptor FLS2 and BAK1 initiates plant defence. *Nature*, 448, 497–500.

Choi, J.J., Klosterman, S.J., and Hadwiger, L.A. (2004) A promoter from pea gene DRR206 is suitable to regulate an elicitor-coding gene and develop disease resistance. *Phytopathol.*, 94, 651–660.

Dagdas, Y.F., Belhaj, K., Maqbool, A., Chaparro-Garcia, A., Pandey, P., Petre, B., Tabassum, N., Cruz-Mireles, N., Hughes, R.K., Sklenar, J., Win, J., Menke, F., Findlay, K., Banfield, M.J., Kamoun, S. and Bozkurt, T.O. (2016) An effector of the Irish potato famine pathogen antagonizes a host autophagy cargo receptor. *eLife*, 5, e10856.

de Jonge, R., Bolton, M.D. and Thomma, B.P. (2011) How filamentous pathogens co-opt plants: the ins and outs of fungal effectors. *Curr. Opin. Plant Biol.*, 14, 400–406.

Dixon, M.S., Jones, D.A., Keddie, J.S., Thomas, C.M., Harrison, K. and Jones, J.D.G. (1996) The tomato Cf-2 disease resistance locus comprises two functional genes encoding leucine-rich repeat proteins. *Cell*, 84, 451–459.

Djamei, A., Schipper, K., Rabe, F., Ghosh, A., Vincon, V., Kahnt, J., Osorio, S., Tohge, T., Fernie, A.R., Feussner, I., Feussner, K., Meinicke, P., Steirhof, Y.D., Schwarz, H., Macek, B., Mann, M. and Kahmann, R. (2011) Metabolic priming by a secreted fungal effector. *Nature*, 478, 395–398.

Doehlemann, G. and Hemetsberger, C. (2013) Apoplastic immunity and its suppression by filamentous plant pathogens. *New Phytol.*, 198, 1001–1016.

Dodds, P. N. and Rathjen, J. P. (2010) Plant immunity: towards an integrated view of plant-pathogen interactions. *Nature Reviews Genetics*, 11(8), 539–48.

Dodds PN, Lawrence GJ, Catanzariti AM, Ayliffe MA, Ellis JG. (2004) The *Melampsora lini* AvrL567 avirulence genes are expressed in haustoria and their products are recognized inside plant cells. *Plant Cell*, 16, 755–68.

Dou, D. and Zhou, J-M. (2012) Phytopathogen Effectors Subverting Host Immunity: Different Foes, Similar Battleground. *Cell Host Microbe*, 12, 484–495.

Dowen, R.H., Engel, J.L., Shao, F., Ecker, J.R. and Dixon, J.E. (2009) A family of bacterial cysteine protease type III effectors utilizes acylation-dependent and -

independent strategies to localize to plasma membranes. *J. Biol. Chem.*, 284, 15867–15879.

Duplessis, S., Cuomo, C.A., Lin, Y.C., Aerts, A., Tisserant, E., Veneault-Fourrey, C., Joly, D.L., Hacquard, S., Amselem, J., Cantarel, B., Chiu, R., Coutinho, P., Feau, N., Field, M., Frey, P., Gelhaye, E., Goldberg, J., Grabherr, M., Kodira, C., Kohler, A., Hües, U., Lindquist, E.A., Lucas, S., Mago, R., Mauceli, E., Morin, E., Murat, C., Pangilinan, J.L., Park, R., Pearson, M., Quesneville, H., Rouhier, N., Sakthikumar, S., Schmutz, J., Selles, B., Shapiro, H., Tanguay, P., Tuskan, G.A., Henrissat, B., Van de Peer, Y., Rouzé, P., Ellis, J.G., Dodds, P.N., Schein, J.E., Zhong, S., Hamelin, R.C., Grigoriev, I.V., Szabo, L.J. and Martin, F. (2011) Obligate biotrophy features unravelled by the genomic analysis of rust fungi. *Proc. Natl. Acad. Sci. U.S.A.*, 108, 9166–9171.

Earley, K. W., Haag, J. R., Pontes, O., Opper, K., Juehne, T., Song, K., & Pikaard, C. S. (2006) Gateway-compatible vectors for plant functional genomics and proteomics. *The Plant Journal*, 45(4), 616-629.

Eriksson, J., & Henning, E. (1896) Die Getreideroste. Ihre Geschichte und Natur sowie Massregeln gegen Dieselben. Verlag von P. A. Norstedt & Soner, Stockholm.

Fang, A., Han, Y., Zhang, N., Zhang, M., Liu, L., Li, S., Lu, F. and Sun, W. (2016) Identification and Characterization of Plant Cell Death–Inducing Secreted Proteins From *Ustilaginoidea virens*. *Mol. Plant Microbe-Interact.*, 29, 405-416.

Farman, M.L., Eto, Y., Nakao, T., Tosa, Y., Nakayashiki, H., et al. (2002) Analysis of the structure of the AVR1-CO39 avirulence locus in virulent rice-infecting isolates of *Magnaporthe grisea*. *Mol. Plant-Microbe Interact.*, 15, 6–16.

Fellbrich, G., Romanski, A., Varet, A., Blume, B., Brunner, F., et al. (2002) NPP1, a *Phytophthora*-associated trigger of plant defense in parsley and *Arabidopsis*. *Plant J.*, 32, 375–390.

- Fernandez, D., Tisserant, E., Talhinas, P., Azinheira, H., Vieira, A., Petitot, A.S., Loureiro, A., Poulain, J., Da Silva, C., Silva Mdo, C. and Duplessis, S. (2012) 454-pyrosequencing of *Coffea arabica* leaves infected by the rust fungus *Hemileia vastatrix* reveals in planta-expressed pathogen-secreted proteins and plant functions in a late compatible plant–rust interaction. *Mol. Plant Pathol.*, 13, 17–37.
- Filichkin, S.A., Leonard, J.M., Monteros, A., Liu, P.P. and Nonogaki, H. (2004) A novel endo-beta-mannanase gene in tomato *LeMAN5* is associated with anther and pollen development. *Plant Physiol.*, 134, 1080-1087.
- Fudal, I., Bohnert, H.U., Tharreau, D. and Lebrun, M.H. (2005) Transposition of MINE, a composite retro- transposon, in the avirulence gene ACE1 of the rice blast fungus *Magnaporthe grisea*. *Fungal Genet. Biol.*, 42,761–72.
- Gamm, M., Héloir, M-C., Kelloniemi, J., Poinsot, B., Wendehenne, D. and Adrian, M. (2011) Identification of reference genes suitable for qRT-PCR in grapevine and application for the study of the expression of genes involved in pterostilbene synthesis. *Molecular Genetics and Genomics*, 285, 273 – 285.
- Giannakopoulou, A., Steele, J.F., Segretin, M.E., Bozkurt, T., Zhou, J., Robatzek, S., Banfield, M.J., Pais, M. and Kamoun, S. (2015) Tomato I2 immune receptor can be engineered to confer partial resistance to the oomycete *Phytophthora infestans* in addition to the fungus *Fusarium oxysporum*. *Mol. Plant-Microbe Interact.*, 28, 1316–1329.
- Gilroy EM, Taylor RM, Hein I, Boevink P, Sadanandom A, Birch PRJ (2011) CMPG1-dependent cell death follows perception of diverse pathogen elicitors the host plasma membrane and is suppressed by *Phytophthora infestans* RXLR effector AVR3a. *New Phytologist*, 6y, 653–666.
- Godfrey, D., Böhlenius, H., Pedersen, C., Zhang, Z., Emmersen, J. and Thordal-Christensen, H. (2010) Powdery mildew fungal effector candidates share N-terminal Y/F/WxC-motif. *BMC Genomics*, 11, 317-329.

Gout, L., Fudal, I., Kuhn, M.L., Blaise, F., Eckert, M., et al. (2006) Lost in the middle of nowhere: the AvrLm1 avirulence gene of the *Dothideomycete* *Leptosphaeria maculans*. *Mol. Microbiol.*, 60, 67–80.

Hacquard, S., Joly D.L., Lin, Y-C., Tisserant, E., Feau, N., Delaruelle, C., Legué, V., Kohler, A., Tanguay, P., Petre, B., Frey, P., Van de Peer Y., Rouzé, P., Martin, F., Hamelin, R.C. and Duplessis, S. (2012) A comprehensive analysis of genes encoding small secreted proteins identifies candidate effectors in *Melampsora larici-populina* (poplar leaf rust). *Mol. Plant-Microbe Interact.*, 25, 279–293.

Hartley, J. L. (2000) DNA Cloning Using In Vitro Site-Specific Recombination. *Genome Research*, 10, 1788-1795.

Hall, R. (2004) Co-immunoprecipitation as a strategy to evaluate receptor–receptor or receptor–protein interactions. *Receptor Biochemistry and Methodology*. John Wiley & Sons, Inc, 165–178.

Houterman, P.M., Speijer, D., Dekker, H.L., De Koster, C.G., Cornelissen, B.J.C. and Rep, M. (2007) The mixed xylem sap proteome of *Fusarium oxysporum*-infected tomato plants. *Molecular Plant Pathol.*, 8, 215–221.

He K., Gou X., Yuan T., Lin H., Asami T., Yoshida S., Russell S.D. and Li J. (2007). BAK1 and BKK1 regulate brassinostroid-dependent growth and brassinostroid-independent cell-death pathways. *Curr. Biol.*, 17, 1109–1115.

Hecht, V., Vielle-Calzada, J.P., Hartog, M.V., Schmidt, E.D.L., Boutilier, K., Grossniklaus, U. and de Vries, S.C. (2001) The *Arabidopsis SOMATIC EMBRYOGENESIS RECEPTOR KINASE 1* gene is expressed in developing ovules and embryos and enhances embryogenic competence in culture. *Plant Physiol.*, 127, 803-816.

Heese, A., Hann, D.R., Gimenez-Ibanez, S., Jones, A.M.E., He, K., Li, J., Schroeder, J.I., Peck, S.C., and Rathjen, J.P. (2007) The receptor-like kinase SERK3/BAK1 is a

central regulator of innate immunity in plants. *Proc. Natl. Acad. Sci. U.S.A.*, 104, 12217–12222.

Hematy, K., Cherk, C. and Somerville, S. (2009) Host-pathogen warfare at the plant cell wall. *Curr. Opin. Plant Biol.* 12, 406–413.

Hoson T. 1998. Apoplast as the side of response to environmental signals. *Journal of Plant Research* 111: 167–177.

Jashni, M. K., Mehrabi, R., Collemare, J., Mesarich, C. H. and de Wit, P. (2015) The battle in the apoplast: Further insights into the roles of proteases and their inhibitors in plant-pathogen interactions. *Front. Plant Sci.*, 6, 584.

Jones D.A. and Jones,J.D.G. (1997) The role of leucine-rich repeat proteins in plant defences. *Adv. Bot. Res.*, 24, 89–167.

Jones, J. D. G., & Dangl, J. L. (2006) The plant immune system. *Nature*, 444, 323–329.

Joosten, M.H.A.J., Cozijnsen, T.J. and De Wit, P.J.G.M. (1994) Host resistance to a fungal tomato pathogen lost by a single base-pair change in an avirulence gene. *Nature*, 367, 384–386.

Kamoun, S. (2006) A catalogue of the effector secretome of plant pathogenic oomycetes. *Annu. Rev. Phytopathol.*, 44, 41–60.

Kamoun, S., van West, P., de Jong, A.J., de Groot, K., Vleeshouwers, V., Govers, F. (1997a) A gene encoding a protein elicitor of *Phytophthora infestans* is down-regulated during infection of potato. *Mol. Plant Microbe. Interact.*, 10, 13–20.

Kamoun, S., Lindqvist, H. and Govers, F. (1997b) A novel class of elicitin-like genes from *Phytophthora infestans*. *Mol. Plant Microbe. Interact.*, 10, 1028–1030.

Kang, S., Sweigard, J.A. and Valent, B. (1995) The PWL host specificity gene family in the blast fungus *Magnaporthe grisea*. *Mol. Plant-Microbe Interact.*, 8, 939–948.

Karimi, M., Inzé, D., & Depicker, A. (2002) Gateway vectors for Agrobacterium-mediated plant transformation. *Trends in Plant Science*. 7, 193-195.

Keller, H., Pamboukdjian, N., Ponchet, M., Poupet, A., Delon, R., Verrier, J.L., Roby, D. and Ricci, P. (1999) Pathogen-induced elicitin production in transgenic tobacco generates a hypersensitive response and nonspecific disease resistance. *Plant Cell*, 11, 223–235.

Khalimonchuk, O. and Winge, D.R. (2008) Function and redox state of mitochondrial localized cysteine-rich proteins important in the assembly of cytochrome c oxidase. *Biochim. Biophys. Acta.*, 1783, 618–628.

Khang, C.H., Park, S.Y., Lee, Y.H., Valent, B. and Kang, S. (2008) Genome organization and evolution of the AVR-pita avirulence gene family in the *Magnaporthe grisea* species complex. *Mol. Plant-Microbe Interact.*, 21, 658–670.

Kim, H.J. and Ryu, S.B (2014) sPLA₂ and PLA₁: Secretory Phospholipase A₂ and Phospholipase A₁ in Plants. In: Wang, X. ed. *Phospholipases in Plant Signaling*. Springer, Heidelberg, 109–118.

Lauge, R., Goodwin, P.H., De Wit, P.J.G.M. and Joosten, M.H.A.J. (2000) Specific HR-associated recognition of secreted proteins from *Cladosporium fulvum* occurs in both host and non-host plants. *Plant J.*, 23, 735–745.

Lee, H.A., Kim, S.Y., Oh, S.K., Yeom, S.I., Kim, S.B., Kim, M.S., Kamoun, S. and Choi, D. (2014) Multiple recognition of RXLR effectors is associated with nonhost resistance of pepper against *Phytophthora infestans*. *New Phytol.*, 203, 926–938.

- Lee, L. Y., & Gelvin, S. B. (2008) T-DNA binary vectors and systems. *Plant Physiology*, 146, 325-332.
- Leipe, D.D., Koonin, E.V. and Aravind, L. (2004) STAND, a class of P-loop NTPases including animal and plant regulators of programmed cell death: multiple, complex domain architectures, unusual phyletic patterns, and evolution by horizontal gene transfer. *Journal of Molecular Biology*, 343, 1-28.
- Li, J., Wen, J., Lease, K.A., Doke, J.T., Tax, F.E., and Walker, J.C. (2002). BAK1, an *Arabidopsis* LRR receptor-like protein kinase, interacts with BRI1 and modulates brassinosteroid signaling. *Cell*, 110, 213–222.
- Lindbo, J. A. (2007) TRBO: a high-efficiency tobacco mosaic virus RNA-based overexpression vector. *Plant Physiology*, 145, 1232-1240.
- Liu, Z., Bos, J.I.B., Armstrong, M., Whisson, S.C., da Cunha, L., et al. (2005) Patterns of diversifying selection in the phytotoxin-like scr74 gene family of *Phytophthora infestans*. *Mol. Biol. Evol.*, 22, 659–672.
- Liu, Y., Schiff, M. and Dinesh-Kumar, S. P. (2002) Virus-induced gene silencing in tomato. *Plant J.*, 31, 777–786.
- Liu, D., Shi, L., Han, C., Yu, J., Li, D. and Zhang, Y. (2012) Validation of Reference Genes for Gene Expression Studies in Virus-Infected *Nicotiana benthamiana* Using Quantitative Real-Time PCR. *PLoS ONE*, 7, e46451.
- Livak, K.J. and Schmittgen, T.D. (2001) Analysis of relative gene expression data using real-time quantitative PCR and the $2\Delta\Delta C(T)$ Method. *Methods*, 25, 402–408.
- Lund, S.T., Peng, F.Y., Nayar, T., Reid, K.E. and Schlosser, J. (2008) Gene expression analyses in individual grape (*Vitis vinifera L.*) berries during ripening initiation reveal that pigmentation intensity is a valid indicator of developmental staging within the cluster. *Plant Mol. Biol.*, 68, 301–315.

Ma, Z., Song, T., Zhu, L., Ye, W., Wang, Y., Shao, Y., Dong, S., Zhang, Z., Dou, D., Zheng, X., Tyler, B.M. and Wang, Y. (2015) A *Phytophthora sojae* Glycoside Hydrolase 12 Protein Is a Major Virulence Factor during Soybean Infection and Is Recognized as a PAMP. *Plant Cell*, 27, 2057–2072.

Macfarlane, S.A. (1999). Molecular biology of the tobaviruses. *J. Gen. Virol.*, 80, 2799–2807

Maddison, A. C., & Manners, J. G. (1972) Sunlight and viability of cereal rust uredospores. *Transaction of British Mycological Society*. 59, 429–443.

Maiorino, M., Roveri, A., Benazzi, L., Bosello, V., Mauri, P., Toppo, S., Tosatto, S.C.E. and Ursini, F. (2005) Functional interaction of phospholipid hydroperoxide glutathione peroxidase with sperm mitochondrion-associated cysteine-rich protein discloses the adjacent cysteine motif as a new substrate of the selenoperoxidase. *J. Biol. Chem.*, 280, 38395–38402.

Marillonnet S, Thoeringer C, Kandzia R, Klimyuk V, Gleba Y (2005) Systemic Agrobacterium tumefaciens-mediated transfection of viral replicons for efficient transient expression in plants. *Nat. Biotechnol.*, 23, 718–723.

Markell, S., Milus, E.A., Cartwright, R., & Hedge, J. (2006) Rust diseases of wheat. *University of Arkansas. CES FSA*, 7547, 1-4.

Martin, G. B. (1999) Functional analysis of plant disease resistance genes and their downstream effectors. *Current Opinion in Plant Biology*, 2, 273-279.

McHale, L., Tan, X., Koehl, P., & Michelmore, R. W. (2006). Plant NBS-LRR proteins: adaptable guards. *Genome Biology*, 7, 212.

Miller, S.M., Moore, M.J., Massey, V., Williams, C.H., Jr., Distefano, M.D., Ballou, D.P. and Walsh, C.T. (1989) Evidence for the participation of Cys558 and Cys559 at the active site of mercuric reductase. *Biochemistry*, 28, 1194–1205.

- Morais do Amaral, A., Antoniw, J., Rudd, J.J. and Hammond-Kosack, K.E. (2012) Defining the Predicted Protein Secretome of the Fungal Wheat Leaf Pathogen *Mycosphaerella graminicola*. *PLoS ONE*, 7, e49904.
- Nakagawa, T., Suzuki, T., Murata, S., Nakamura, S., Hino, T., Maeo, K., Tabata, R., Kawai, T., Tanaka, K., Niwa, Y., Watanabe, Y., Nakamura, K., Kimura, T. and Ishiguro, S. (2007) Improved Gateway binary vectors: high performance vectors for creation of fusion constructs in transgenic analysis of plants. *Biosci. Biotechnol. Biochem.*, 71, 2095–2100.
- Nam, K.H., and Li, J. (2002). BRI1/BAK1, a receptor kinase pair mediating brassinosteroid signaling, *Cell*, 110, 203–212.
- Nurnberger, T., Nennstiel, D., Jabs, T., Sacks, W.R., Hahlbrock, K. and Scheel, D. (1994) High affinity binding of a fungal oligopeptide elicitor to parsley plasma membranes triggers multiple defense responses. *Cell*, 78, 449–460.
- O'Leary, B.M., Rico, A., McCraw, S., Fones, H.N. and Preston, G.M. (2014) The Infiltration-centrifugation Technique for Extraction of Apoplastic Fluid from Plant Leaves Using *Phaseolus vulgaris* as an Example. *J. Vis. Exp.*, 94, e52113.
- Oliva, R., Win, J., Raffaele, S., Boutemy, L., Bozkurt, T.O., Chaparro-Garcia, A., Segretain, M.E., Stam, R., Schornack, S., Cano, L.M., van Damme, M., Huitema, E., Thines, M., Banfield, M.J. and Kamoun, S. (2010) Recent developments in effector biology of filamentous plant pathogens. *Cell. Microbiol.*, 12, 705–715.
- Olsen, K.M., Hehn, A., Jugde, H., Slimestad, R., Larbat, R., Bourgaud, F. and Lillo, C. (2010) Identification and characterisation of CYP75A31, a new Flavonoid 35-hydroxylase, isolated from *Solanum lycopersicum*. *BMC Plant Biol.*, 10, 21.
- Opabode, J. (2006) Agrobacterium-mediated transformation of plants: emerging factors that influence efficiency. *Biotechnology and Molecular Biology Review*, 1, 12–20.

Orbach, M.J., Farrall, L., Sweigard, J.A , Chumley, F.G., Valent,B. (2000) A telomeric avirulence gene determines efficacy for the rice blast resistance gene *Pi-ta*. *Plant Cell*, 12, 2019–2032.

Osman, H., Mikes, V., Milat, M.L., Ponchet, M., Marion, D., et al. (2001) Fatty acids bind to the fungal elicitor cryptogein and compete with sterols. *FEBS Lett.*, 489, 55–58.

Orsomando, G., Lorenzi, M., Ferrari, E., de Chiara, C., Spisni, A. and Ruggieri S. (2003) Pcf protein from *Phytophthora cactorum* and its recombinant homologue elicit phenylalanine ammonia lyase activation in tomato. *Cell. Mol. Life Sci.*, 60, 1470–1476.

Orsomando, G., Lorenzi, M., Raffaelli, N., Dalla Rizza, M., Mezzetti, B. and Ruggieri S. (2001) Phytotoxic protein Pcf, purification, characterization, and cDNA sequencing of a novel hydroxyproline-containing factor secreted by the strawberry pathogen *Phytophthora cactorum*. *J. Biol. Chem.*, 276, 21578–21584.

Park, C. and Raines, R.T. (2001) Adjacent cysteine residues as a redox switch. *Protein Eng.*, 14, 939–942.

Parlange, F., Daverdin, G., Fudal, I., Kuhn, M-L., Balesdent, M-H., et al. (2009) *Leptosphaeria maculans* avirulence gene AvrLm4-7 confers a dual recognition specificity by the Rlm4 and Rlm7 resistance genes of oilseed rape, and circumvents Rlm4-mediated recognition through a single amino acid change. *Mol. Microbiol.*, 71, 851–863.

Petersen, T.N., Brunak, S., von Heijne, G. and Nielsen, H. (2011) SignalP 4.0: discriminating signal peptides from transmembrane regions. *Nature Methods*, 8, 785–786.

Petre, B., Joly, D.L. and Duplessis, S. (2014) Effector proteins of rust fungi. *Front. Plant Sci.*, 5, 416.

- Petre, B., Saunders, D.G.O., Sklenar, J., Lorrain, C., Krasileva, K.V., Win, J., Duplessis, S. and Kamoun, S. (2016) Heterologous expression screens in *Nicotiana benthamiana* identify a candidate effector of the wheat yellow rust pathogen that associates with processing bodies. *PLoS ONE*, 11, e0149035.
- Petre, B., Saunders, D.G., Sklenar, J., Lorrain, C., Win, J., Duplessis, S. and Kamoun, S. (2015) Candidate Effector Proteins of the Rust Pathogen *Melampsora larici-populina* Target Diverse Plant Cell Compartments. *Mol. Plant-Microbe Interact.*, 28, 689–700.
- Pike, L.J. (2006) Rafts defined: a report on the Keystone Symposium on Lipid Rafts and Cell Function. *J. Lipid Res.*, 47, 1597–1598.
- Pitzschke, A., & Hirt, H. (2010) New insights into an old story: Agrobacterium-induced tumour formation in plants by plant transformation. *The EMBO Journal*, 29, 1021-32.
- Qiu, D., Mao, J., Yang, X. and Zeng, H. (2009) Expression of an elicitor-encoding gene from *Magnaporthe grisea* enhances resistance against blast disease in transgenic rice. *Plant Cell Rep.*, 28, 925–933.
- Raffaele, S., Bayer, E., Lafarge, D., Cluzet, S., German Retana, S., Boubekeur, T., Leborgne-Castel, N., Carde, J.P., Lherminier, J., Noirot, E., Satiat-Jeunemaitre, B., Laroche-Traineau, J., Moreau, P., Ott, T., Maule, A.J., Reymond, P., Simon-Plas, F., Farmer, E.E., Bessoule, J.J. and Mongrand S. (2009) Remorin, a Solanaceae protein resident in membrane rafts and plasmodesmata, impairs potato virus X movement. *Plant Cell*, 21, 1541–1555.
- Rafiqi, M., Gan, P.H., Ravensdale, M., Lawrence, G.J., Ellis, J.G., Jones, D.A., Hardham, A.R. and Dodds, P.N. (2010) Internalization of flax rust avirulence proteins into flax and tobacco cells can occur in the absence of the pathogen. *Plant Cell*, 22, 2017-2032.

Rapilly F (1979) Yellow rust epidemiology. *Annu Rev Phytopathol*, 17, 59–73.

Reese, M.G. and Eeckman, F.H. (1995) Novel neural network algorithms for improved eukaryotic promoter site recognition. The Seventh International Genome Sequencing and Analysis Conference, Hilton Head Island.

Rep, M., Meijer, M., Houterman, P.M., Van Der Does, H.C. and Cornelissen, B.J.C. (2005) *Fusarium oxysporum* evades I-3-mediated resistance without altering the matching avirulence gene. *Mol. Plant-Microbe Interact.*, 18, 15–23.

Ricci, P., Bonnet, P., Huet, J-C., Sallantin, M., Beauvais-Cante, F., et al. (1989) Structure and activity of proteins from pathogenic fungi *Phytophthora* eliciting necrosis and acquired resistance in tobacco. *Eur. J. Biochem.*, 183, 555–563.

Ridout, C.J., Skamnioti, P., Porritt, O., Sacristan, S., Jones, J.D.G. and Brown, J.K.M. (2006) Multiple avirulence paralogues in cereal powdery mildew fungi may contribute to parasite fitness and defeat of plant resistance. *Plant Cell*, 18, 2402–2414.

Rigaut, G., Shevchenko, A., Rutz, B., Wilm, M., Mann, M., and Seraphin, B. (1999). A generic protein purification method for protein complex characterization and proteome exploration. *Nature biotechnology*, 17, 1030-1032.

Robinovich, L. and Weiss, D. (2010) The Arabidopsis cysteine-rich protein GASA4 promotes GA responses and exhibits redox activity in bacteria and in *planta*. *The Plant Journal*, 64, 1018-1027.

Rohe, M., Gierlich, A., Hermann, H., Hahn, M., Schmidt, B., et al. (1995) The race-specific elicitor, NIP1, from the barley pathogen, *Rhynchosporium secalis*, determines avirulence on host plants of the Rrs1 resistance genotype. *EMBO J.*, 14, 4168–4177.

Rooney, H.C., Van't Klooster, J.W., van der Hoorn, R.A., Joosten, M.H., Jones, J.D. and de Wit, P.J. (2005) Cladosporium Avr2 inhibits tomato Rcr3 protease required for Cf-2-dependent disease resistance. *Science*, 308, 1783–1786.

Rose, J.K., Ham, K.S., Darvill, A.G., Albersheim, P. (2002) Molecular cloning and characterization of glucanase inhibitor proteins: coevolution of a counterdefense mechanism by plant pathogens. *Plant Cell*, 14, 1329–1345.

Sacks W, Nurnberger T, Hahlbrock K, Scheel D. (1995) Molecular characterization of nucleotide sequences encoding the extracellular glycoprotein elicitor from *Phytophthora megasperma*. *Mol. Gen. Genet.*, 246, 45–55.

Sattelmacher, B. (2001) The apoplast and its significance for plant mineral nutrition. *New Phytologist*, 149, 167–192.

Saunders, D.G., Win, J., Cano, L.M., Szabo, L.J., Kamoun, S., and Raffaele, S. 2012. Using hierarchical clustering of secreted protein families to classify and rank candidate effectors of rust fungi. *PLOS ONE*. 7:e29847.

Segonzac, C., Feike, D., Gimenez-Ibanez, S., Hann, D.R., Zipfel, C. and Rathjen JP. (2011) Hierarchy and roles of pathogen-associated molecular pattern-induced responses in *Nicotiana benthamiana*. *Plant Physiol.*, 156, 687–699.

Sejalon-Delmas, N., Villalba Mateos, F., Bottin, A., Rickauer, M., Dargent, R. and Esquerre - Tugaye , M.T. (1997) Purification, elicitor activity, and cell wall localization of a glycoprotein from *Phytophthora parasitica* var. *nicotianae*, a fungal pathogen of tobacco. *Phytopathology*, 87, 899–909.

Seraphin, B. and Puig, O. (2002) Tandem affinity purification to enhance interacting protein identification. *Protein-Protein Interactions: A Molecular Cloning Manual*, 313–328.

Shabab, M., Shindo, T., Gu, C., Kaschani, F., Pansuriya T, Chinthia, R., Harzen, A., Colby, T., Kamoun, S. and van der Hoorn, R.A. (2008) Fungal effector protein

AVR2 targets diversifying defense-related cys proteases of tomato. *Plant Cell*, 20, 1169–1183.

Shan, L., He, P., Li, J., Heese, A., Peck, S.C., Nürnberg, T., Martin, G.B. and Sheen, J. (2008) Bacterial effectors target the common signaling partner BAK1 to disrupt multiple MAMP receptor signaling complexes and impede plant immunity. *Cell Host Microbe*, 4, 17–27.

Shuman, S. (1994) Novel approach to molecular cloning and polynucleotide synthesis using vaccinia DNA topoisomerase. *The Journal of Biological Chemistry*, 269(51), 32678-32684.

Simons, K. and Gerl, M.J. (2010) Revitalizing membrane rafts: new tools and insights. *Nat. Rev. Mol. Cell Biol.*, 11, 688–699.

Solovyev, V.V., Shahmuradov, I.A. and Salamov, A.A. (2010) Identification of promoter regions and regulatory sites. *Methods Mol Biol.*, 674, 57-83.

Spoel, S.H. and Dong, X. (2012) How do plants achieve immunity? Defence without specialized immune cells. *Nat Rev Immunol.* 12, 89–100.

Stergiopoulos I & de Wit PJGM (2009) Fungal effector proteins. *Annu Rev Phytopathol.*, 47, 233–263.

Sweigard, J.A., Carroll, A.M., Kang, S., Farrall, L., Chumley, F.G. and Valent, B. (1995) Identification, cloning, and characterization of PWL2, a gene for host species specificity in the rice blast fungus. *Plant Cell*, 7, 1221–33.

Thordal-Christensen, H., Zhang, Z., Wei, Y. and Collinge, D.B. (1997) Subcellular localization of H₂O₂ in plants, H₂O₂ accumulation in papillae and hypersensitive response during barley-powdery mildew interaction. *Plant J.*, 11, 1187–1194.

- Toth RL, Pogue GP, Chapman S (2002) Improvement of the movement and host range properties of a plant virus vector through DNA shuffling. *Plant J.*, 30, 593–600.
- Tör, M. (2008) Pattern-recognition receptors PRRs in plants. *Journal of Leukocyte Biology*, A1 - A2.
- Upadhyaya, N.M., Mago, R., Staskawicz, B.J., Ayliffe, M.A., Ellis, J.G. and Dodds, P.N. (2014) A Bacterial Type III Secretion Assay for Delivery of Fungal Effector Proteins into Wheat. *Mol. Plant-Microbe Interact.*, 27, 255–264.
- Van Den Ackerveken, G.F.J.M., van Kan, J.A., Joosten, M.H.A.J., Muisers, J.M., Verbakel, H.M., De Wit, P.J.G.M. (1993) Characterization of two putative pathogenicity genes of the fungal tomato pathogen *Cladosporium fulvum*. *Mol. Plant-Microbe Interact.*, 6, 210–215.
- van Esse, H.P., Thomma, B.P.H.J., van't Klooster, J.W. and de Wit, P.J.G.M. (2006) Affinity-tags are removed from *Cladosporium fulvum* effector proteins expressed in the tomato leaf apoplast. *J. Exp. Bot.*, 57, 599–608.
- Veit, S., Worle, J.M., Nurnberger, T., Koch, W. and Seitz, H.U. (20019) A novel protein elicitor (PaNie) from *Pythium aphanidermatum* induces multiple defense responses in carrot, *Arabidopsis*, and tobacco. *Plant Physiol.*, 127, 832–841.
- Velásquez, A.C., Chakravarthy, S. and Martin, G.B. (2009). Virus-induced gene silencing (VIGS) in *Nicotiana benthamiana* and tomato. *J. Vis. Exp.*, pii, 1292.
- Vidhyasekaran, P. (2016) Switching on Plant Innate Immunity Signaling Systems: Bioengineering and Molecular Manipulation of PAMP-PIMP-PRR Signaling Complex. *Springer*, Switzerland, 142–156.
- Villalba Mateos, F., Rickauer, M. and Esquerre-Tugaye, M.T. (1997) Cloning and characterization of a cDNA encoding an elicitor of *Phytophthora parasitica* var. *nicotianae* that shows cellulose-binding and lectin-like activities. *Mol. Plant Microbe Interact.*, 10, 1045–1053.

Wang, J. W., Ungar, L. H., Tseng, H. and Hannenhalli, S. (2007) MetaProm: a neural network based meta-predictor for alternative human promoter prediction. *BMC Genomics*, 8, 374.

Wang, X., et al. (2010) Differential gene expression in incompatible interaction between wheat and stripe rust fungus revealed by cDNA-AFLP and comparison to compatible interaction, *BMC Plant Biol.*, 10, 9.

Westerink, N., Brandwagt, B.F., De Wit, P.J.G.M. and Joosten, M.H.A.J. (2004) *Cladosporium fulvum* circumvents the second functional resistance gene homologue at the Cf-4 locus (Hcr9-4E) by secretion of a stable avr4E isoform. *Mol. Microbiol.*, 54, 533–545.

Whisson, S.C., Boevink, P.C., Moleleki, L., Avrova, A.O., Morales, J.G., Gilroy, E.M., Armstrong, M.R., Grouffaud, S., van West, P., Chapman, S., Hein, I., Toth, I.K., Pritchard, L., Birch, P.R. (2007) A translocation signal for delivery of oomycete effector proteins into host plant cells. *Nature*, 450, 115-118.

Win, J., Chaparro-Garcia, A., Belhaj, K., Saunders, D. G. O., Yoshida, K., Dong S., Schornack, S., Zipfel, C., Robatzek, S., Hogenhout, S. A. and Kamoun, S. (2012) Effector biology of plant-associated organisms: concepts and perspectives. *Cold Spring Harbor Symp. Quant. Biol.*, 77, 235–247.

Win, J., Kamoun, S. and Jones, A.M. (2011) Purification of effector-target protein complexes via transient expression in *Nicotiana benthamiana*. *Methods Mol. Biol.*, 712, 181–194.

Witte, C.P., Tiller, S., Isidore, E., Davies, H.V. and Taylor, M.A. (2005) Analysis of two alleles of the urease gene from potato: Polymorphisms, expression, and extensive alternative splicing of the corresponding mRNA. *J. Exp. Bot.*, 56, 91-99.

- Wroblewski, T., Tomczak, A., & Michelmore, R. (2005) Optimization of Agrobacterium-mediated transient assays of gene expression in lettuce, tomato and Arabidopsis. *Plant Biotechnology Journal*, 3, 259–273.
- Wydro, M., Kozubek, E., & Lehmann, P. (2006) Optimization of transient Agrobacterium-mediated gene expression system in leaves of *Nicotiana benthamiana*. *Acta Biochimica Polonica*, 53, 289-98.
- Xiang T, Zong N, Zou Y, Wu Y, Zhang J, Xing W, Li Y, Tang X, Zhu L, Chai J, et al. (2008) *Pseudomonas syringae* effector AvrPto blocks innate immunity by targeting receptor kinases. *Curr. Biol.*, 18, 74–80.
- Xin, D.W., Liao, S., Xie, Z.P., Hann, D.R., Steinle, L., et al. (2012) Functional Analysis of NopM, a Novel E3 Ubiquitin Ligase (NEL) Domain Effector of Rhizobium sp. Strain NGR234. *PLoS Pathog.*, 8, e1002707.
- Xue, J.L., Salem, T.Z., Turney, C.M. and Cheng, X.W. (2010) Strategy of the use of 28S rRNA as a housekeeping in real-time quantitative PCR analysis of gene transcription in insect cells infected by viruses. *J. Virol. Methods*, 163, 210-215.
- Yin, C., Chen, X., Wang, X., Han, Q., Kang, Z., & Hulbert, S. H. (2009) Generation and analysis of expression sequence tags from haustoria of the wheat stripe rust fungus *Puccinia striiformis* f. sp. *tritici*. *BMC Genomics*, 10, 626-634.
- Zadoks, J. C. (1961) Yellow rust on wheat studies in epidemiology and physiologic specialization. *Tijdschr Plantenziekten* 67, 69–256.
- Zeng L, Velasquez AC, Munkvold KR, Zhang J, Martin GB. (2012) A tomato LysM receptor-like kinase promotes immunity and its kinase activity is inhibited by AvrPtoB. *Plant J.*, 69, 92–103.
- Zheng, W., Huang, L., Huang, J., Wang, X., Chen, X., Zhao, J., Guo, J., Zhuang, H., Qiu, C., Liu, J., Liu, H., Huang, X., Pei, G., Zhan, G., Tang, C., Cheng, Y., Liu, M., Zhang, J., Zhao, Z., Zhang, S., Han, Q., Han, D., Zhang, H., Zhao, J., Gao, X., Wang, J., Ni, P., Dong, W., Yang, Y., Yang, H., Xu, J-R., Zhang, G. and Kang, Z.

(2013) High genome heterozygosity and endemic genetic recombination in the wheat stripe rust fungus. *Nat. Commun.*, 4, 2673.

Zipfel, C. (2008) Pattern-recognition receptors in plant innate immunity. *Curr. Opin. Immunol.*, 20, 10–16.

Zipfel, C., & Felix, G. (2005) Plants and animals: a different taste for microbes?. *Current Opinion in Plant Biology*, 8(4), 353-360.

Zhang, S. and Xu, J-R. (2014) Effectors and Effector Delivery in *Magnaporthe oryzae*. *PLoS Pathogen*, 10, e1003826.

Zhao, R. Y., Xiao, W., Cheng, H. L., Zhu, P., and Cheng, K. D. (2010) Cloning and characterization of squalene synthase gene from *Fusarium fujikuroi* (Saw.) Wr. *J. Ind. Microbiol. Biotechnol.*, 37, 1171-1182.

APPENDIX-A

pBSK-PstSCR1 (or pBSK-PSTHA2A5) PLASMID INFORMATION AND SEQUENCE

LOCUS GS50144_pBSK-PTSha2a5 3292 bp DNA circular SYN 18-OCT-2010
DEFINITION Ligation of inverted PTSha2a5 into modified pBluescript
ACCESSION GS50144_pBSK-PTSha2a5
KEYWORDS .
SOURCE Unknown.
ORGANISM Unknown
Unclassified.
REFERENCE 1 (bases 1 to 3292)
AUTHORS Self
JOURNAL Unpublished.
COMMENT SECID/File created by SciEd Central, Scientific & Educational Software
COMMENT SECNOTES|Vector molecule: modified pBluescript
Fragment ends: EcoRV
Fragment size: 2857
Insert molecule: PTSha2a5
Fragment ends: blunt
Fragment size: 435
FEATURES Location/Qualifiers
CDS 21..327
/gene="f1 origin"
/SECDrawAs="Gene"
misc_feature 600..643
/gene="T7/M13F"
/SECDrawAs="Region"
CDS complement (460..615)
/gene="LacZ"
/SECDrawAs="Gene"
CDS complement (656..1088)
/gene="PTSha2a5"
/SECDrawAs="Gene"
misc_feature complement (1103..1159)
/gene="T3/M13R"
/product="T3 primer"
/SECDrawAs="Region"
misc_feature 1489..2156

CDS /gene="pUC origin"
/SECDrawAs="Region"
complement (2307..3164)
/gene="Ampcillin"
/SECDrawAs="Gene"

ORIGIN

APPENDIX-B

pBSK-PstSCR1 (pBSK-PSTHA2A5) PLASMID MAP

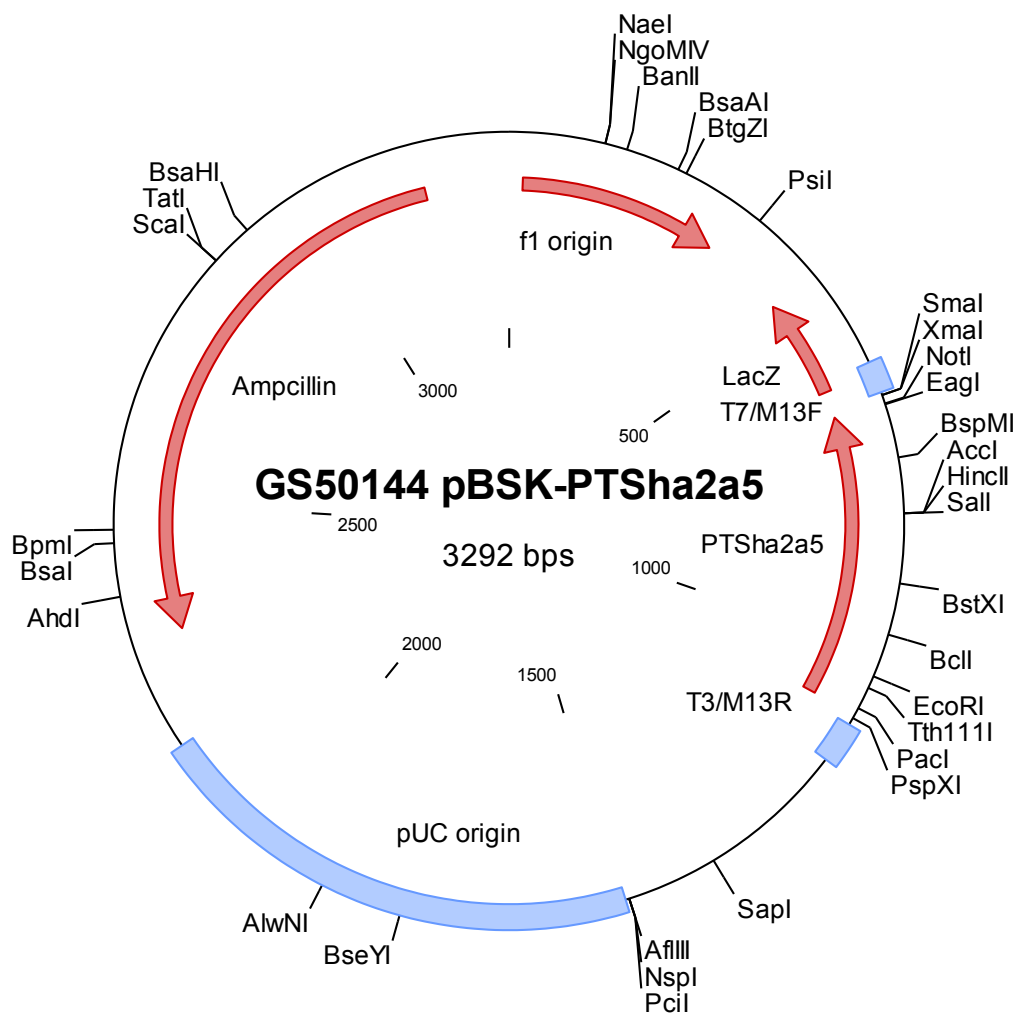


Figure B: pBSK-PstSCR1 plasmid map. PstSCR1 (PstHa2a5) synthetic gene was cloned into pBluescript II SK derivative at *Eco*RV site (lacking its multiple cloning sites).

APPENDIX-C

SEQUENCING RESULTS OF DNA BANDS IN FIGURE 3.5 A AND B IN SECTION 3.2

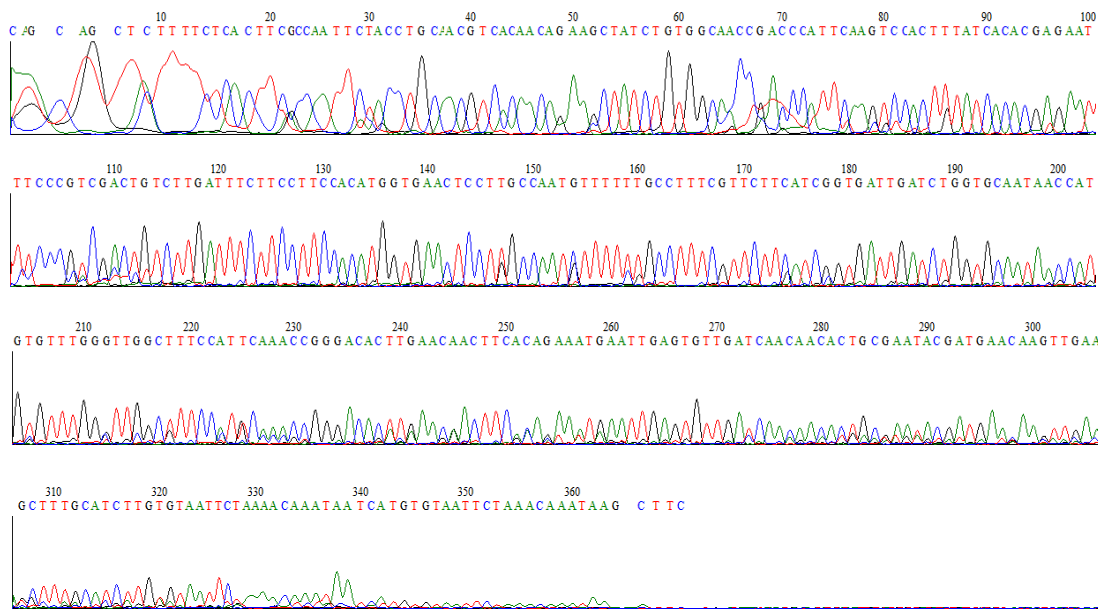


Figure C-1 The chromatogram of the sequenced DNA band of Figure 3.5A. The sequencing was carried out with PstSCR1-SP-5-UTR-F primer.

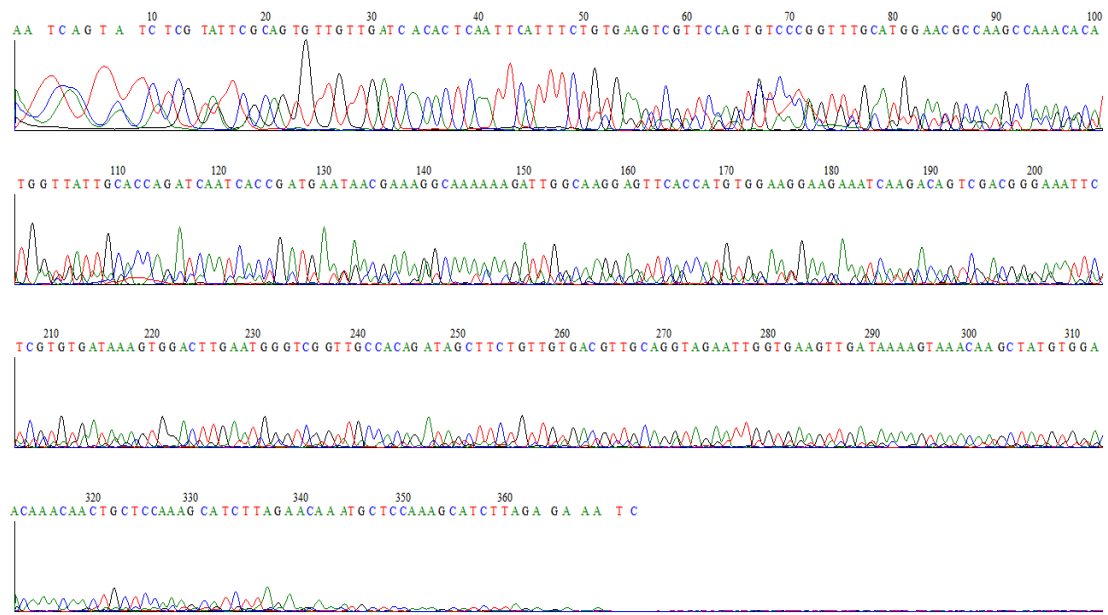


Figure C-2 The band of Figure 3.5A sequencing chromatogram. The sequencing was carried out with PstSCR1-Rev primer.

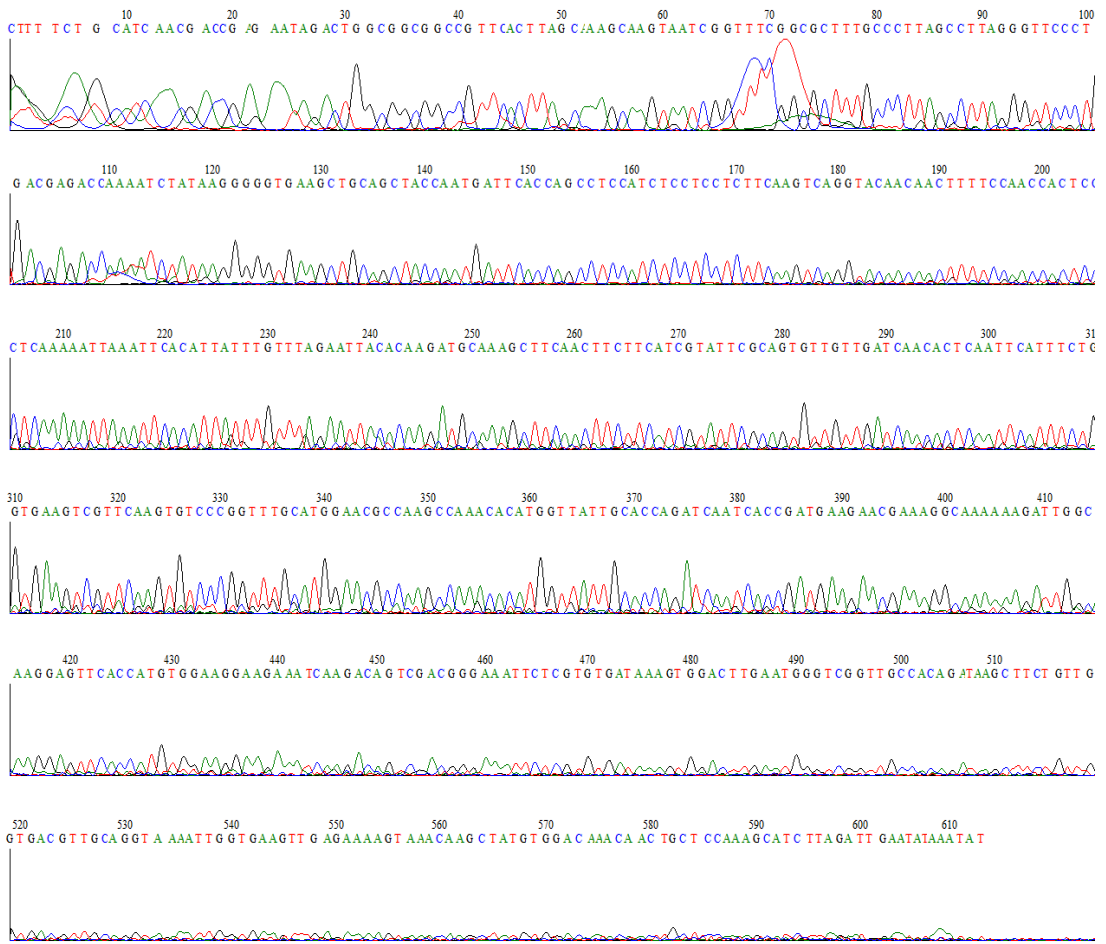


Figure C-3 The band (a) of Figure 3.5B sequencing chromatogram. The sequencing was carried out with PstSCR1-TM-5-UTR-F primer.

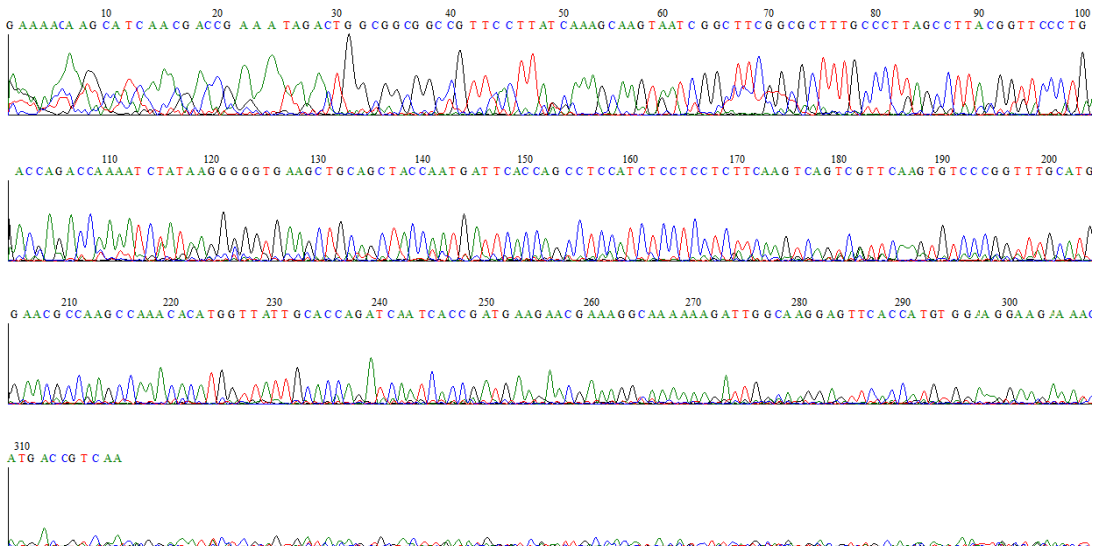


Figure C-4 The band (b) of Figure 3.5B sequencing chromatogram. The sequencing was carried out with PstSCR1-TM-5-UTR-F primer.

Score	Expect	Identities	Gaps	Strand
		324/333(97%)	2/333(0%)	Plus/Plus
Query 29	ATTATTGTAGAATTACACAAGATGCAAAGCTTCAACTTGTTCATCGTATTCGCAGT		88	
Sbjct 49	TTG-TTTAGAATTACACAAGATGCAAAGCTTCAACTTCTTCATCGTATTCGCAGT			107
Query 89	GTTGTTGATCAACACTCAATTCAATTCTGTGAAGTTGTTCAAGTGTCCGGTTGAATGG			148
Sbjct 108	TTGATCAACACTCAATTCAATTCTGTGAAGTCGTTCAAGTGTCCGGTTGCATGG			167
Query 149	AAAGCCAACCCAAACACATGGTATTGCACCAAGATCAATCACCGATGAAGAACGAAAGGC			208
Sbjct 168	AACGCCAACGCAAACACATGGTATTGCACCAAGATCAATCACCGATGAAGAACGAAAGGC			227
Query 209	AAAAAACATTGGCAAGGAGTTCACCATGTGGAAGGAAGAAATCAAGACAGTCGACGGAA			268
Sbjct 228	AAAAAGATTGGCAAGGAGTTCACCATGTGGAAGGAAGAAATCAAGACAGTCGACGGAA			287
Query 269	ATTCTCGTGTGATAAAAGTGGACTTGAATGGTCGGTTGCCACAGATAGCTTCTGTTGTGA			328
Sbjct 288	ATTCTCGTGTGATAAAAGTGGACTTGAATGGTCGGTTGCCACAGATAGCTTCTGTTGTGA			347
Query 329	CGTTGCAGGTAGAATTGGCGAAGT-GAGAAAAG	360		
Sbjct 348	CGTTGCAGGTAGAATTGGTGAGTTGAGAAAAG	380		

Figure C-5 The alignment of sequenced PCR product in Figure 3.5A by PstSCR1-SP-5-UTR-F primer was aligned with EST of PstSCR1.

Score 584 bits(316)	Expect 2e-171	Identities 325/329(99%)	Gaps 1/329(0%)	Strand Plus/Plus
Query 11	TCGTATTCGCACTGGTGTGATC-ACACTCAATTCAATTCTGTGAAGTCGTTCCAGTGTC	69		
Sbjct 95				
Query 70	CCGGTTGCATGGAACGCCAAGCCAAACACATGGTTATTGCACCAAGATCAATCACCGATG	129		
Sbjct 155	CCGGTTGCATGGAACGCCAAGCCAAACACATGGTTATTGCACCAAGATCAATCACCGATG	214		
Query 130	AATAACGAAAGGCAAAAAAGATTGGCAAGGAGTTACCATGTGGAAGGAAGAAATCAAGA	189		
Sbjct 215				
Query 190	AAGAACGAAAGGCAAAAAAGATTGGCAAGGAGTTACCATGTGGAAGGAAGAAATCAAGA	274		
Sbjct 275	CAGTCGACGGAAATTCTCGTGTGATAAAGTGGACTTGAATGGTCGGTTGCCACAGATA	334		
Query 250	GCTTCTGTTGTGACGTTGCAGGTAGAATTGGTGAAGTTGATAAAAGTAAACAAGCTATGT	309		
Sbjct 335				
Query 310	GGACAAACAACTGCTCCAAGCATCTTAG	338		
Sbjct 395	GGACAAACAACTGCTCCAAGCATCTTAG	423		

Figure C-6 The alignment of sequenced PCR product in Figure 3.5A by PstSCR1-Rev primer was aligned with EST of PstSCR1.

Score		Expect	Identities	Gaps	Strand
765 bits(414)		0.0	419/421(99%)	1/421(0%)	Plus/Plus
Query 178	CAGGTACAACAACTTTCCAACCACCTCCTCAAAAATTAAATTACACATTATTTGTTAGAA				237
Sbjct 4					63
Query 238	TTACACAAGATGCAAAGCTTCAACTTCTTCATCGTATTGCAGTGTGTTGATCAACACT				297
Sbjct 64					123
Query 298	CAATTCACTTCTGTGAAGTCGTTCAAGTGTCCGGTTGCATGGAACGCCAAGCCAAACAA				357
Sbjct 124					183
Query 358	CATGGTTATTGCACCAAGATCAATCACCGATGAAGAACGAAAGGCAAAAAAGATTGGCAAG				417
Sbjct 184					243
Query 418	GAGTTCACCATGTGGAAGGAAGAAATCAAGACAGTCGACGGGAAATTCTCGTGTGATAAA				477
Sbjct 244					303
Query 478	GTGGACTTGAATGGGTCGGTTGCCACAGATAAGCTTCTGTTGTGACGTTGCAGGTAAAAT				537
Sbjct 304					362
Query 538	TGGTGAAGTTGAGAAAAGTAAACAAGCTATGTGGACAAACAACGTCTCCAAAGCATCTTA				597
Sbjct 363					422
Query 598	G 598				
Sbjct 423	G 423				

Figure C-7 The alignment of sequenced PCR product (**a**) in Figure 3.5B by PstSCR1-TM-5-UTR-F primer was aligned with EST of PstSCR1.

Range 1: 16 to 444

Alignment statistics for match #1

Score	Expect	Identities	Gaps	Strand
774 bits(419)	0.0	426/429(99%)	2/429(0%)	Plus/Plus
Query 7	TGCATC-AACGACCGAG-AATA	GACTGGCGCGCCGTCACTTAGCAAAGCAAGTAATC	64	
Sbjct 16	TGCATCAAACGACCGAGAA	ATAAGACTGGCGCGCCGTCACTTAGCAAAGCAAGTAATC	75	
Query 65	GGTTTCGGCGCTTGC	CCCTAGGCCCTAGGGTCCCTGACGAGACAAAATCTATAAGGG	124	
Sbjct 76	GGTTTCGGCGCTTGC	CCCTAGGCCCTAGGGTCCCTGACGAGACAAAATCTATAAGGG	135	
Query 125	GTGAAGCTGCAGCTACCA	AATGATTACCAACCAGCCTCCATCTCCTCCTCAAGTCAGGTAC	184	
Sbjct 136	GTGAAGCTGCAGCTACCA	AATGATTACCAACCAGCCTCCATCTCCTCCTCAAGTCAGGTAC	195	
Query 185	AACAACTTTCCAACC	ACTCCTCAAAAATTAAATTCACATTATTGTTAGAATTACACA	244	
Sbjct 196	AACAACTTTCCAACC	ACTCCTCAAAAATTAAATTCACATTATTGTTAGAATTACACA	255	
Query 245	AGATGCAAAGCTTCAACT	TCTCATCGTATTGCAGTGTTGATCAACACTCAATTCA	304	
Sbjct 256	AGATGCAAAGCTTCAACT	TATTATCGTATTGCAGTGTTGATCAACACTCAATTCA	315	
Query 305	TTTCTGTGAAGTCGTT	CAAGTGTCCCCGGTTGCATGGAACGCCAACACATGGT	364	
Sbjct 316	TTTCTGTGAAGTCGTT	CAAGTGTCCCCGGTTGCATGGAACGCCAACACATGGT	375	
Query 365	ATTGCACCA	GATCAATCACCGATGAAGAACGAAAGGAAAAAGATTGGCAAGGAGTTCA	424	
Sbjct 376	ATTGCACCA	GATCAATCACCGATGAAGAACGAAAGGAAAAAGATTGGCAAGGAGTTCA	435	
Query 425	CCATGTGGA	433		
Sbjct 436	CCATGTGGA	444		

Range 2: 517 to 631

Alignment statistics for match #2

Score	Expect	Identities	Gaps	Strand
198 bits(107)	7e-55	114/117(97%)	2/117(1%)	Plus/Plus
Query 434	AGGAAGAAATCAAGACAGTCGAC	GGGAAATTCTCGTGTGATAAAAGTGGACTTGAATGGGT	493	
Sbjct 517	AGGAAGAAATCAAGACAGTCGAC	GGGAAATTCTCGTGTGATAAAAGTGGACTTGAATGGGT	576	
Query 494	CGGTTGCCACAGATAAGCTT	CTGTGACGTTGCAGGTAAAATTGGTGAAGTTGAG	550	
Sbjct 577	CGGTTGCCACAGAT-AGCTT	CTGTGACGTTGCAGGTAGAATTGGTGAAGT-GAG	631	

Range 3: 714 to 766

Alignment statistics for match #3

Score	Expect	Identities	Gaps	Strand
99.0 bits(53)	7e-25	53/53(100%)	0/53(0%)	Plus/Plus
Query 545	GTTGAGAAAAGTAA	ACAAGCTATGTGGACAAACAACTGCTCAAAGCATCTTA	597	
Sbjct 714	GTTGAGAAAAGTAA	ACAAGCTATGTGGACAAACAACTGCTCAAAGCATCTTA	766	

Figure C-8 The alignment of sequenced PCR product (a) in Figure 3.5B by PstSCR1-TM-5-UTR-F primer was aligned with whole genome shotgun sequence of PstSCR1 homolog.

Range 1: 12 to 191

Alignment statistics for match #1

Score	Expect	Identities	Gaps	Strand
278 bits(150)	4e-79	171/180(95%)	5/180(2%)	Plus/Plus
Query 5	ACAA-GCATC-AACGACC--GAAATAGACTGGCGCGCCGTTTC-CTTATCAAAGCAAGT			59
Sbjct 12	ACAATGCATCAAACGACCGAGAAAATAGACTGGCGCGCCGTTCACTTAGCAAAGCAAGT			71
Query 60	AATCGGCTTCGGCGCTTGCCCTTAGCCTACGGTCCCTGACCAGACAAAATCTATAA			119
Sbjct 72	AATCGGTTTCGGCGCTTGCCCTAGCCTAGGGTCCCTGACGAGACAAAATCTATAA			131
Query 120	GGGGGTGAAGCTGCAGCTACCAATGATTACCCAGCCTCCATCTCCTCCTCTCAAGTCAG			179
Sbjct 132	GGGGGTGAAGCTGCAGCTACCAATGATTACCCAGCCTCCATCTCCTCCTCTCAAGTCAG			191

Range 2: 325 to 444

Alignment statistics for match #2

Score	Expect	Identities	Gaps	Strand
222 bits(120)	2e-62	120/120(100%)	0/120(0%)	Plus/Plus
Query 178	AGTCGTTCAAGTGTCCC GGTTTGCATGGAACGCCAACACATGGTTATTGCACCA			237
Sbjct 325	AGTCGTTCAAGTGTCCC GGTTTGCATGGAACGCCAACACATGGTTATTGCACCA			384
Query 238	GATCAATCACCGATGAAGAACGAAAGGCAAAAAAGATTGGCAAGGAGTTCACCATGTGGA			297
Sbjct 385	GATCAATCACCGATGAAGAACGAAAGGCAAAAAAGATTGGCAAGGAGTTCACCATGTGGA			444

Figure C-9 The alignment of sequenced PCR product (b) in Figure 3.5B by PstSCR1-TM-5-UTR-F primer was aligned with whole genome shotgun sequence of PstSCR1 homolog.



Figure C-10 Schematic view of the PCR product (b) in Figure 3.5B after sequencing.

APPENDIX-D

pTRBO CONSTRUCT SEQUENCES

<i>PacI</i>	<i>SP</i>	
GCGTTAATTAAATGcaaagcttcaacttcttcattcgatgttttatcaacactcaat		
tcatttctgtgaagtgcgttcaagtgtcccggttgcattggaaacgccaagccaaacacatggatt		
gcaccagatcaatcaccatggaaacgaaaggcaaaaaagattggcaaggagttcaccatgtgga		
aggaagaaatcaagacagtcgacggaaattctcgatgataaagtggacttgaatggcggttg		
ccacagatagcttctgttgacgttgcaggtagaattggatgagaaaagtaaacaagcta		
tgtggacaaacaactgctccaaagcatctGTCAAGCTTCTCGAGAATTCCGACTACAAGGACGACG		
ATGACAAAat	GCGCCGCAAT	Linker
<i>NotI</i>		Flag-Tag

Figure D-1 PstSCR1 with SP fused with FLAG at C-terminus, and *PacI* at 5' and *NotI* at 3' end restriction site extensions.

<i>PacI</i>		
GAGTTAATTAAATGttcaagtgtcccggttgcattggaaacgccaagccaaacacatggttattgca		
ccagatcaatcaccatggaaacgaaaggcaaaaaagattggcaaggagttcaccatgtggaagg		
agaaatcaagacagtcgacggaaattctcgatgataaagtggacttgaatggcggttgcca		
cagatagcttctgttgacgttgcaggtagaattggatgagaaaagtaaacaagctatgt		
ggacaaacaactgctccaaagcatctGTCAAGCTTCTCGAGAATTCCGACTACAAGGACGACGATG		
ACAAAat	GCGCCGCAAT	Linker
<i>NotI</i>		Flag-Tag

Figure D-2 PstSCR1 without SP fused with FLAG at C-terminus, and *PacI* at 5' and *NotI* at 3' end extensions.

PacI
GAGTTAATTAAATGttcaagtgtcccggttgcattggaaacgccaagccaaacacatggttattgca
ccagatcaatcaccgatgaagaacgaaaggcaaaaaagattggcaaggagttcaccatgtggagg
aagaaatcaagacagtgcacggaaatttcgtgtataaagtggacttgaatgggtcggttgcca
cagatagcttctgttgtgacgtgcaggtagaattggtaagttgagaaaagtaaacaagctatgt
ggacaaacaactgctccaaagcatcttagGCGGCCGC AAT
NotI

Figure D-3 PstSCR1 without SP fused with FLAG at C-terminus, and *PacI* at 5' and *NotI* at 3' end extensions.

PacI SP
GAGTTAAT TAAATGcaaagctcaacttcttcatgtattcgcaagtgttgcattcaacactcaat
tcatttctgtgaagtcgaagggtggcgccgaccagcttcttgcataaagtggatataca
tggtagcagggcgaggagctgttcccggtggccatccgtcgagctggacggcgacg
taaacggccacaagtcagcgtgtccggcgagggcgagggcgatgccacctacggcaagctgacc
tgaagttcatctgcaccaccggcaagctgcccgtgcctggccaccctcgtgaccaccctgac
acggcgtgcagtgcctcagccgttcccgaccatgaagcagcacgacttctcaagtccgcca
tgccccgaaaggctacgtccaggagcgcaccatcttctcaaggacgacggcaactacaagaccccg
ccgaggtgaagttcgagggcgacaccctggtaaccgcattcgagctgaagggcatcgacttcaagg
aggacggcaacatccgtgggcacaagctggagtacaactacaacagccacaacgttatcatgg
ccgacaagcagaagaacggcatcaaggtgaacttcaagatccgcccacaacatcgaggacggcagcg
tgcagctcgccgaccactaccaggcagaacaccccatcgccgacggcccgatgcgtgcggcaca
accactacctgagcaccaggatccgcctgagcaaaagaccccaacgagaagcgcgatcacatggtcc
tgctggagttcggtgaccggccggatcactctcgcatggacgagctgtacaag GTCAAGCTTC
TCGAGAATTCCGACTACAAGGACGACGATGACAAA tag GCGGCCGC AAT
Linker Flag-Tag NotI

Figure D-4 GFP with SP fused with FLAG at C-terminus, and *PacI* at 5' and *NotI* at 3' end extensions.

APPENDIX-E

SCR1-FLAG AND SP-SCR1-FLAG AMPLIFICATION

Primary PCR:

PacI-noSP-SCR1-F

gagtttaattaaatgttcaagtgtcccggttgcattgg →
..... **tgaagtgc** **ttcaagtgtcccggttgcattgg** aacgccaagccaaacacatggttat
tgcaccagatcaatcaccatcgatgaagaacgaaaggcaaaaaagattggcaaggagttcaccatgtggaa
gaaagaaaatcaagacacatcgacggaaattctcgatgtgataaagtggacttgaatggcggttgc
cagatagcttctgtgtgcacgttgcaggttagaattggtaagttgagaaaagtaaacaagctatgtgg
acaa**acaactgtccaaagcatct** **taggcggccaaatccc**
← acaactgtccaaagcatctgtcaagcttctcgagaattccgactacaagg

SCR1-C-FLAG-R2

Secondary PCR:

PacI-noSP-SCR1-F

gagtttaattaaatgttcaagtgtcccggttgcattgg →
gagtttaattaaatgttcaagtgtcccggttgcattgg aacgccaagccaaacacatggttattgcacc
agatcaatcaccatcgatgaagaacgaaaggcaaaaaagattggcaaggagttcaccatgtggaaaggaa
aatcaagacacatcgacggaaattctcgatgtgataaagtggacttgaatggcggttgcacagata
gcttcgttgtgcacgttgcaggttagaattggtaagttgagaaaagtaaacaagctatgtggacaaac
aactgtccaaagcatctgtcaagct**tctcgagaattccgactacaagg**
← **tctcgagaattccgactacaaggacgacgtgacaaataaggc**

SCR1-C-FLAG-R1

Target PCR product:

PacI

gagtttaattaaatgttcaagtgtcccggttgcattgg aacgccaagccaaacacatggttattgcacc
agatcaatcaccatcgatgaagaacgaaaggcaaaaaagattggcaaggagttcaccatgtggaaaggaa
aatcaagacacatcgacggaaattctcgatgtgataaagtggacttgaatggcggttgcacagata
gcttcgttgtgcacgttgcaggttagaattggtaagttgagaaaagtaaacaagctatgtggacaaac
aactgtccaaagcatct**gtcaagcttctcgagaattccgactacaaggacgacgtgacaaataaggc**
gccccaaat Linker Flag-Tag
NotI

Figure E-1 Sequence view of amplification of SCR1-FLAG construct.

Primary PCR:

PacI-SP-SCR1-F

gggttaattaaatgcaaagcttcaacttcttcattcgatcgcaag →
.....acgacaag **caaagcttcaacttcttcattcgatcgcaag**tgttgttatcaacact
caattcattctgtgaagtgcgttcaagtgtcccggttgcattggaaacgccaagccaaacacatggta
ttgcaccagatcaatcacgatgaaagaacgaaaggaaaaagattggcaaggagttcaccatgtgga
aggaagaaaatcaagacagtcgacggaaattctcgatgataaagtggacttgaatggcggttgcc
acagatagottctgttgtgacgtgcaggtagaattgtgaaatggacttgaatggcggttgcc
gacaaa**acaactgctccaaagcatct**tagggccgcaatatccc.....
← **acaactgctccaaagcatctgtcaagcttctcgagaattccgactacaagg**

SCR1-C-FLAG-R2



Secondary PCR:

PacI-SP-SCR1-F

gggttaattaaatgcaaagcttcaacttcttcattcgatcgcaag →
gggttaattaaatgcaaagcttcaacttcttcattcgatcgcaagtgttgttatcaacactcaattc
atttctgtgaagtgcgttcaagtgtcccggttgcattggaaacgccaagccaaacacatgttattgcac
cagatcaatcacgatgaaagaacgaaaggaaaaagattggcaaggagttcaccatgtggaaggaaag
aaatcaagacagtcgacggaaattctcgatgataaagtggacttgaatggcggttgccacagat
agcttctgttgtgacgtgcaggtagaattgtgaaatggacttgaatggcggttgccacagat
caactgctccaaagcatctgtcaagct**tctcgagaattccgactacaagg**
← **tctcgagaattccgactacaaggacgacgatgacaaatag**

SCR1-C-FLAG-R1



Target PCR product:

PacI SP
gggttaattaaatgcaaagcttcaacttcttcattcgatcgcaag →
gggttaattaaatgcaaagcttcaacttcttcattcgatcgcaagtgttgttatcaacactcaattc
atttctgtgaagtgcgttcaagtgtcccggttgcattggaaacgccaagccaaacacatgttattgcac
cagatcaatcacgatgaaagaacgaaaggaaaaagattggcaaggagttcaccatgtggaaggaaag
aaatcaagacagtcgacggaaattctcgatgataaagtggacttgaatggcggttgccacagat
agcttctgttgtgacgtgcaggtagaattgtgaaatggacttgaatggcggttgccacagat
caactgctccaaagcatct**gtcaagcttctcgagaattccgactacaaggacgacgatgacaaatag**
cgccgcaat Linker Flag-Tag
NotI

Figure E-2 Schematic view of amplification of SP-SCR1-FLAG construct.

APPENDIX-F

pTRBO CONSTRUCTS SEQUENCING CHROMATOGRAMS

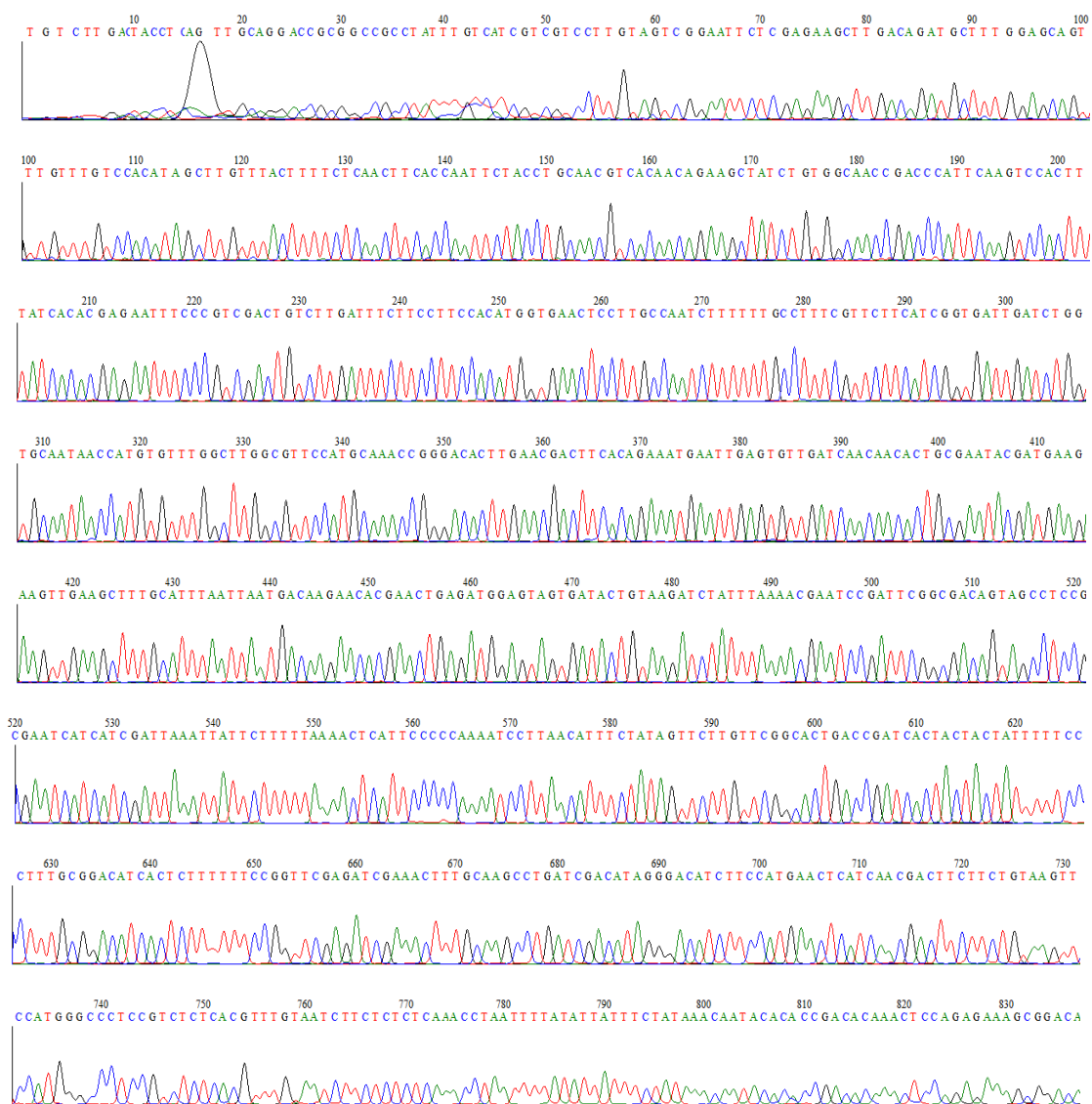


Figure F-1 pTRBO/SP-SCR1-FLAG sequencing chromatogram. The sequencing was carried out with pTRBO-seq-R primer.



Figure F-2 pTRBO/SCR1-FLAG sequencing chromatogram. The sequencing was carried out with pTRBO-seq-R primer.

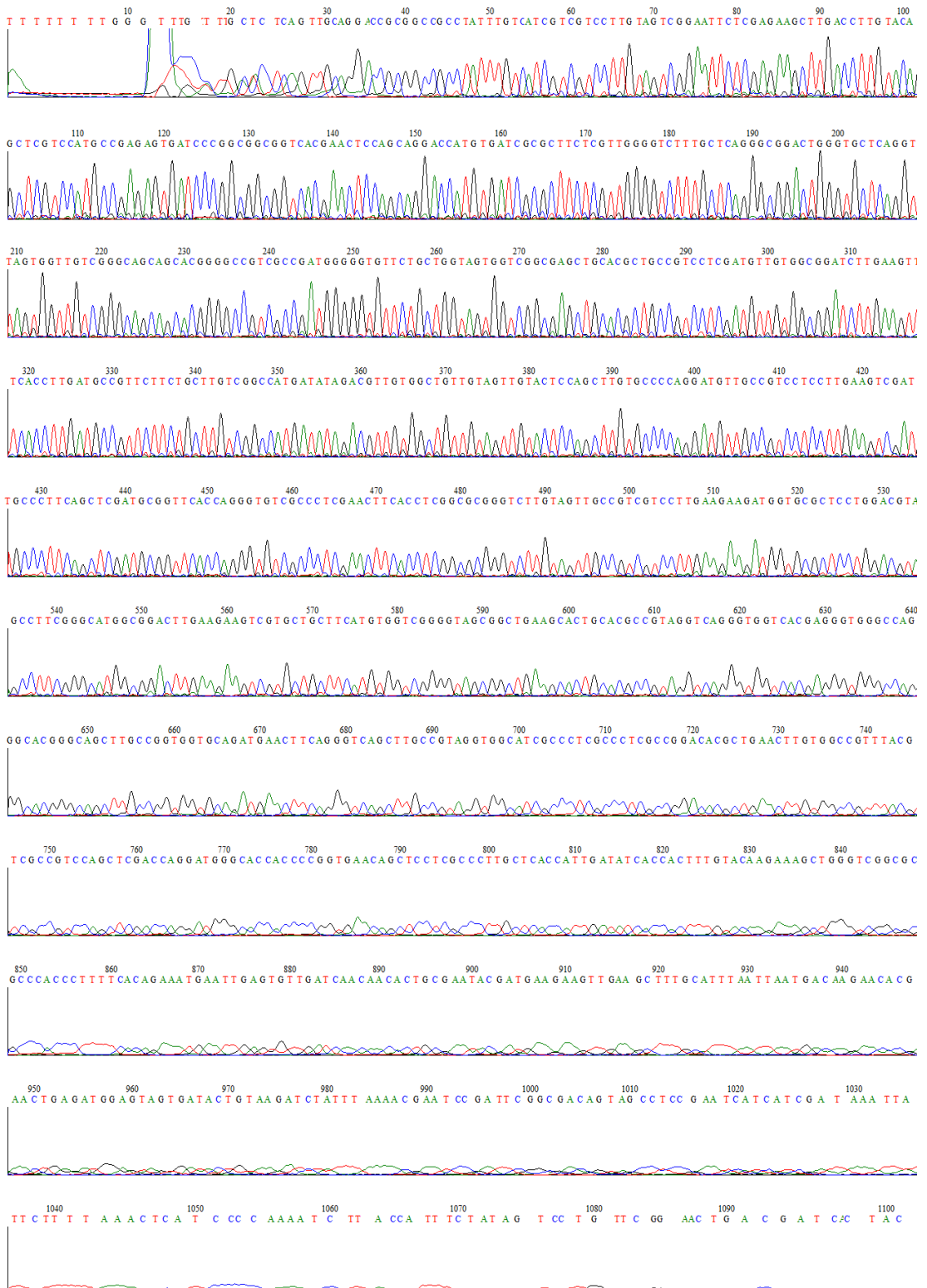


Figure F-3 pTRBO/SP-GFP-FLAG sequencing chromatogram. The sequencing was carried out with pTRBO-seq-R primer.

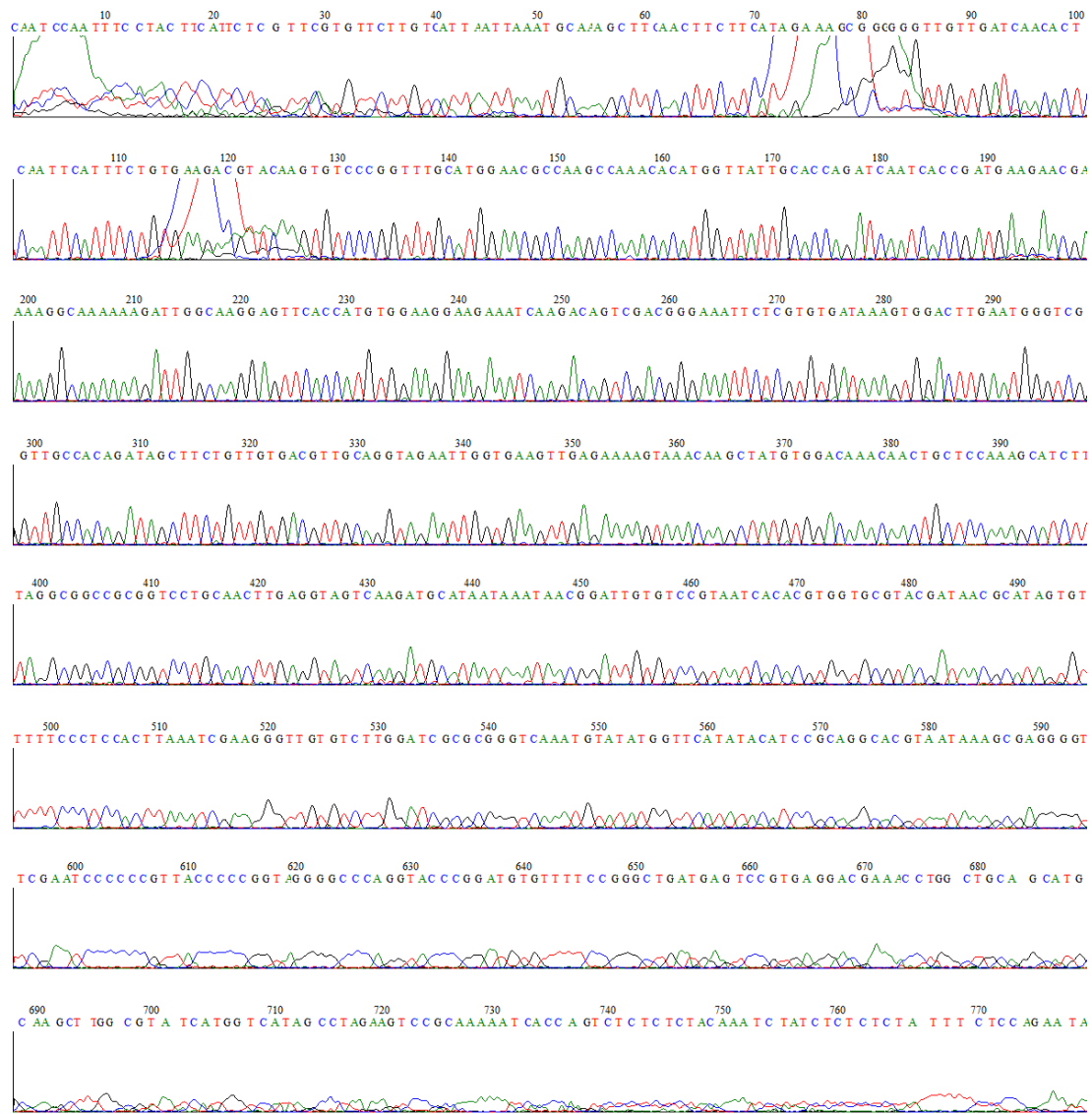


Figure F-4 pTRBO/SP-SCR1 sequencing chromatogram. Sequencing was carried out with pTRBO-seq-F primer.

APPENDIX-G

pJL48-TRBO VECTOR SEQUENCE

(Lindbo, 2007)

```
>pJL48 vector sequence (10606 bp): (nucleotide 1 = first nucleotide  
of TMV)  
gtattttacaacaattaccaacaacaacaacaaacaacagacaacattacaatttacaattaca  
atggcatacacacacagacagctaccacatcagcttgcggacactgtccgaggaaacaactccttggt  
caatgatctagcaaagcgctgtcttacgacacagcgggtgaagagtttaacgcgtgcgtgaccgcaggc  
ccaaggtaactttcaaaaagtaataagcgaggagcagacgcatttgcgtacccgggtatccagaa  
ttccaaattacatttataacacgcaaaatgcgtgcattgcgtcagggtggattgcgtatctttaga  
actggaatatctgtatgcattccctacggatcattgacttatgacataggcgaaattttgcatt  
cgcatctgtcaaggacgagcatatgtacactgctgcattgcgtgcgtgcggatccatgc  
cgacgaaaggccagaaagacagtattgaactataccttctaggctagagagagggggaaaacagt  
ccccaaacttccaaaagaaagcatttgcgtacagatacgcagaaatttgcgtacacaga  
cttccagacatgcgaacatcagccgatgcagcaatcaggcagagtgtatgcattgcgtacacaga  
atataatgacataccagccgatgcgttgcgggcacttgcgttgcgttgcgttgcgttgcgt  
cgcttcacttctccgagaacctgttgcgttgcgttgcgttgcgttgcgttgcgttgcgt  
gttttcgcgcgatggagacaagggttgcgttgcgttgcgttgcgttgcgttgcgttgcgt  
agttattctaatttgcgttgcgttgcgttgcgttgcgttgcgttgcgttgcgttgcgt  
gaaggagtttttagtcaccagagtttgcgttgcgttgcgttgcgttgcgttgcgttgcgt  
tgtacaaagggttgcgttgcgttgcgttgcgttgcgttgcgttgcgttgcgttgcgt  
cattacaaaaagacttgcgttgcgttgcgttgcgttgcgttgcgttgcgttgcgttgcgt  
ttactggttccaaaatgaggatatggtcatcgatcattgcgttgcgttgcgttgcgttgcgt  
agaggacgcgaaggaagtcttagtgcgttgcgttgcgttgcgttgcgttgcgttgcgt  
taccaggcgaagcttgcgttgcgttgcgttgcgttgcgttgcgttgcgttgcgttgcgt  
cattaaacgggttgcgttgcgttgcgttgcgttgcgttgcgttgcgttgcgttgcgt  
cggtttacctgcataactaagcttgcgttgcgttgcgttgcgttgcgttgcgttgcgt  
tcgaaaacgggttgcgttgcgttgcgttgcgttgcgttgcgttgcgttgcgttgcgt  
gaaagagaggcttgcgttgcgttgcgttgcgttgcgttgcgttgcgttgcgttgcgt  
atctatatgtgaccttccacgcacagattgtgactgtgacttgcgttgcgttgcgttgcgt  
gacatttaggaagaagatggaagaaacggaaatgttgcgttgcgttgcgttgcgttgcgt  
ggagtctgacaaattcgatgttgcgttgcgttgcgttgcgttgcgttgcgttgcgt  
cgccagcgaaggatgttgcgttgcgttgcgttgcgttgcgttgcgttgcgttgcgt  
actgaggcgaatgttgcgttgcgttgcgttgcgttgcgttgcgttgcgttgcgttgcgt  
ctcaagagaagttgttgcgttgcgttgcgttgcgttgcgttgcgttgcgttgcgt  
ttgcgttgcgttgcgttgcgttgcgttgcgttgcgttgcgttgcgttgcgttgcgt  
atggcgcacggcagattcgatgttgcgttgcgttgcgttgcgttgcgttgcgttgcgt  
tcagcaaatttgcgttgcgttgcgttgcgttgcgttgcgttgcgttgcgttgcgt  
agatcctcaaaatgcgttgcgttgcgttgcgttgcgttgcgttgcgttgcgttgcgt  
tcttaggaatgttgcgttgcgttgcgttgcgttgcgttgcgttgcgttgcgttgcgt  
gaagtatgttgcgttgcgttgcgttgcgttgcgttgcgttgcgttgcgttgcgttgcgt  
tagctgttagctgttagctgttagctgttagctgttagctgttagctgttagctgttag  
cgaaacggagaaccgcgttgcgttgcgttgcgttgcgttgcgttgcgttgcgttgcgt  
aacccaaagaaattcttccagggttgcgttgcgttgcgttgcgttgcgttgcgttgcgt  
cgaaatgtcagaagacgtgcgttgcgttgcgttgcgttgcgttgcgttgcgttgcgt  
gttgcgttgcgttgcgttgcgttgcgttgcgttgcgttgcgttgcgttgcgttgcgt  
agggttgcgttgcgttgcgttgcgttgcgttgcgttgcgttgcgttgcgttgcgt  
tttacggagacacacagcagattccatcatcaatagatgttgcgttgcgttgcgttgcgt  
gccaatttgcgttgcgttgcgttgcgttgcgttgcgttgcgttgcgttgcgttgcgt  
ttatctgaacaggagatgttgcgttgcgttgcgttgcgttgcgttgcgttgcgttgcgt
```

agatggtcggcggagccgcgtgatcaatccgatctcaaaaacccttgcattggcaagatcttgacttt
acccaatcgataaagaagctctgtttcaagaggatttcagatgtcacactgtgcataatgcagg
aggcggagacatactctgtatgtttacttagttacttagttacccctacaccggctccatcattgcagg
acagcccacatgtttggtcgttcaggcacactgttcgtcaagtaactacactgtttagtat
gatccttagtttagttagtattcattagagatcttagagaaacttagtgcgtactttagatgtataaggt
cgatgcaggaacacaatagcaattacagatgtactcggttcaaggttcaatctttgttgcag
cgccaaagactggtgatattctgtatgcagtactatgataagtgtctcccaggcaacagcacc
atgtatgtatgtatgtatgttaccatgaggactgacatttcattgtataatgtcaagatgt
atggatatgtctaagtctgtgtgcgtcaaggatcaaaccactaatactatgttagaa
cgccggcagaaatgccacgcagactggactattggaaaatttagtggcgttcaatgttgcag
aacgcacccagttgtctggcatcattgtatattgaaaactgcacatcttgggttagataagt
tgatagttatgtcttaaagaaaaagaaaaaccataaaaatgtttcttgcgttagagatgt
tcaatagatgttagaaaagcaggaacaggtaacaataggccagtcgcagatattgttgcgt
ttgcccagttgtatcagtacagacacatgattaaagcacaacccaaacaaaatggacacttcaat
ccaaacggagtacccggcttgcagacgatgtgttaccattcaaaaaagatcaatgcac
cgtttagttagtgcgttacttaggaattactggacagtgttgcgttgcgttgcgttgcgt
agaaagacaccagcgcagatttgcgttgcgttgcgttgcgttgcgttgcgttgcgt
ggagctggatatacataacgacaaatctcagaatgttgcgttgcgttgcgttgcgt
ggcaagatgggtttcaagacttgcgttgcgttgcgttgcgttgcgttgcgttgcgt
aaggattataccgcaggatataaaaacttgcgttgcgttgcgttgcgttgcgt
cattggaaacactgtgtatcattgcgttgcgttgcgttgcgttgcgttgcgt
gagcctttgcgttgcgttgcgttgcgttgcgttgcgttgcgttgcgttgcgt
tccgcgaatcttatgttgcgttgcgttgcgttgcgttgcgttgcgttgcgt
ttatagatgctctaggatgttgcgttgcgttgcgttgcgttgcgttgcgt
gaagatcttaccgtcgttgcgttgcgttgcgttgcgttgcgttgcgt
ttcatgagaatgagtcatgttgcgttgcgttgcgttgcgttgcgttgcgt
gtctgttagccgggttgcgttgcgttgcgttgcgttgcgttgcgttgcgt
cgtgtgtctggggacaaaaggatggaaagagccgcacggccactctcggt
ctgcaaaagaaaagatttcaggatgttgcgttgcgttgcgttgcgt
aacgtctggcaagtttagttaatattagaaatgtgaagatgtcagcgggttgcgt
ggagtttgtcggtgttgcgttgcgttgcgttgcgttgcgttgcgt
acgtgagagacggaggccatggaaacttacagaagaatgtcgttgcgt
atgtcgatcaggcttgcgttgcgttgcgttgcgttgcgttgcgt
tagtagtagtgcgttgcgttgcgttgcgttgcgttgcgt
ttaaaaagaataatgttgcgttgcgttgcgttgcgttgcgt
gatcttacagtatcactactccatctcgttgcgttgcgttgcgt
cggtctgcgttgcgttgcgttgcgttgcgttgcgttgcgt
gctacgataacgcataatgttgcgttgcgttgcgttgcgt
caaatgtatatgttgcgttgcgttgcgttgcgttgcgt
ccccggtagggcccaaggatccggatgttgcgttgcgttgcgt
agcatgcgttgcgttgcgttgcgttgcgttgcgt
acaaatctatctctatgttgcgttgcgttgcgttgcgt
tctttaggtttcgctcatgtgttgcgttgcgttgcgt
acttctatcaataaaaattctaaatcccaatcccaatcc
cactagcagattgtcgttgcgttgcgttgcgt
aaacctaagaaaaagagcgatgttgcgttgcgt
ttcgccattgtatgtcgttgcgttgcgttgcgt
gaactgaccacacaaggccctagcgttgcgttgcgt
aggccgttgcgttgcgttgcgttgcgt
atccgatccgcacatgaggcggaaagggttgcgttgcgt
agtcgaacatccgtcggccgtcggcgt
tcgcccagcaacacgcacgc
gtccaggacgcggaaagcggtgcagc
ccatcgccgtcgcgttgcgttgcgttgcgt

APPENDIX-H

pK7FWG2 GATEWAY DESTINATION VECTOR SEQUENCE

(Karimi *et al.*, 2002)

>pK7FWG2,0 standard; circular DNA; 11880 bp.
ggccctctagaggatccccggtaaccctgaattatcatacatgagaattaaggagtcacgttatga
ccccccgcgatgacgcggacaagccgtttacgttggactgacagaaccgcaacgttgaaaggagc
caactcagcccgggttctggagttaatgagctaagcacatacgtcagaaaaccattattgcgcgttc
aaaagtgcctaaggctactatcagtagcaaatttctgtcaaaaatgtccactgacgttccat
aaattccctcggtatccaatttagagtctcatattcactctcaactcgatcgaggcatgattgaacaa
gatggattgcacgcaggttctccggccgctgggtggagaggctattcggtatgactgggcacaaca
gacaatcggtctgtatgcccgtgtccggctgtcagcgcaggggcggccggtttttgtca
agaccgacctgtccggtgcctgaatgaactccaagacgaggcagcgcggctatgtggctggccacg
acgggcgttccctgcgcagctgtctgcacgttgcactgaagcggaaaggactggctgttattgg
cgaagtgcggggcagatctctgtcatctcaccttgcctgcggccgatccatcatggctg
atgcaatgcggcggctgcatacgcctgtatccggctacgcgcggccattcgaccaccaagcgaacatcgc
atcgagcgcacgtactcgatggaaagccggcttgcgtatcaggatgatctggacgaaagacatca
ggggctcgccgcagccaaactgttgcgcaggctcaaggcgcggatgcccgcacggcggatctcg
tgaccacggcgatgcctgttgcgcgaaatcatggggaaaatggccgcatttgcgtatcgac
tgtggccggctgggtgtggcgaccgcgtatcaggacatagcgttgcgttgcgtatattgctgaaga
gcttggccggcgaatgggtgaccgcctctcgatgcggactctgggtcgactctagatgcgt
tcgccttctatgcctcttgcgcgatgcggacttgcgttgcgttgcgtatcgac
caagcagatcgtaaaacatttgcataaaagttcttaagattgaatcctgttgcggcttgcgt
gattatcatataatttgcgttgcataacatgttaagcgtatgcataatgcgttat
ttatgagatgggttttatgattagactgcgcattatacgtatgcgtatgcgtatgcgt
tagcgcgcggaaactaggataattatgcgcgcgggtcatctatgttacttagatgcgcggcatgc
gctgataattcaattcgccgttaattcgtacattaaaacgtccgcataatgttattaaagtgtct
acgcgtcaatttgcgttgcacccacaatatcctgcgcaccagccacgcgtccccgaccggc
cgccacaaaatcaccactcgatcaggcagccatcagtcgggacggcgtcagcggagagccgtt
taaggccgcagactttgcgtatgttaccgtatcgttgcgttgcgttgcgttgcgttgcgtt
aaacacggatgtatcgcggagggttagcatgttgcgttgcgttgcgttgcgttgcgtt
caattcgggcacgaacccagtgacataaggcctcggtcgtaagctgtatgcacgt
ctgccgtacgcacactggccagaacccatgttgcacgcacgcgttgcgttgcgtt
catggcttctgttatgacatgtttttgggtacagtctatgcctcggtatccaaacgc
cggtacgcgtgggtcgatgttgcgttgcgttgcgttgcgttgcgttgcgttgcgtt
taaaacaaaatcatcatggggaaagcgggtatcgcgcgaaatgcgtatcgactcaactatc
ttggcgcatcgacgcgcattcgaaccgcacgttgcgttgcgttgcgttgcgttgcgtt
ggccgcctgaagccacacagtgtatgttgcgttgcgttgcgttgcgttgcgttgcgtt
gcggcgagcgttgcgttgcgttgcgttgcgttgcgttgcgttgcgttgcgttgcgtt
ctgttagaagtccatgttgcacgcacatcatccgtggcgttgcgttgcgttgcgtt
caatttggagaatggcagcgcacatgcacatttgcgttgcgttgcgttgcgttgcgtt
tctggctatcttgcgttgcacaaaagcaagagaacatagcgttgcgttgcgttgcgtt
tctttgatccgggttcttgcacacaggatcttgcgttgcgttgcgttgcgttgcgtt
ccgccccgactgggctggcgtatgcgttgcgttgcgttgcgttgcgttgcgttgcgtt
aacccggcaaaatcgcgcgcgaaatgcgttgcgttgcgttgcgttgcgttgcgtt
agcccgctcatacttgcgttgcgttgcgttgcgttgcgttgcgttgcgttgcgtt
gatcagttgcgttgcgttgcgttgcgttgcgttgcgttgcgttgcgttgcgtt
agctagaaattcggttgcgttgcgttgcgttgcgttgcgttgcgttgcgttgcgtt
cataatttgcgttgcgttgcgttgcgttgcgttgcgttgcgttgcgttgcgttgcgtt

gtcaggctccttatacacagccagtctgcaggtcgaccatagtgactggatatgttggtttacag
tattatgttagtctgttttatgcaaaatctaatttatatttatatttatcatttacgttac
tcgttcagcttcttgacaaagtggtgatataatgtgacatgtgagcaagggcgaggagctgttacccgggg
tggtgcccacatcctggcgagctggacggcgaacgtaaaacggccacaagttcagcgtgtccggcgagggg
gagggcgatgccacctacggcaagctgaccctgaagttcatctgcaccaccggcaagctgcccgtgcc
ctggcccacccctcgtaaccctgacctacggcgtgcagtgcattcagccgttaccccgaccacatga
agcagcacgacttcttcaagtccgcattccccgaaggctacgtccaggagcgcaccatcttcaag
gacgacggcaactacaagaccgcgcgcgaggtaagttcgagggcgacaccctggtaaccgcacatcg
gctgaaggcatcgacttcaaggaggacggcaacatctggggcacaagctggagtacaactacaaca
gccacaacgtctatatcatggccgacaagcagaagaacggcatcaaggtaacttcaagatccgcac
aacatcgaggacggcagcgtcagctcgccgaccactaccagcagaacaccccccattggcgacggccc
cgtgctgctgcccgcacaaccactacctgagccacccagtccgcctgagcaaagaccccaacgagaagc
gcgatcacatggctctgtggaggttcgatggccgcggatcaactctcgcatggacgagctgtac
aagtaaccgcggccatgctagatgtggatgttcccgataaggaaattagggttctatagggttcgctc
atgtgttgcataaaaaacccttagtatgttattgttataaaaacttctatcaataaaaatt
tctaattccaaaaacccttgcacgtgcaggcatgcgacgtcg

APPENDIX-I

THE C_T VALUES OF qPCR IN *BAK1* SILENCING EXPERIMENT

Table I. The C_T values of qPCR in *BAK1* silencing experiment

RNA samples	Gene amplification	Ct (dR)
Bak1 silenced(rep1)	Bak1	33.88
Bak1 silenced(rep2)	Bak1	No Ct*
Bak1 silenced(rep3)	Bak1	33.59
GFP silenced(rep1)	Bak1	30.67*
GFP silenced(rep2)	Bak1	31.04
GFP silenced(rep3)	Bak1	31.1
- (rep1)	Bak1	No Ct
- (rep2)	Bak1	No Ct
- (rep3)	Bak1	No Ct
Bak1 silenced(rep1)	EF1 α	25.95
Bak1 silenced(rep2)	EF1 α	25.94
Bak1 silenced(rep3)	EF1 α	26.04
GFP silenced(rep1)	EF1 α	25.39
GFP silenced(rep2)	EF1 α	25.37
GFP silenced(rep3)	EF1 α	25.5
- (rep1)	EF1 α	No Ct
- (rep2)	EF1 α	No Ct
- (rep3)	EF1 α	No Ct
Bak1 silenced(rep1)	-	No Ct
Bak1 silenced(rep2)	-	No Ct
GFP silenced(rep1)	-	No Ct
GFP silenced(rep2)	-	No Ct

*Ct values not included in Δ Ct and $\Delta\Delta$ Ct calculations.

APPENDIX-J

THE AVERAGE OF C_T VALUES AND ΔΔC_T CALCULATION OF qPCR IN *BAK1* SILENCING EXPERIMENT

Table J Averages and standard deviations of Ct values.

Gene Amplification	<i>NbBAK1/SERK3</i>		<i>NbEF1α</i>	
	Bak1 silenced	GFP silenced	Bak1 silenced	GFP silenced
Ct Mean	33.735	31.07	25.976	25.42
Ct StDev	0.205	0.042	0.055	0.07

1) $\Delta Ct_{(BAK1)} = Ct(\text{Bak1 silenced-Bak1 amplification}) - Ct(\text{Bak1 silenced-EF1}\alpha \text{ amplification}) = 33.735 - 25.97667 = 7.75833$

$\Delta Ct_{(GFP)} = Ct(\text{GFP silenced-Bak1 amplification}) - Ct(\text{GFP silenced-EF1}\alpha \text{ amplification}) = 30.93667 - 25.42 = 5.517$

2) $s_{(BAK1)} = ((0.205061)^2 + (0.055076)^2)^{1/2} = 0.212$

$s_{(GFP)} = ((0.042426)^2 + (0.07)^2)^{1/2} = 0.081853316$

3) $\Delta\Delta Ct = \Delta Ct_{(BAK1)} - \Delta Ct_{(GFP)} = 7.758 \pm 0.212 - 5.517 \pm 0.0818 = 2.10833 \pm 0.212$

Figure J The ΔΔCt calculation.

APPENDIX-K

DAB STAINING OF *N. BENTHAMIANA* LEAF TREATED WITH PURIFIED SCR1

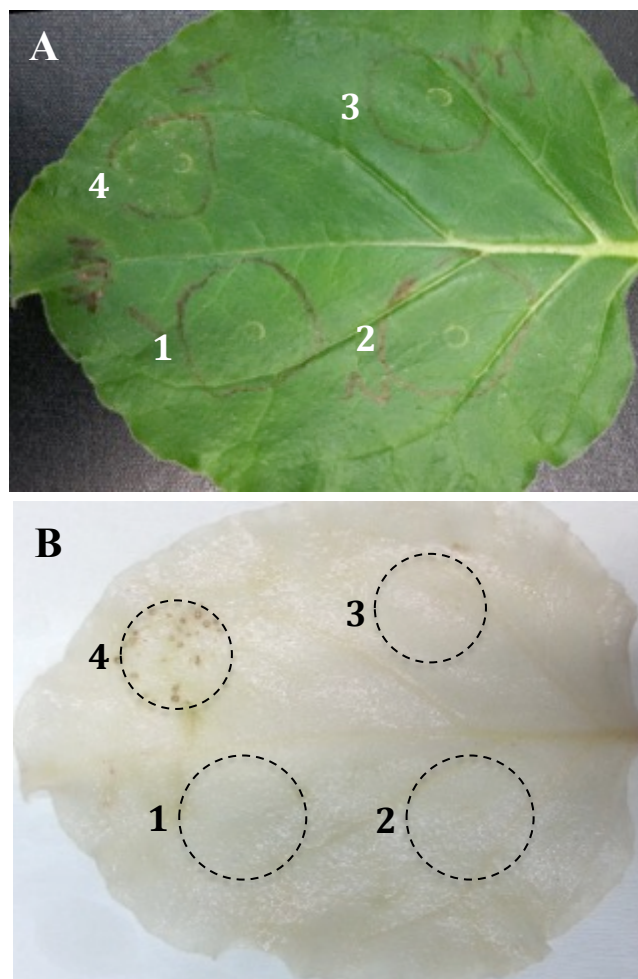


Figure K DAB staining of *N. benthamiana* leaves (4-dpi) infiltrated with purified SCR1. **1)** and **2)** GFP and SCR1 purified using apoplastic fluids isolated from *N. benthamiana* leaves expressing SP-GFP-FLAG and SP-SCR1-FLAG, respectively. **3)** and **4)** apoplastic fluids isolated from *N. benthamiana* leaves expressing SP-GFP-FLAG and SP-SCR1-FLAG, respectively. **A)** Representatvie *N. benthamiana* leaf. **B)** Representatvie *N. benthamiana* leaf after DAB staining.

APPENDIX-L

APOPLASTIC FLUID AND TOTAL PROTEIN WITH SCR1 INFILTRATION INTO *N. BENTHAMIANA*

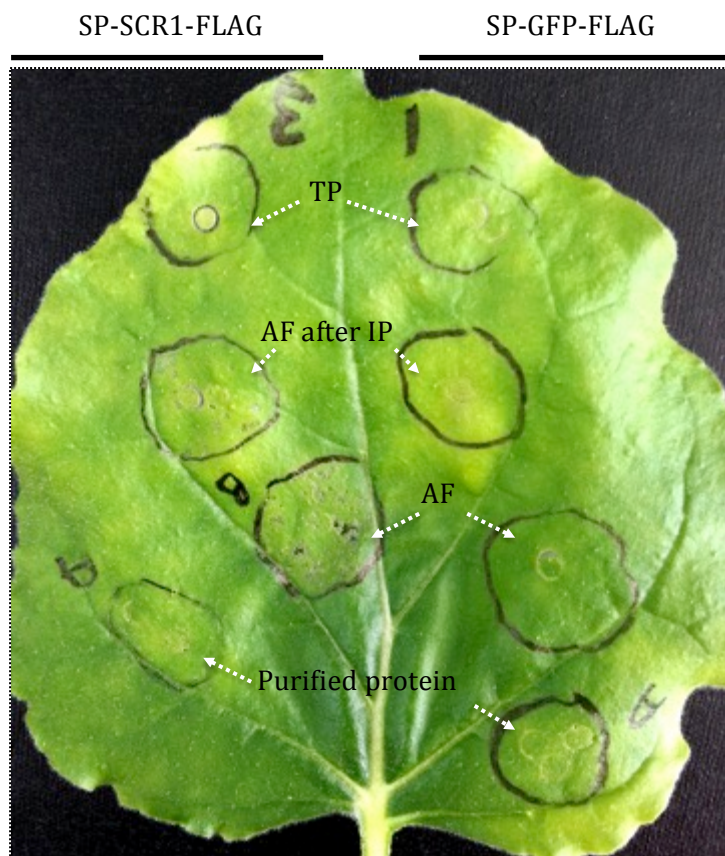


Figure L Representative *N. benthamiana* leaf infiltrated with samples possessing SCR1 protein. Apoplastic fluid (AF) isolated from pJL48-TRBO/SP-SCR1-FLAG or pJL48-TRBO-SP-GFP-FLAG expressing *N. benthamiana* (3dpi). AF, AF after Immunoprecipitation (IP) of FLAG, Purified protein (SCR1) from apoplastic fluid, and total protein (TP) from *N. benthamiana* expressing pJL48-TRBO/SP-SCR1-FLAG or pJL48-TRBO-SP-GFP-FLAG were infiltrated on the same leaf.

APPENDIX-M

AMINO ACID SEQUENCE OF PstSCR1 (GH737102.1)

MQSFNFFIVFAVLLINTQFISVKSFKCPGLHGTPSQTHGYCTRSITDEERKAKK
IGKEFTMWKEEIKTVDGKFCDKVDLNGSVATDSFCCDVAGRIGEVEKSKQ
AMWTNNCSKAS

//

CURRICULUM VITAE

PERSONAL INFORMATION

Surname, Name: Dagvadorj, Bayantes
Nationality: Mongolian
Date and Place of Birth: 10 February 1986, Mongolia
Marital Status: Married
Phone: +90 312 210 31 97
e-mail: bayantes.dagvadorj@metu.edu.tr

EDUCATION

Degree	Institution	Year of Graduation
MS	METU, Biotechnology	2012
BS	METU, Molecular Biology and Genetics	2010

FOREIGN LANGUAGES

Advanced English, Fluent Turkish

AWARDS

2013-2015, Graduate Scholarship for International Students (TUBITAK-2215)
2012-2013, Ali Kuşçu Science and Technology Scholarship, Turkey Scholarships
2010-2012, Graduate scholarship from Ministry of National Education, Turkey

MEETING ABSTRACTS

Bayantes Dagvadorj, Tolga Osman Bozkurt, Mahinur S. Akkaya. In search for subcellular localization and host interactors of a candidate effector of *Puccinia striiformis* f. sp. *tritici*. 13th ICRPMC, Aug 28 - Sept 1 2012, Beijing, China.